Synthesis, Characterization and Protonolysis mechanistic studies of diimine Pt diphenyl complexes of relevance to C-H activation

Faculty of Mathematics and Natural Sciences

University of Oslo
2009

Jérôme Parmene

Series of dissertations submitted to the
Faculty of Mathematics and Natural Sciences, University of Oslo
No. 934

ISSN 1501-7710

Cover: Inger Sandved Anfinsen.
Printed in Norway: AiT e-dit AS.

Produced in co-operation with Unipub.
The thesis is produced by Unipub merely in connection with the
thesis defence. Kindly direct all inquiries regarding the thesis to the copyright
holder or the unit which grants the doctorate.

Acknowledgement

The work presented in this thesis was carried out between 2006 and 2009 at the Department of Chemistry, University of Oslo in the group of professor Mats Tilset, and for two periods of one and two months at the Department of Chemistry and Pharmacy, University of Erlangen-Nürnberg in the group of professor Rudi van Eldik. The Norwegian Research Council and the Deutsche Forschungsgemeinschaft are gratefully acknowledged for financial support.

First of all, I would like to thank my principal supervisor Mats Tilset, for giving me the opportunity to join his group, and for introducing me to what he mentioned early on as the far from trivial topic. I can now acknowledge: C-H activation is not trivial at all. Thank you for all the suggestions and useful discussions, and especially for never lowering your standards. This has been demanding but rewarding as well.

Specials thanks go to all the past and present members of the Tilset group that I had the pleasure to work with. Without you, experimenting wouldn't have been so fun. I also would like to thank many people from the Chemistry and Pharmacy departments for making life in Oslo not so depressing during the long, cold and dark winter days. I have no doubt they will recognize themselves.

I would like to express my recognition to Rudi van Eldik and Ivana Ivanović-Burmazović for the great time I spent in there labs. I didn't expect to learn that much of every single little pieces of a UV-vis spectrometer. This has been quite an experience.

I also want to thank Dirk Petersen for his friendly attitude towards myself and his assistance with NMR. Also, thank you to Alexander Krivokapic for your assistance with X-ray crystallography.

Finally, I would like to thank my family for their support and encouragements; a special one to Aude.

Olso, July 2009

Jérôme Parmene

Abstract

In the late 60's, it was reported that aqueous Pt salts solution were capable of activating hydrocarbons C-H bonds. First encountered by deuterium incorporation in series of arenes, the reaction was found to be effective as well with methane. This reaction was further improved and the scientific community gained interest in this new field when the catalytic conversion of methane into methanol was achieved. The reaction consumed stoechiometric quantities of expensive Pt(IV) salts that limited its application. Since then, the quest for a catalytic system capable of activating un-reactive C-H bond has proven a great challenge for the chemist community. Numerous mechanistic studies have been reported, but due to the difficult observation in the rather harsh conditions of the system that proved to be efficient in the C-H activation reaction, a practical strategy that we intensively used during this thesis is the study of the microscopic reverse reaction, *i.e.* the protonolysis reaction of Pt–aryl/alkyl complexes.

Platinum complexes supported by diimine ligands have been used widely as models system of the catalytic system, and our group has presented evidence that such system were capable of activating C-H bond. Protonolysis of such diimine complexes permit to gain new insight into the C-H activation mechanism of methane and benzene but several element of the mechanism remained unclear and further study were needed. Of particular interest is the plausible difference in reactivity between a Pt-methyl and Pt-aryl complex. The present thesis is focused on the synthesis and protonolysis reaction mechanism of diimine platinum diphenyl complex and the influence solvent, temperature, pressure and structure of the diimine ligand on the complex reactivity has been widely investigated. A more detailed introduction to the field is presented in Chapter 1.

The second chapter presents a detailed kinetic investigation of an Ar-DAB diimine Pt diphenyl complex protonolysis reaction and offers direct comparison with the dimethyl, and methyl/phenyl analogues complex. Similarly, the kinetic site of protonation appears to be the metal. The study do not allow to assert firmly whether the protonation event in coordinating solvent mixture is simultaneous with the metal coordination to form an hexacoodinated Pt(IV) complex or is a stepwise process. The study allowed us to review some key mechanistic features from previous reports regarding the intramolecular proton exchange mechanism at (diimine)PtPh(η^2-C_6H_6)$^+$ between the phenyl and the benzene ligand. It appears that a direct σ-bond metathesis mechanism is more likely, in opposition to an oxidative addition/reductive

elimination sequence. Benzene elimination from (diimine)$PtPh_2H(NCMe)^+$ appears to proceed through acetonitrile dissociation, followed by reductive coupling. The kinetics of the two consecutive steps are strongly influence by the diimine ligand. Finally, kinetic evidences for an associative benzene substitution mechanism in the presence of acetonitrile are presented.

A great advantage of the diimine complex lies in the diimine ligand itself where its structure permits steric and electronic tunings of the complex. In Chapter 3, the synthesis of new Ar-BIAN and Ar-BICAT diimine complexes is described. ^{195}Pt NMR spectroscopy was used to establish the electronic influence of such ligand variation. Ar-BIAN ligands are found to be less electron donating to the metal than the Ar-DAB system previously mentioned, and the Ar-BICAT appears to be a stronger electron donating diimine ligand system. The protonolysis of the diimine complexes appear to proceed through the same intermediates in all cases. Electronic and steric effects on the protonolysis reaction are discussed. Steric factors appear to be of primary importance. ^{195}Pt NMR spectroscopy suggests that electronic tuning of the complex is best achieved by varying the diimine backbone as compared to the *N*-aryl groups.

A more rigorous mechanistic study of the steric and electronic effects was undergone combining UV-vis stopped flow and NMR techniques and the results are presented in Chapter 4. The study supports the main mechanistic view of the protonolysis mechanism. Further evidences for a metal center protonation event are presented. The influence of the electron-tuning of the diimine on the kinetics is discussed.

Chapter 5 deals specifically with the protonolysis mechanism investigation of two (Ar-BIAN)$PtPh_2$ complexes in ether dichloromethane solvent mixtures by UV-vis stopped flow spectroscopy.

Table of Contents

Acknowledgement 1

Abstract 2

Table of Contents 4

List of Papers 6

List of contributors 6

Abbreviations 7

Numbering 8

1. Introduction and Scope 9

1.1. Introduction 9
1.2. Hydrocarbon C-H activation 11
1.2.1 "Shilov's" chemistry 11
1.2.2 The Catalytica system 12
1.2.3 Mechanistic fundamentals 13
1.3. Platinum diimine complexes in C-H activation 15
1.3.1 C-H activation with diimine Pt complexes 15
1.3.2 Protonolysis reaction of (Ar-DAB)$PtMe_2$ 17
1.4. Aromatic C-H activation 19
1.4.1 Platinum scorpionate complex in arene C-H activation 19
1.4.2 Intramolecular proton exchange at (Ar-DAB)$PtPh(\eta^2\text{-}C_6H_6)^+$ complexes 20
1.5. Methods and techniques used 21
1.5.1 NMR 21
1.5.2 Stopped-flow UV-vis spectroscopy 22
1.6. Scope 22

2. Combined low temperature rapid scan and ^1H NMR mechanistic study of the protonation and subsequent benzene elimination from a (diimine)platinum(II) diphenyl complex 24

2.1. Introduction 24
2.2. Results 25
2.2.1 Protonation of (Ar-DAB)$PtPh_2$ in the presence of MeCN 25
2.2.2 Elimination of benzene from (Ar-DAB)$PtPh_2H(NCMe)^+$ 28
2.2.3 The second protonation and benzene elimination 31
2.2.4 Substitution of benzene on (Ar-DAB)$PtPh(\eta^2\text{-}C_6H_6)^+$ by acetonitrile in dichloromethane 34
2.3. Discussion 36
2.3.1 Low-Temperature Protonation of (Ar-DAB)$PtPh_2$ 36
2.3.2 Reductive Coupling and Oxidative Cleavage 39
2.3.3 Elimination of Benzene from (Ar-DAB)$PtPh_2H(NCMe)^+$ 41
2.3.4 Substitution of Benzene by Acetonitrile at (Ar-DAB)$PtPh(\eta^2\text{-}C_6H_6)^+$ 42
2.3.5 Protonation and Benzene Elimination at (Ar-DAB)$PtPh(NCMe)^+$ 4a 43
2.4. Summary and concluding remarks 44
2.5. Experimental Section 45

3. Synthesis, Characterization, and Protonation Reactions of new Ar-BIAN and Ar-BICAT Diimine Platinum Diphenyl Complexes 47

3.1. Introduction....47
3.2. Results and Discussion....48
3.2.1 Synthesis and characterization of metal complexes....48
3.2.2 Low-temperature protonation of (N–N)$PtPh_2$ in the presence of acetonitrile....50
3.2.3 Low-temperature protonation of (N–N)$PtPh_2$ in the absence of acetonitrile....51
3.2.4 Protonation of 1b-h in the presence of acetonitrile at ambient temperature....53
3.2.5 Protonation of 1b-g in the presence of acetonitrile at elevated temperatures....53
3.2.6 X-ray crystal structures....54
3.3. Mechanistic issues....60
3.4. Conclusions....62
3.5. Experimental section....63
3.5.1 General considerations....63
3.5.2 X-ray crystallographic structure determinations....63
3.5.3 Synthetic procedures....64
4. Steric and electronic effect investigation on the protonolysis reaction mechanism at a series of (N-N)$PtPh_2$ complexes by complementary ^{1}H NMR and UV-Vis spectroscopy....75
4.1. Introduction....75
4.2. Results and discussion....76
4.2.1 Low-temperature protonation of (N-N)$PtPh_2$ in the presence of acetonitrile....76
4.2.2 Protonation in poorly coordinating solvent mixtures of ether in dichloromethane....80
4.2.3 Study of the benzene elimination from (N-N)$PtPh_2H(NCMe)^+$ 2b-f, h at higher temperature....82
4.2.4 Benzene substitution reaction from π-benzene complex 3b....85
4.3. Suggested mechanism and diimine electronic and steric influence on the processes investigated....88
4.3.1 Protonation....89
4.3.2 Benzene elimination....90
4.3.3 Benzene substitution....94
4.4. Summary and concluding remarks....95
5. UV-vis stopped-flow investigation of the protonolysis reaction of (Ar-BIAN)$PtPh_2$ complexes 1b and 1e in ether dichloromethane solvent mixtures....97
5.1. Introduction....97
5.2. Results....98
5.2.1 Protonation and benzene substitution reactions from (Ar-BIAN)$PtPh_2$ 1e....98
5.2.2 Protonation of (Ar-BIAN)$PtPh_2$ 1b complex with $HBF_4.Et_2O$ and consecutive benzene substitution reaction....100
5.2.3 Protonation of (Ar-BIAN)$PtPh_2$ 1b with triflic acid and benzene substitution reaction....103
5.2.4 Ion pair and salt inhibition effect....104
5.3. Discussion....106
5.4. Conclusion....107
6. Conclusion and perspectives....108
7. References....110
Appendix: Papers and Manuscript **1-3**

List of Papers

1. Combined low temperature rapid scan and ^{1}H NMR mechanistic study of the protonations and subsequent benzenes eliminations from a (diimine)platinum(II) diphenyl complex relevant to arene C-H activation. Parmene, J.; Ivanović-Burmazović, I.; Tilset, M.; van Eldik, R., *Inorg. Chem.* **2009**, *48*, 9092-9103

2. Synthesis, Characterization, and Protonation Reactions of new Ar-BIAN and Ar-BICAT Diimine Platinum Diphenyl Complexes. Parmene, J.; Krivopavic, A.; Tilset, M., **2009**, submitted

3. Steric and electronic effect investigation on the protonolysis reaction mechanism at a series of (N-N)$PtPh_2$ ((N-N) = diimine = Ar-BIAN with Ar = 2,6-$Me_2C_6H_3$ (a), 2,4,6-$Me_3C_6H_2$ (b), 4-Br-2,6-$Me_2C_6H_2$ (c), 3,5-$Me_2C_6H_3$ (d), 4-MeC_6H_4 (e), and Ar'BICAT with Ar'= 4-MeC_6H_4 (f)) complexes by complementary ^{1}H NMR and UV-Vis spectroscopy. Parmene, J.; Ivanović-Burmazović, I.; Tilset, M.; van Eldik, R. *Preliminary manuscript*

List of contributors

Jerome Parmene (experimental work, NMR, UV-vis stopped-flow, Papers 1-3)
Ivana Ivanović-Burmazović (UV-vis stopped-flow, Papers 1 and 3)
Alexander Krivopavic (crystallographic work, Paper 2)

Abbreviations

DAB	1,4- diaza-1,3-butadiene
BIAN	bis(aryl-imino)acenaphtene
BICAT	bis(aryl-imino)catechol
bpy	bipyridine
bpym	bipyrimidine
Cp	cyclopentadienyl
Cp*	(1,2,3,4,5- pentamethyl)cyclopentadienyl
Tp	hydridotris(pyrazolyl)borate
Tp'	hydridotris(3,5-dimethylpyrazolyl)borate
tmeda	tetramethylethylenediamine
Me	methyl
Ar	aryl
Ph	phenyl
o	ortho
m	meta
p	para
i	ipso
Et_2O	diethylether
MeCN	acetonitrile
CH_2Cl_2	dichloromethane
TFE	trifluoroethanol
TfOH	triflic acid
$HBF_4.Et_2O$	fluoroboric acid diethylether complex
NMR	nuclear magnetic resonance
δ	chemical shift (NMR)
ppm	part per million
EXSY	exchange spectroscopy
KIE	kinetic isotope effect
IR	infra red
ν	stretching frequency
σ-CAM	sigma- complex assisted metathesis
DFT	density functional theory

Numbering

The following numbering scheme has been chosen for the diimine Pt complexes discussed in the thesis. The letters design the diimine ligand (Table A) and the numbers refer to the substituent bounded to the metal center (Table B).

Table A: Numbering of diimine ligands

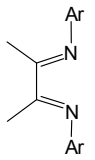

ligand	Ar
a	2,6-$Me_2C_6H_3$

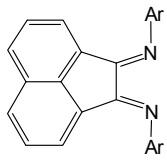

ligand	Ar
b	2,6-$Me_2C_6H_3$
c	2,4,6-$Me_3C_6H_2$
d	4-Br-2,6-$Me_2C_6H_2$
e	3,5-$Me_2C_6H_3$
f	4-MeC_6H_4
g	4-$CF_3C_6H_4$

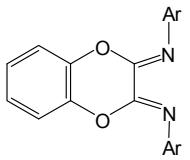

ligand	Ar
h	4-MeC_6H_4

As a reference to the diimine backbone substitution, ligand **a** is also designated as Ar-DAB, whereas ligands **b-h** are referred to as Ar-BIAN, and ligand **h** to as Ar-BICAT respectively.

Table B: Numbering of Pt complexes

#	Pt(II) neutral	#	Pt(IV) cationic	#	Pt(II) cationic	#	Pt(II) dicationic
1	$PtPh_2$	**2**	$PtPh_2H(NCMe)^+$	**3**	$PtPh(\eta^2\text{-}C_6H_6)^+$	**7**	$Pt(NCMe)_2^{2+}$
				4	$PtPh(NCMe)^+$		
				5	$PtPh(CO)^+$		
				6	$PtPh(solv)^+$		

Anions used include BF_4^- and TfO^- and will be specified were appropriate although the BF_4^- anion is undermined when no specification.

1. Introduction and Scope

1.1. *Introduction*

Hydrocarbons are the simplest class of organic molecules. They consist of a chain of carbon and hydrogen atoms. Alkanes, or aliphatic hydrocarbons are a sub-class of hydrocarbons.[1] The most elementary compound of this sub-class is methane, CH_4. It is the main component of natural gas, and since it only releases CO_2 and H_2O upon combustion, is considered a clean fuel. Methane, H_2O and CO_2 are all green house gazes, but the methane contribution to global warming is considered 23 times higher than its equivalent in CO_2.[2] As such, its releasing, and the gases it releases upon combustion in the atmosphere is a major concerned for the environment. Methane is used industrially as the principal starting material for the production of hydrogen, methanol, and acetic acid.[3] When used to produce any of these chemicals, methane is first converted to *Synthesis Gas*, a mixture of carbon monoxide and hydrogen, by a process termed steam reforming, Scheme 1. This process is heterogeneous in nature and requires high temperature.[4,5]

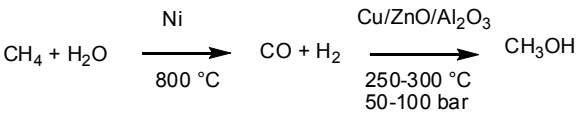

Scheme 1

Another sub-class of hydrocarbon is termed aromatic hydrocarbons, or arenes.[1] The simplest cyclic hydrocarbon member of this sub-class is the benzene molecule, C_6H_6. In the 19th and early-20th centuries, benzene was used as an after-shave because of its "pleasant" smell, thereby the aromatic denomination encountered for this class of compounds. It was also used as a solvent but when its toxicity became obvious, benzene was supplanted by other solvents, especially toluene, which has similar physical properties but is not as carcinogenic.[6,7] Benzene, in organic chemistry, reacts classically by electrophilic aromatic substitution sometimes abbreviated SE_{Ar}. Common reactions are acylation and alkylation (also termed Friedel-Crafts reactions),[8-10] sulfonation,[11] nitration,[12] and halogenation reactions.[13] In such reactions, benzene is considered a nucleophile, and reacts with an activated electrophile reagent. Alternatively, benzene can be hydrogenate and furnish cyclohexane. This chemistry has limitation, due mainly to the poor reactivity of benzene, and rather harsh conditions used.

The C-H bonds of hydrocarbons are very strong (the bond dissociation energy of methane is 440 kJ mol^{-1} at 25 °C,[14] the one of benzene is 469 kJ mol^{-1} at 25 °C[15]) and the selective cleavage of these is difficult to perform. The development of catalytic systems capable of selectively functionalized C-H bond in mild conditions is an area of research with great possible input for the industry but is also a fascinating subject for the academic community.[14,16-18] Practical application for C-H bond activation do not only implies that a C-H bond has to be broken, but also the functionalization of the resulting carbon entity by introduction of a heteroatom or formation of a new C-C bond. Systems involving transition metal complexes have proven to be good candidate and a few promising homogeneous systems have been developed[3,19-30] with a particular interest for Pt(II) square planar metal complexes that will be addressed further. Extensive research has been aimed at studying the details of the selective functionalization of hydrocarbons. The work presented here browse a series of recent contributions that deal with the mechanistic studies of arene C-H bond formation and cleavage, by studying its microscopic reverse reaction, *i.e.* the protonolysis of phenyl-metal complex, and is specifically intended to gain further understanding of benzene C-H activation mechanism.

1.2. *Hydrocarbon C-H activation*

1.2.1 "Shilov's" chemistry

Garnett and Hodges reported during the late 1960's that aqueous Pt(II) salts were able to catalyse the H/D exchange in aromatic hydrocarbons.[31,32] Certainly inspired by their work, Shilov and his co-workers extended that reaction to the aliphatic hydrocarbons, Scheme 2.[33,34]

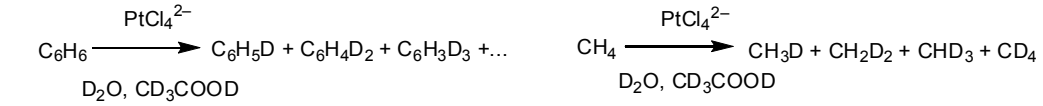

Scheme 2

The reaction was further developed into catalytic systems in which methane was converted into methanol using stoechiometric amounts of $PtCl_6^{2-}$ as an oxidant, Scheme 3. The catalytic Shilov system is believed to process through a three steps general mechanism.[16,18,19,31,35-41] The first is the C-H activation, where a hydrocarbon coordinates to the Pt(II) metal complex and one C-H bond is broken. This leads to the formation of an alkyl Pt(II) metal complex and a proton is liberated. After oxidation of the Pt(II) alkyl intermediate to Pt(IV) by a redox process with $PtCl_6^{2-}$, a water molecule reacts with the Pt(IV) alkyl to liberate the functionalized alkyl and the Pt(II) metal centre is regenerated.

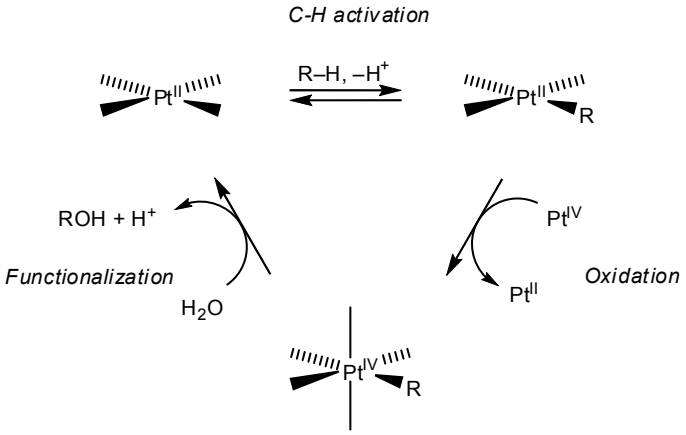

Scheme 3

The individual steps if the Shilov mechanism have been extensively studied, and both alkane and arene activation follow this simple outline. Although useful as a model, this mechanism is a simplification of the chain of events that occur during the C-H activation and functionalization reactions. Several organometallic complexes capable of activating

hydrocarbons have been made and many ingeniously designed experiments combined with careful spectroscopic observations have provided more detailed insight into the simple three steps outline of the Shilov system. Numerous experimental techniques and theoretical studies have revealed many mechanistic details of the C-H activation steps that led to an increased understanding of the reaction mechanism.[18,37,38] Key intermediates have been characterized. Of particular interest are the σ–methane and benzene ones that have been first implied by isotopic scrambling experiments and by multiple deuterium incorporation from deuterated solvent.[31,42]

1.2.2 The Catalytica system

The most impressive catalytic system described yet for catalytic conversion of methane to methanol is the Catalytica system, Scheme 4, developed by Periana.[5] It operates under rather harsh condition of SO_3/H_2SO_4 at 150 °C where the catalyst decomposes, but the combination of ligand, bipyrimidine (bpym), and hot sulphuric acid assure the dissolution of metallic Pt. An ingenious way to keep the catalyst alive that assures its efficiency. Turnover numbers greater than 300, high yield (70 % based on methane) and impressive selectivity (90 %) have been reported.

DFT calculations were used to map out the underlying C-H activation mechanism in this system.[43,44] The methane coordination appeared to be rate determining. An electrophilic substitution mechanism revealed to be less energetically demanding than the oxidative addition observed in the Shilov system, and it is assume to be resulting from the enhanced electrophilicity of the metal because of the ligand protonation at a *N* non-ligated atom.[45] The functionalization step proceeds via a reductive cleavage to form methylsufonate (CH_3OSO_3H), further hydrolyzed to methanol, rather than by water nucleophilic attack at the methyl-Pt bond, observed in the original Shilov system.

This emphasize the complexity of hydrocarbon activation and functionalization studies, where conclusions obtained from one particular set of metal, ligand, and conditions, although resulting in the same product formation, may not be valid for another set of experimental conditions.

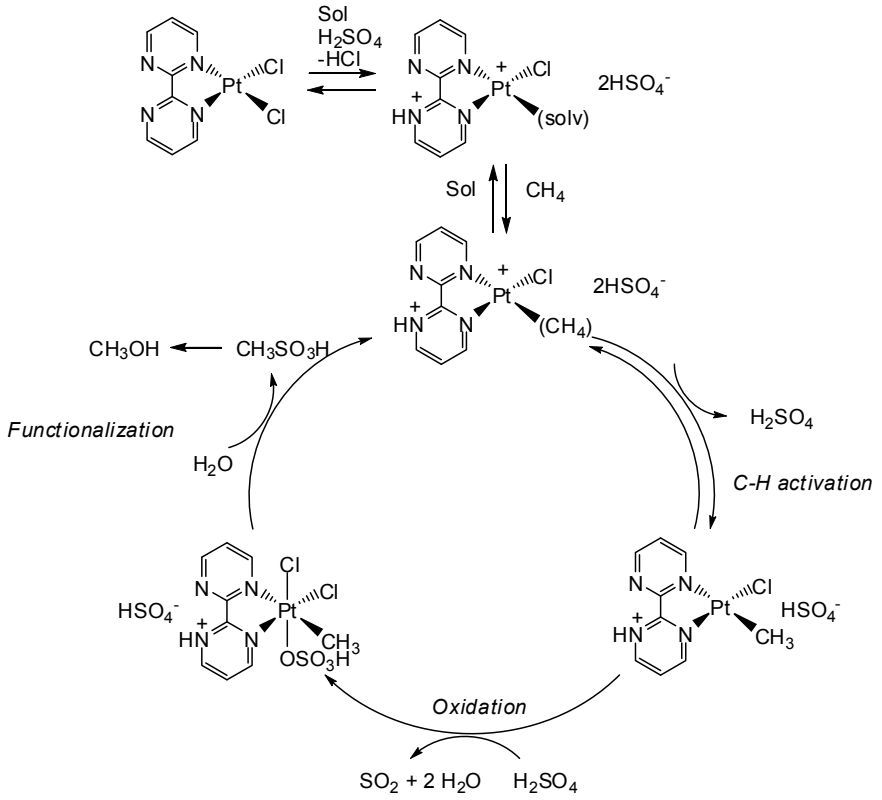

Scheme 4

1.2.3 Mechanistic fundamentals

As defined by Periana and co-workers, C-H activation is a facile C-H cleavage reaction with an "MX" species that proceeds by coordination of an alkane to the inner-sphere of "M".[19] As such C-H bond activation can be subdivided in two steps: inner-sphere coordination to the metal and C-H bond cleavage.

1.2.3.1 Coordination mode

Arenes C-H bonds are considerably stronger than alkanes C-H bonds, however arene C-H activation is thermodynamically favoured over alkanes C-H activation because of the formation of strong metal-aryl bonds.[46,47] C-H activation of arenes usually follows similar mechanism to aliphatic hydrocarbon, but substantial evidence, although not without exceptions,[48,49] indicates that the mechanism of the addition prior to the oxidative cleavage of arenes at unsaturated metal centres proceeds via η^2–(C,C) pre-complexation.[37,50-59] This is

probably followed by an arene "slip" to a η^2–(C,H)[52,60,61] or a η^1–(C)[62] coordination, and finally oxidative cleavage of one of the C-H bond to form a hydrido aryl complex, Scheme 5.

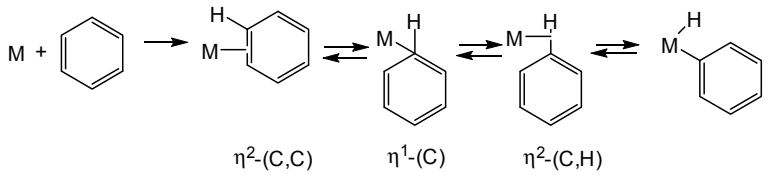

Scheme 5

Different intermediate or coordination modes can interconvert, and the actual conditions employed will make the system shift between these different coordination modes.

1.2.3.2 Mechanism of activation

The C-H activation of hydrocarbon involves the breaking of a C-H bond. Five different mechanistic pathways are considered as potentially operating depending on the conditions used: oxidative addition, σ-bond metathesis, electrophilic addition, 1,2 addition and metalloradical activation.[37]

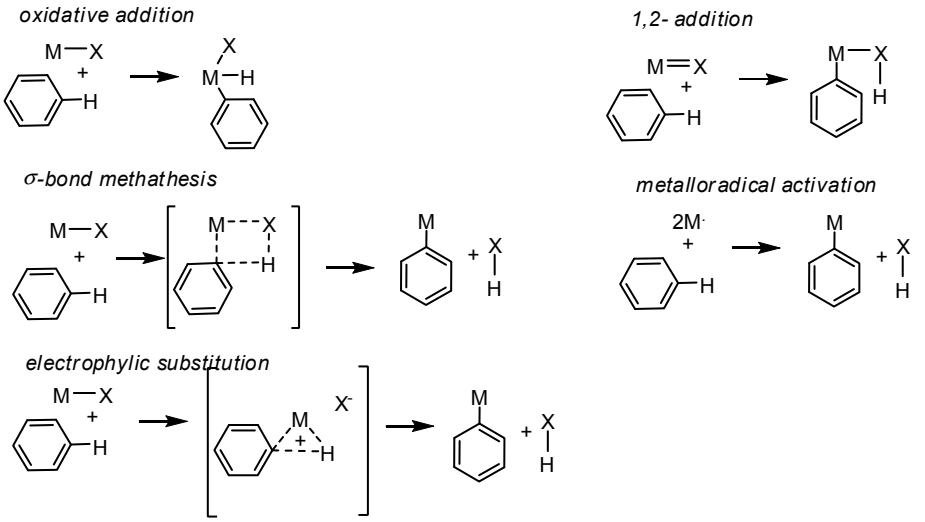

Scheme 6

The oxidative addition is expected to be operational for reactions at electron rich, low oxidation state metal centre complexes and implies the availability for higher oxidation state of the metal. The σ-bond metathesis involves the direct transfer of hydrogen through a 4

centres, 4 electrons transition state by avoiding the necessity for a change in the oxidation state of the metal. So it is pertinent for d^0 metals. An alternative denomination as σ-complex assisted metathesis (σ-CAM) has been recently proposed.[63] The distinction between electrophilic substitution and σ-bond metathesis is less obvious. It is based on the deprotonation event of the C-H bond. If effective from a basic enough group, that is not link to the metal, the former term is prefered.[18]

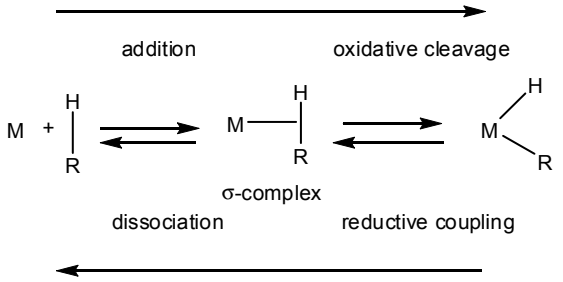

Scheme 7

It is now established that the oxidative addition mechanism proceeds in two elementary steps; coordination to the metal that can be associative or dissociative in nature, and oxidative cleavage of the C-H bond. The reverse reaction, formally a reductive elimination, can as well be decomposed in two elementary steps as implied by microscopic reversibility arguments and is termed reductive coupling, which is followed by hydrocarbon dissociation, Scheme 7.[64,65]

1.3. *Platinum diimine complexes in C-H activation*

1.3.1 C-H activation with diimine Pt complexes

Among the most crucial intermediates in the C-H activation reaction are the C-H σ-coordinated alkyl and aryl complexes and the corresponding hydridoalkyl and hydridoaryl complexes that were first implied by H/D exchange, Scheme 8.

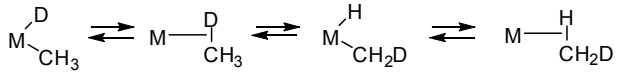

Scheme 8

Under C-H activation conditions, theses intermediates are normally too unstable to be directly observed by standard spectroscopic methods. A common strategy to elucidate the C-H bond

activation mechanism is the study of its microscopic reverse reaction, *i.e.* protonolysis of Pt-(alkyl/ aryl) complexes. Early on, it was postulated that protonation of this type of complexes could occur at a ligand, at the Pt-C bond or directly at the metal. The Bercaw group established on a tmeda-Pt(II) model system that hydridoalkylplatinum(IV) species were involved in the protonolysis reaction.[66,67] Other studies also observed hydridoalkylplatinum(IV) species during low-temperature protonation.[68-72] This lead to the assumption of an oxidative addition mechanism of an alkane to the metal, presumably from a Pt(II) σ-methane complex, leading to a Pt(IV) hydrido intermediate by oxidative cleavage of the C-H bond. Reaction of [(tmeda)Pt(CH_3)(pentafluoropyridine)][$BArf_4$] (tmeda = tetamethylethylendiamine) with benzene-d_6 resulted in the observation of deuterated methane (CH_4, CH_3D, CH_2D_2 and CHD_3).[73] Arene C-H activation was expected to follow similar patterns to aliphatic hydrocarbon C-H activation: associative displacement of a ligand by the hydrocarbon to form a Pt(II) η^2-benzene intermediate,[74] followed by an oxidative cleavage to furnish a Pt(IV) hydrido/phenyl intermediate. The rates of the reaction of benzene with cationic Pt(II) centres were found to be faster with more electron rich ligands. Later studies provided insights into how the substitution pattern on the aryl rings of the diimine ligands affect the rate determining step for C-H activation of benzene by [(diimine)Pt(CH_3)(L)]$^+$ with TFE as the reaction medium.[75] With bulky substituent in the ortho position of the diimine ligand, η^2-benzene coordination appeared rate limiting while in the absence of ortho substituent, the C-H cleavage became the rate determining step. This was explained by steric destabilisation of both the intermediate π–benzene complex and the transition state by the ortho methyl group. The relative energy levels of the transition states in the reaction appeared not very sensitive to electronic properties of the ligand, independently of the different substitution pattern on the aryl groups. The introduction of stronger electron donating ancillary ligand led to destabilisation of the ground state aqua complexes resulting in faster C-H activation rates.

Pt(IV) species have also been proposed to be involved in arene C-H activation at (diimine)PtMe(solv)$^+$ (diimine = ArN=CR-CR=NAr, R = H, Me, Ar = substituted aryl) species, where solv is a solvent molecule, in solution. One important finding has been that low-temperature protonation of (diimine)Pt(II) dialkyl and Pt(II) diaryl complexes lead to observable, but thermally sensitive, Pt(IV) hydridoalkyl and hydridoaryl complexes that eliminate the respective hydrocarbons upon heating.[60,76-81] Scheme 9 summarizes the mechanistic picture that has emerged for these reactions at (diimine)Pt(II) systems[60,63,74,82-85] and at related Pt species with bidentate ligands.[66,86-94]

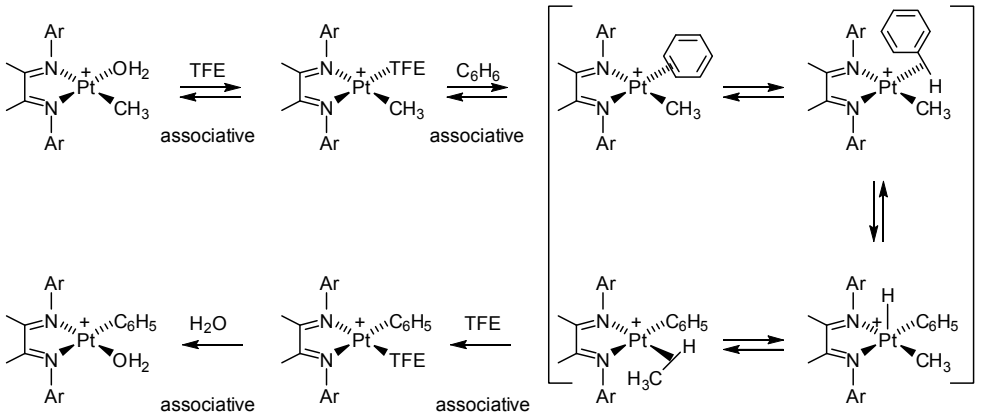

Scheme 9

Substitution of π-benzene for an aqua (or TFE) ligand occurs as a solvent assisted process for which there is controversy over an associative mechanism.[85,95-97] Although not observed during C-H activation experiments, the π-benzene complex was independently generated and observed by NMR at low temperatures.[60] From then the mechanism postulated is a Pt(II) oxidative insertion into a C-H bond of the π-benzene complex, presumably via an unobserved η^2-(C,H) benzene complex that proceeds with the oxidative cleavage. The resulting penta coordinate Pt(IV) species may be stabilized by coordinating a weakly bonded solvent molecule or proceed by C-H reductive coupling to yield σ–methane complex which finally furnishes the Pt(II) phenyl product by associative displacement of coordinated methane.

1.3.2 Protonolysis reaction of (Ar-DAB)$PtMe_2$

Further evidence of such postulated oxidative addition mechanism, was presented when studying the protonolysis reaction of (diimine)$PtMe_2$, where diimine = Ar-DAB = ArN=CMe-CMe=NAr, Ar = 2,6-$Me_2C_6H_4$, complex in acetonitrile solvent mixtures.[80] Protonation in acetonitrile solvent mixture led to the observation of (diimine)$PtMe_2H(NCMe)^+$ at low temperature. The intermediate suggested but didn't prove that the metal was the kinetic site of protonation. It could have been the thermodynamic product resulting from rapid protonation at a methyl to from the σ-methane intermediate followed by rapid oxidative cleavage and trapping by acetonitrile. Our group later elucidated the kinetic site of protonation using the competitive trapping methodology, Scheme 10.[76,79]

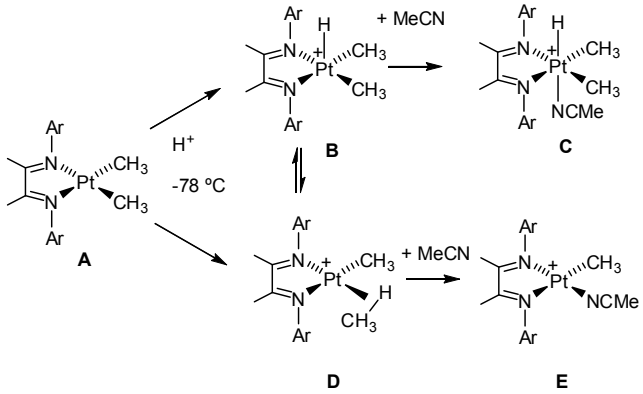

Scheme 10

It was reasoned that protonation might occur either at a coordinated methyl ligand to produce the σ-methane complex **D** or at the metal, and produce a pentacoordinate platinum(IV) hydride species **B**. Upon addition of a trapping agent, in this case acetonitrile, these species produce either the platinum(II) solvento complex **E** or the hexacoordinate platinum(IV) solvento complex **C**, respectively. The kinetically preferred site can be assessed provided that a [MeCN]-dependent product distribution is observed. Kinetic protonation at Pt should under such circumstances lead to a **C**/**E** ratio that increases with increasing [MeCN], whereas a kinetic preference for protonation at Ph should lead to a **C**/**E** ratio that decreases with increasing [MeCN]. Protonation of (diimine)$PtMe_2$ in dichloromethane-d_2 at -78 °C in the presence of MeCN led to mixtures of (diimine)$PtMe(NCMe)^+$ **E** and (diimine)$PtMe_2H(NCMe)^+$ **C**. Increasing concentrations of MeCN led to reduced **E**/**C** product ratios. This is consistent with protonation occurring at Pt rather than at a methyl group.[76]

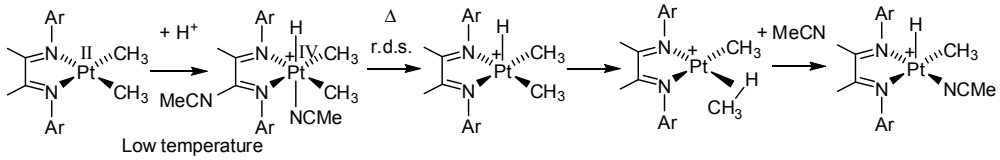

Scheme 11

The (diimine)$PtMe_2H(NCMe)^+$ intermediate is only stable at low temperature. The mechanism of the ensuing methane elimination was later investigated. It appeared to proceed by rate limiting acetonitrile dissociation, followed by reductive coupling and finally by associative methane substitution to yield (diimine)$PtMe(NCMe)^+$ according to Scheme 11.[80]

1.4. Aromatic C-H activation

1.4.1 Platinum scorpionate complex in arene C-H activation

Tremendous amounts of information have been collected on arene C-H activation by the use of Pt complexes with anionic Tp' ligand (Tp' = hydridotris(3,5-dimethylpyrazolyl)borate) also called scorpionate. This ligand is a strong electron donor that presents the additional particularity to be negatively charged and to be able to coordinate in a κ^3 fashion. Those characteristics have been exploited with success by Templeton's group to observe octahedral Pt(IV) dihydride complexes formed via arene C-H bond activation. In 2001, they even reported a X-Ray structure for the relatively stable π-benzene complex $[\kappa^2\text{-(Tp')Pt(H)}(\eta^2\text{-}C_6H_6)]^+$.[98] Templeton also described that related scorpionate Pt system: $[\kappa^2\text{-(HTp')Pt(Ph)}(\eta^2\text{-}C_6H_6)]$[BArf] (Tp'= hydridotris(3,5-dimethylpyrazole)borate), upon addition of a trapping agent such as a strongly coordinating acetonitrile ligand didn't lead to benzene substitution at low temperature but to the formation of a Pt(IV) hydrido complex, seen as the resultant of the oxidative C-H bond cleavage and trapping of the Pt hydride, Scheme 12.[99]

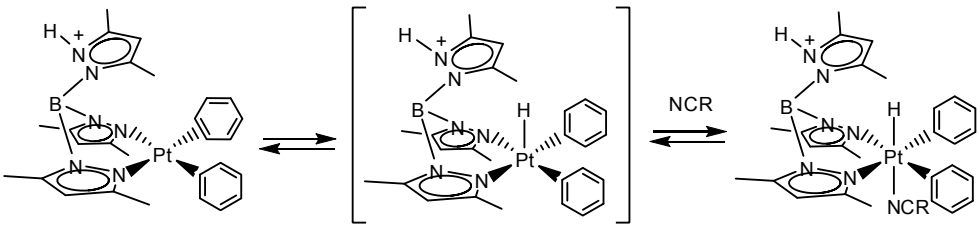

Scheme 12

The η^2-coordinated π-benzene complex, believed to be an important intermediate in aromatic C-H activation, exhibited dynamic NMR behaviour indicating intramolecular exchange reactions.[69] The dynamic process was demonstrated for the complex $[(\kappa^2\text{-(HTp')Pt}(C_6H_5)(\eta^2\text{-}C_6H_6)]^+$ causing an averaging of the protons signals between the phenyl and the coordinated benzene. These reports lead to the early assumption that the arene C-H activation, proceeded via oxidative addition, at electron-rich metal complex.

1.4.2 Intramolecular proton exchange at (Ar-DAB)PtPh(η^2-C_6H_6)$^+$ complexes

Our group reported that protonation of a series of (diimine)$PtPh_2$ complexes (diimine = Ar-N=CMe-CMe=N-Ar with differently substituted *N*-aryl groups) in dichloromethane at -78 °C resulted in the formation of (diimine)PtPh(η^2-C_6H_6)$^+$ complexes that were characterized by ^{1}H NMR spectroscopy.[81] A rapid site exchange of protons between the phenyl and π-benzene moieties was observed. The kinetics of the exchange processes were established by quantitative 2D EXSY NMR measurements. A rapid proton exchange that involved oxidative cleavage to furnish a putative (diimine)$PtPh_2H(L)^+$ intermediate (L = loosely coordinated ligand or vacant site) between each benzene ring and the metal site was originally postulated.[81] Such hexa-coordinated Pt hydrides were reported when protonation was conducted in coordinating solvent mixture of acetonitrile in dichloromethane, where the acetonitrile serves as an external ligand to stabilize the intermediate. The existence of penta coordinated Pt(IV) hydride has not been observed but Pt-alkyl analogues have been characterized.[38,98,100,101]

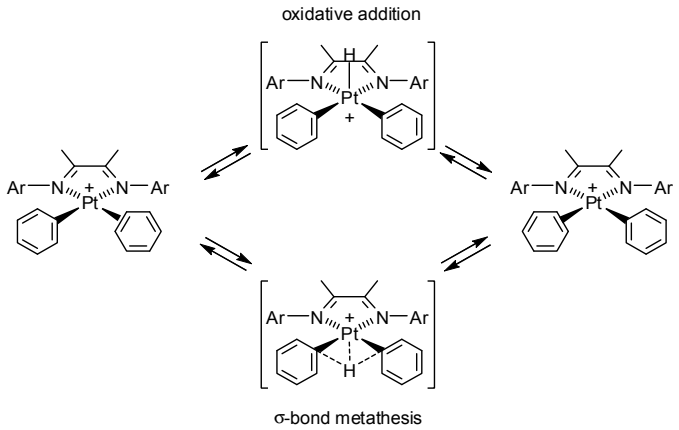

Scheme 13

The EXSY measurement did not offer clear evidence for any preferable mechanism, and the oxidative cleavage-reductive coupling mechanism was postulated. However, a direct proton transfer by a σ-bond metathesis (or σ-complex assisted metathesis, σ-CAM[63]) pathway was later described as "more likely" to occur based on DFT calculations.[102] The distinction between the two possibilities is of importance and will be addressed in details.

1.5. Methods and techniques used

Synthetic and analytic techniques used during this thesis are standard for organic and metal organic chemist, except for ^{195}Pt NMR and 2D EXSY NMR experiments that were introduced previously in our group.[81] IR spectra were recorded on a Perkin Elmer Spectrum One spectrometer. Elemental analyses were performed by Mikro Kemi AB, Uppsala, Sweden. Mass spectra were recorded on a Waters Micromass Q-TOF2W instrument. MS data are given as *m/z* values. Kinetic and thermodynamic data for mechanistic information have been acquired using less common temperature controlled NMR and stop-flow UV-vis spectroscopy. Experimental details are provided in the following.

1.5.1 NMR

NMR spectra were recorded on Bruker DPX200, DPX300, and DRX500 instruments. Deuterated solvents were used as received without further drying (CD_2Cl_2, Et_2O-d_{10}, CD_3CN). ^{1}H NMR chemical shifts (δ) are reported in parts per million (ppm) relative to TMS using the residual proton resonances of the solvent (δ 1.94 in CD_3CN, 5.32 in CD_2Cl_2). 2D ^{1}H,^{1}H-COSY and ^{1}H,^{1}H-NOESY NMR experiments were recorded on the Bruker DPX300 spectrometer equipped with a 5 mm QNP probe to help the assignments of ^{1}H NMR signals. ^{19}F NMR shifts (δ) are reported using CCl_3F as an internal reference.

^{195}Pt NMR shifts (δ) are referenced according to the 2001 IUPAC "unified scale" recommendation with Ξ = 21.496784.[103] All chemical shifts are reported such that lower frequencies give more negative shifts. ^{195}Pt NMR spectra were acquired with a 20 ms acquisition time and 500 ms relaxation time. Backward linear prediction to recalculate the 50 first points of the FID gave good baselines (Bruker settings: ME-mod = LPbc, ncoef = 200, Lpbin = 130, TDOFF = 50).

2D EXSY NMR was used according to published experimental protocol[81] using a Bruker pulse program (noesygpph) with a 900 ms mixing time and 1.5 s recycling time between scans.

The temperature calibration for the low-temperature experiments was done using a thermocouple situated inside a thin glass tube that was inserted into an NMR tube with methanol. Kinetics data extracted by this method were obtained by integration of a selected peak after normalization with the solvent peak at different times. Mathematical treatment of the integrated values as a function of time allows the determination of the rate law as k_{obs}.

1.5.2 Stopped-flow UV-vis spectroscopy

To study the progress of a reaction on a faster time scale than accessible by NMR, UV-vis spectroscopy was used. The basic component of a stop-flow UV-vis spectrometer is a rapid-scan UV-vis instrument with a flow-cell immersed in a cooling medium. Low temperature kinetic data can be obtained by recording time resolved UV-vis spectra using a stopped flow module in combination with cryo-stopped-flow accessories. UV-vis spectra were recorded on Shimadzu UV-2102 and Hewlett Packard 8542A spectrophotometers. Low-temperature kinetic data were obtained by recording time-resolved UV-vis spectra using a modified Bio-Logic stopped-flow module μSFM-20 combined with a cryo-stopped-flow accessory (Huber CC90 cryostat) equipped with a J & M TIDAS high-speed diode array spectrometer with a combined deuterium and tungsten lamp (200-1015 nm bandwidth). Isolast "O" rings were used for all sealing purposes. The acquired data is the processed and analyzed by suitable Bio-Kine software packages version 4.44, software package Specfit/32 global analysis program to extract the rates of the reactions measured. If the reaction is dissociative, the rate limiting step will involve increased volume. High pressure will counteract the volume increase, and slow the reaction down. If the volume of activation is negative, the reaction rate ill increase at high pressure. In this work, measurements under high pressure were made using an in-house constructed high pressure stop-flow instrument.[104,105] The values of $\Delta H^{\#}$ and $\Delta S^{\#}$ are obtained by calculation from the slope and intercepts of Eyring plots (ln(k/T) versus 1/T), respectively. The $\Delta V^{\#}$ is calculated from the slope of plots of ln(k) versus pressure.[106]

1.6. Scope

In Chapter 2, a mechanistic study of the protonolysis reaction of (Ar-DAB)$PtPh_2$ complex is presented. This report allows direct comparison with dimethyl analogues complexes already reported by our group and permits the refinement and reinterpretation of mechanistic issues from previously published studies.

Chapter 3 deals with the synthesis and characterization of new (Ar-BIAN)$PtPh_2$ and (Ar-BICAT)$PtPh_2$ complexes. A qualitative description of the protonolysis events is presented. Key element to appreciate the diimine ligand steric and electron-tuning properties and there relative influence on the complex reactivity are presented. New evidences that confirm our mechanistic proposal are presented and discussed. A comprehensive mechanistic

investigation of the protonolysis reaction for these new diimine complexes is presented in Chapter 4.

In Chapter 5, a study of the protonolysis reaction of two (Ar-BIAN)$PtPh_2$ complexes in ether dichloromethane solvent mixtures by UV-vis spectroscopy is presented.

2. Combined low temperature rapid scan and ^{1}H NMR mechanistic study of the protonation and subsequent benzene elimination from a (diimine)platinum(II) diphenyl complex

The following chapter describes the results of a detailed kinetic study of the two successive protonation and ensuing benzene elimination reactions from (Ar-DAB)$PtPh_2$ **1a.** This complex was chosen to allow direct comparison with the dimethyl analogue complex mentioned in Chapter 1, and to assess the similarities and differences in behavior between methane and benzene C-H activation mechanism.

2.1. Introduction

Our group has presented a detailed account of the kinetics of the rapid protonation of (Ar-DAB)$PtMe_2$ by $HBF_4{\cdot}Et_2O$ to provide the Pt(IV) complex (Ar-DAB)$PtMe_2H(NCMe)^+$ and the subsequent elimination of methane from this Pt(IV) complex.[80] The latter reaction was found to proceed by initial and rate-limiting MeCN dissociation. In this chapter, we present the details of kinetic studies of protonation reactions and benzene-producing reactions at Pt(II) and Pt(IV) species that are derived from (Ar-DAB)$PtPh_2$ **1a**. Concentration, temperature, and pressure-dependent kinetic measurements allow us to evaluate the kinetics for most of the cascade of reactions that are depicted in Scheme 1.

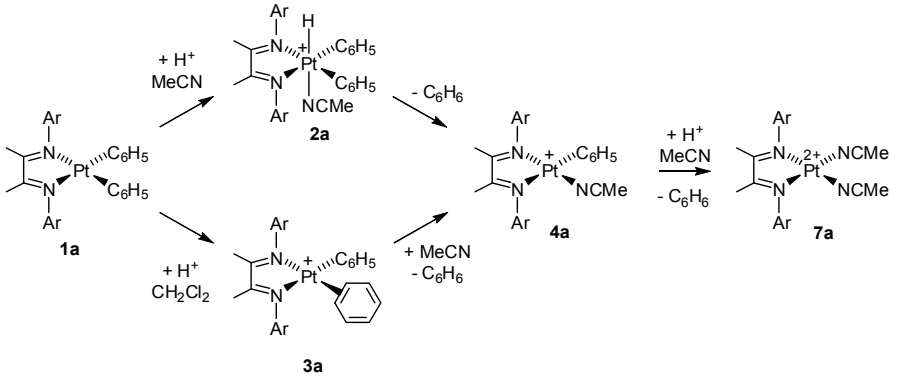

Scheme 1. Sequence of reactions studied in this contribution. Kinetic studies have been performed for all reactions except the lower-left protonation reaction.

2.2. Results

2.2.1 Protonation of (Ar-DAB)$PtPh_2$ in the presence of MeCN

The protonation of (Ar-DAB)$PtPh_2$ **1a** with $HBF_4{\cdot}Et_2O$ in mixtures of dichloromethane-d_2 and acetonitrile-d_3 was previously studied by ^{1}H NMR spectroscopy,[81] and provides (Ar-DAB)$PtPh_2H(NCMe)^+$ **2a** as indicated in Scheme 1. While this Pt(IV) species is stable at -78 °C, benzene is released at ca. -40 °C with concomitant formation of (Ar-DAB)$PtPh(NCMe)^+$ **4a** with no detectable intermediates. When TfOH in acetonitile (expected to be a stronger acid than $HBF_4{\cdot}Et_2O$;[107] protonated Et_2O rather than HBF_4 is here the actual proton source) is employed, a second elimination of benzene is seen at ambient temperature, producing the Pt(II) dication (Ar-DAB)$Pt(MeCN)_2^{2+}$ **7a**. The same species was recently obtained from two successive protonation/methane elimination sequences from (Ar-DAB)$PtMe_2$ and TfOH.[108] This reaction sequence has been subjected to a systematic kinetic investigation by time-resolved stopped-flow techniques with UV-vis monitoring of the reaction, with $HBF_4{\cdot}Et_2O$ or TfOH as acids, in solution mixtures of acetonitrile in dichloromethane, in the temperature range -80 °C to +27 °C. The same three-step sequence was clearly observed by NMR and by UV-vis stopped-flow spectroscopic methods.

The first reaction step, the protonation of (Ar-DAB)$PtPh_2$, was carefully studied by ^{1}H NMR at -78 °C in acetonitrile-d_3 /dichloromethane-d_2 mixtures of different compositions. In all cases, (Ar-DAB)$PtPh_2$ **1a** reacted promptly to give mostly (Ar-DAB)$PtPh_2H(NCMe)^+$ **2a**, with trace quantities (ca. 2-10 %) of (Ar-DAB)$PtPh(NCMe)^+$ **4a** and benzene. There was no clear trend in the relative quantities of (Ar-DAB)$PtPh(NCMe)^+$ as a function of [MeCN] in the range 0.27-8.7 M. This contrasts with the findings from analogous experiments in which the protonation of (diimine)$PtMe_2$ complexes were studied: a consistent decrease in the yield of (diimine)$PtMe(NCMe)^+$, relative to (diimine)$PtMe_2H(NCMe)^+$, with increasing [MeCN] present was taken as evidence that the metal, rather than the methyl ligand, was the kinetically preferred site of protonation (see chapter 1).[76,79] The lack of a clear-cut trend in the present system renders this question unresolved for the time being concerning the protonation of (Ar-DAB)$PtPh_2$. The presence of both products might indicate that two reaction channels are available. In the absence of other, more conclusive evidence, we surmise that the fact that (Ar-DAB)$PtPh_2H(NCMe)^+$ **2a** is the predominant product suggests (but does not prove) that

protonation at the metal is kinetically preferred. This assumption is supported by recent DFT calculations.[102] This subject will be further addressed in the Discussion section.

The protonation event was monitored in the temperature range -80 to -50 °C by time-resolved UV-vis stopped-flow spectroscopy. The concentrations of acid and acetonitrile in the dichloromethane solvent were systematically changed at -80 °C, always in a large excess relative to (Ar-DAB)$PtPh_2$ so as to ensure pseudo-first-order conditions. The protonation results in a characteristic decay in absorbance, and the changes observed in a typical time-resolved experiment are depicted in Figure 1. The spectral changes could in all cases be nicely fitted to a pseudo-first-order decay. The resulting pseudo-first-order rate constant was independent of [MeCN] in the range 0.95-5.7 M (5 to 30 % v/v). Lower [MeCN] could not be used due to the poor solubility of the acid in dichloromethane at low temperatures. The dependence of the pseudo-first-order rate constant on [$HBF_4{\cdot}Et_2O$] (8.8-37.2 mM) at -80 °C in the presence of 30% (v/v) MeCN is shown in Figure 2. Clearly, a first-order dependence is seen and the calculated second-order rate constant by linear regression gives k (-80 °C) = 290 ± 20 M^{-1} s^{-1}.

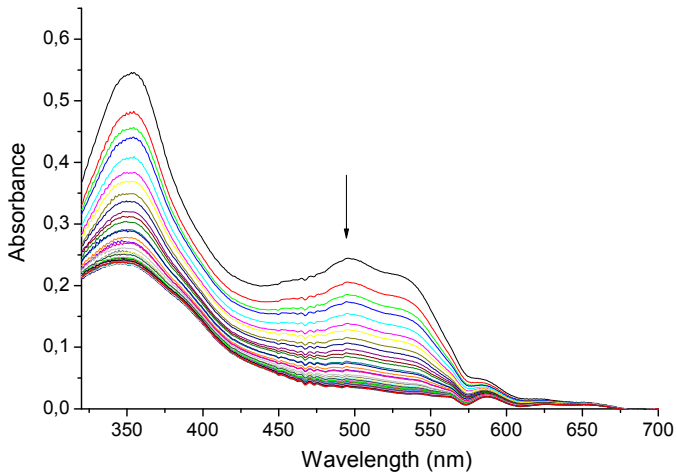

Figure 1. Time-resolved spectra for the protonation of **1a** with $HBF_4{\cdot}Et_2O$ in dichloromethane at -80 °C. Experimental conditions: [Pt] = 0.125 mM, [MeCN] = 5.74 M (30 % v/v), [$HBF_4{\cdot}Et_2O$] = 0.0124 M. The total duration of the experiment was 3.0 s.

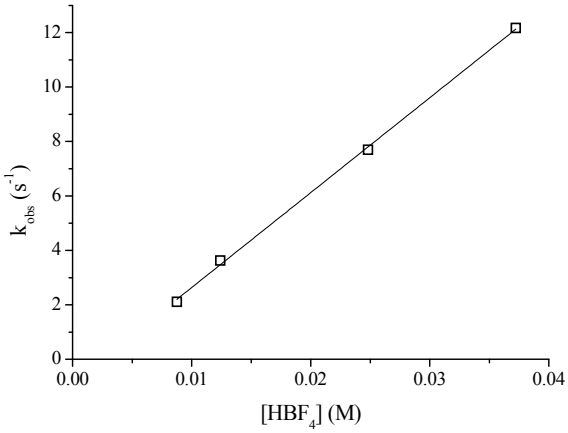

Figure 2. k_{obs} vs [HBF_4·Et_2O] for the protonation of **1a** in CH_2Cl_2 at -80 °C. [Pt] = 0.125 mM, [MeCN] = 5.74 M (30% v/v).

The temperature dependence of the rate constant for protonation was measured by monitoring the reaction of (Ar-DAB)$PtPh_2$ with a 12.4 mM HBF_4·Et_2O solution in dichloromethane-30 % MeCN (v/v; 5.74 M) in the temperature range -80 °C to -50 °C. The Eyring plot in Figure 3 shows an excellent linear fit, and the resulting kinetic parameters are k(-80 °C) = 290 ± 20 M^{-1} s^{-1}, $\Delta H^{\#}$ = 28.8 ± 0.8 kJ mol^{-1} and $\Delta S^{\#}$ = -47 ± 4 J K^{-1} mol^{-1}.

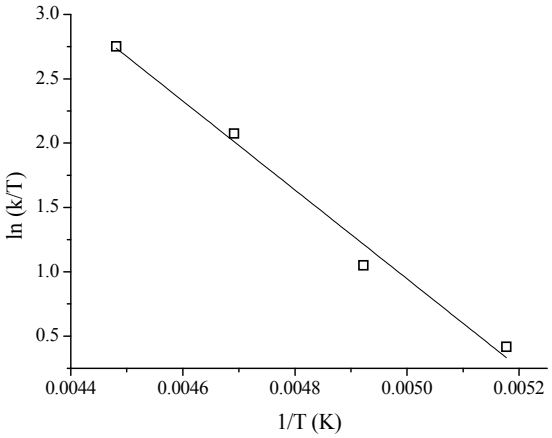

Figure 3. Eyring plot for the protonation of **1a** with HBF_4·Et_2O in CH_2Cl_2. Experimental conditions: [Pt] = 0.125 mM, [MeCN] = 5.74 M (30 % v/v), [HBF_4·Et_2O] = 0.0124 mM.

The protonation has a rather small $\Delta H^{\#}$ and substantially negative $\Delta S^{\#}$ under the studied conditions. This is in accordance with the associative nature of the reaction. These data may be compared with our previously published data[80] on the protonation of (N–N)-$PtMe_2$, viz. $\Delta H^{\#} = 15$ kJ mol^{-1} and $\Delta S^{\#} = -85$ J K^{-1} mol^{-1} were determined and are suggestive of an associative mechanism. The rate constant was reported as 15200 ± 400 M^{-1} s^{-1} at -78 °C. Protonation of the present (Ar-DAB)$PtPh_2$ system appears to be about 40 times slower than protonation of (Ar-DAB)$PtMe_2$ at -78 °C. This may reflect a combined effect of the relative electron withdrawing effect of Ph vs. Me at the metal center and the increased steric bulk of Ph vs. Me. It was suggested that (Ar-DAB)$PtMe_2$ underwent rate-determining protonation to yield a transient five-coordinate species which was rapidly trapped by the apical coordination of MeCN. We assume on the basis of the kinetic data and qualitative similarities (acid and MeCN dependence) that the same holds true for the current system, although a concerted protonation/acetonitrile addition cannot be ruled out on the basis of the available experimental evidence.

2.2.2 Elimination of benzene from (Ar-DAB)$PtPh_2H(NCMe)^+$

Upon warming to temperatures above ca. -40 °C, (Ar-DAB)$PtPh_2H(NCMe)^+$ **2a** starts to release benzene to cleanly furnish (Ar-DAB)$PtPh(MeCN)^+$ **7a** without detectable intermediates, as previously seen by ^{1}H NMR spectroscopy.[81] In the following, we describe the details of a kinetic investigation of this process in the temperature range -10 to +27 °C. The stopped-flow technique allows instant mixing of separately prepared solutions of (Ar-DAB)$PtPh_2$ and $HBF_4{\cdot}Et_2O$ in dichloromethane/acetonitrile mixtures to immediately furnish (Ar-DAB)$PtPh_2H(NCMe)^+$. The ensuing, much slower, benzene elimination can be conveniently monitored by UV-vis spectroscopy at varying [HBF_4], [MeCN], temperatures and pressures. A typical time-resolved UV-vis spectrum of the reaction is depicted in Figure 4 and is characterized by an increase in absorbance in the selected wavelength region with time. The spectral changes are nicely described by first-order kinetics. The kinetic measurements were done by monitoring the spectral changes over the whole spectral range. The excellent first-order kinetic fits that were obtained suggest the smooth transformation of (Ar-DAB)-$PtPh_2H(NCMe)^+$ **2a** to (N–N)$PtPh(NCMe)^+$ **7a** without any observable intermediates.

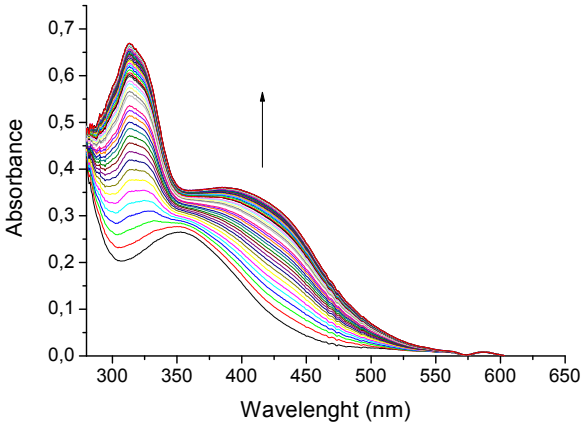

Figure 4. Time-resolved spectra for the elimination of benzene from **2a** in dichloromethane at 0 °C. Experimental conditions: [Pt] = 0.125 mM, [MeCN] = 5.74 M (30 % v/v), [$HBF_4{\cdot}Et_2O$] = 12.4 mM. The total duration of the experiment was 35 s.

The rate of the reaction was studied at different acetonitrile concentrations. In the concentration range 0.95 to 5.7 M, only a slight effect of [MeCN] on the rate of benzene elimination was seen (ca. 20 % rate increase in the concentration range). The kinetics of the benzene elimination were also evaluated at varying [$HBF_4{\cdot}Et_2O$] in dichloromethane containing acetonitrile (5.7 M, 30 % v/v) at 27 °C. No significant effect of the acid concentration on the reaction rate could be discerned.

Variable-temperature kinetic measurements of the benzene elimination were done by recording the time-resolved UV-vis spectra during the elimination of benzene when the initial protonation was done with 12.4 mM $HBF_4{\cdot}Et_2O$ in dichloromethane containing 5.74 M MeCN (30 % v/v) in the temperature range -10 to +20 °C. Figure 5 shows an Eyring plot of the kinetic data, from which the following kinetic parameters were extracted: k (20 °C) = 2.3 s^{-1}, $\Delta H^{\#}$ = 88 ± 2 kJ mol^{-1} and $\Delta S^{\#}$ = +62 ± 6 J K^{-1} mol^{-1}.

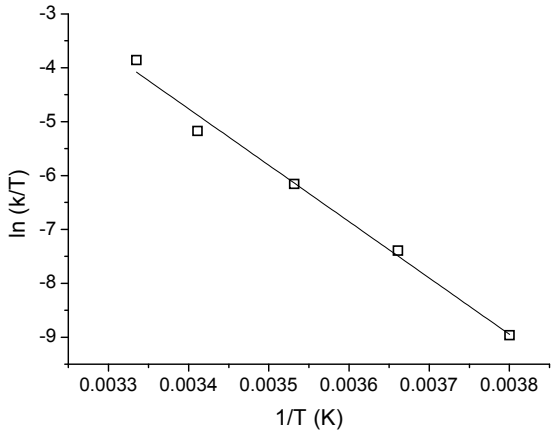

Figure 5. Eyring plot for the kinetic data for the elimination of benzene from **2a** when $HBF_4{\cdot}Et_2O$ was the acid used to initially protonate **1a** (see text). Experimental conditions: [Pt] = 0.125 mM, [MeCN] = 5.7 M (30% v/v), [HBF_4] = 0.0124 M.

Finally, pressure-dependent kinetic measurements were performed for benzene elimination at pressures between 10 and 125 MPa at 20 °C. The volume of activation $\Delta V^{\#}$ was calculated for the reaction from the slope of plots of ln *k* vs pressure (Figure 6) in the way that has been previously thoroughly described,[106] using a 0.125 mM solution of (Ar-DAB)$PtPh_2$ and 0.0062 M $HBF_4{\cdot}Et_2O$ in dichloromethane with 5.7 M MeCN (30 % v/v). The good linear fit that is evident from Figure 6 provides an activation volume $\Delta V^{\#} = +16 \pm 2$ cm^3 mol^{-1}.

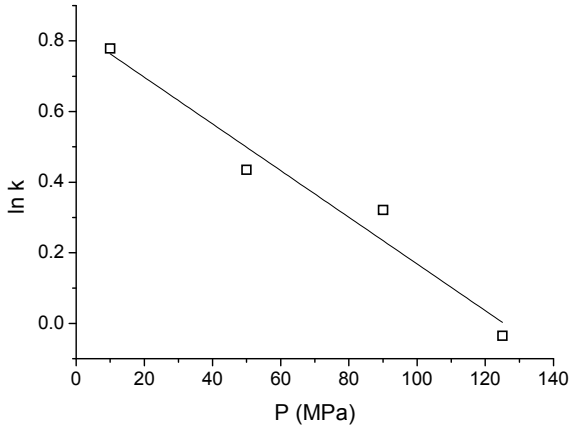

Figure 6. Pressure-dependent rate constants for the elimination of benzene from **2a** at 20 °C. Experimental conditions: [Pt] = 0.125 mM, [MeCN] = 5.7 M (30 % v/v), [$HBF_4{\cdot}Et_2O$] = 0.0062 M.

In summary, the kinetics for the benzene elimination from (Ar-DAB)$PtPh_2H(NCMe)^+$ **2a** exhibits a rather high $\Delta H^{\#}$, a large positive $\Delta S^{\#}$, and a large positive $\Delta V^{\#}$. The collective data strongly suggest a dissociative character of the rate-limiting step, believed to be acetonitrile dissociation, for the benzene elimination. The data are qualitatively similar to those determined[80] for the elimination of methane from (Ar-DAB)$PtMe_2H(NCMe)^+$, for which $\Delta H^{\#} = 75 \pm 1$ kJ mol^{-1}, $\Delta S^{\#} = +38 \pm 5$ J K^{-1} mol^{-1} and $\Delta V^{\#} = +18 \pm 1$ cm^3 mol^{-1}, and for which a mechanism that is dissociative with respect to MeCN was proposed.

2.2.3 The second protonation and benzene elimination

As mentioned in the Introduction, (Ar-DAB)$PtPh_2$ **1a** reacts with TfOH in acetonitrile at ambient temperature to immediately furnish (Ar-DAB)$PtPh(NCMe)^+$ **4a** and then, more slowly, the (Ar-DAB)$Pt(NCMe)_2^{2+}$ dication **7a**. Analogous behavior has been reported for (diimine)$PtMe_2$ species, where treatment with TfOH can ultimately lead to the dicationic Pt complexes.[108]

The kinetics for this protonation/benzene elimination reaction was pursued with the stopped-flow UV-vis spectroscopic method in dichloromethane/acetonitrile mixtures. At 25 °C, the time-resolved UV-vis spectra (Figure 7) show characteristic absorption bands decaying in intensity at 320 and 430 nm, and bands of increasing intensity at 280 and 350 nm. Three well-defined isosbestic points are seen at 300, 346 and 360 nm. The first spectrum is that of (Ar-DAB)$PtPh(NCMe)^+$ **4a** and the last matches that of (N–N)$Pt(NCMe)_2^{2+}$ **7a**, and the isosbestic points establish that no detectable intermediates build up during the reaction. The reaction rate was extracted from the changes in absorbance at 410 nm, and the data were nicely described by a single exponential decay suggestive of pseudo first-order kinetic behavior in [Pt].

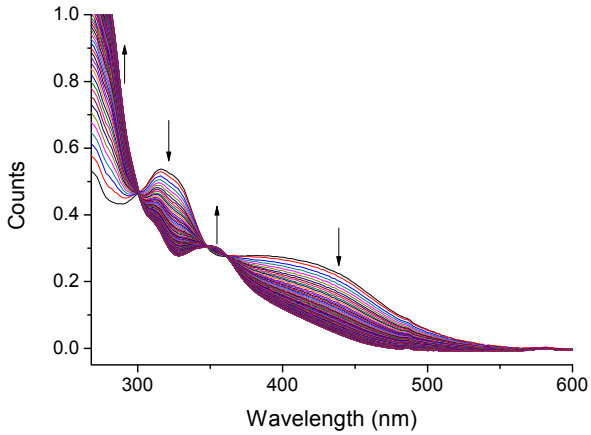

Figure 7. Time-resolved UV-vis spectra for the protonation/benzene elimination sequence from (Ar-DAB)$PtPh_2$ **1a** in dichloromethane/acetonitrile at 25 °C. Experimental conditions: [Pt] = 0.125 mM, [MeCN] = 5.74 M (30 % v/v, [TfOH] = 0.013 M. The total duration of the experiment was 30 min.

The kinetics were further evaluated by UV-vis monitoring of the reaction at 25 °C in order to study the influence of acid concentration on this step by varying [TfOH] in the range 0.013-0.13 M. In each case, the reaction exhibited pseudo-first-order kinetic behavior, and the observed rate increased linearly with [TfOH], Figure 8. Thus, the reaction is first-order with respect to the acid, analogous to the first protonation of (Ar-DAB)$PtPh_2$ **1a** at low temperatures. From the slope of the plot in Figure 8, the second-order rate constant for the protonation was determined as 0.38 ± 0.03 M^{-1} s^{-1} at 25 °C. Interestingly, when $HBF_4{\cdot}Et_2O$ was used as the acid (129 mM), the pseudo-first-order rate constant was estimated to be as low as 3×10^{-5} s^{-1} corresponding to 2.3×10^{-4} M^{-1} s^{-1}. The significantly slower reaction is in accord with $HBF_4{\cdot}Et_2O$ being a considerably weaker acid than TfOH.[109]

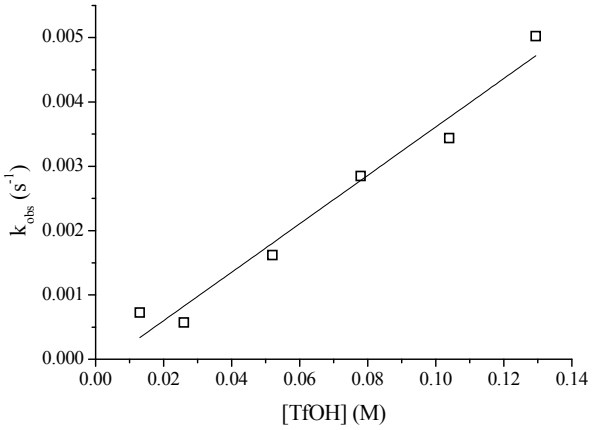

Figure 8. k_{obs} vs [TfOH] for the second protonation/elimination sequence in dichloromethane. Experimental conditions: [Pt^{II}] = 0.125 mM, [MeCN] = 5.74 M (30 % v/v) and T = 25 °C.

Variable-temperature kinetic measurements of the protonation/benzene elimination were done by recording the time-resolved UV-vis spectra for the reaction with 0.13 M TfOH in dichloromethane containing 5.74 M MeCN (30 % v/v) in the temperature range 7- 29 °C. The Eyring plot in Figure 9 shows an excellent linear fit and gives the kinetic parameters: k (25 °C) = 0.033 M^{-1} s^{-1}, $\Delta H^{\#}$ = 68.5 ± 1.0 kJ mol^{-1} and $\Delta S^{\#}$ = -43 ± 3 J K^{-1} mol^{-1}.

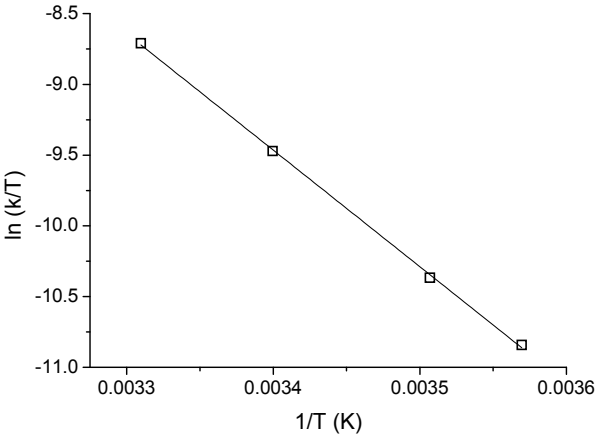

Figure 9. Eyring plot for the kinetic data for the second protonation/benzene elimination sequence from (Ar-DAB)$PtPh_2$ **1a**. Experimental conditions: [Pt] = 0.125 mM, [MeCN] = 5.74 M (30 % in vol), [TfOH] = 0.13 M in dichloromethane.

2.2.4 Substitution of benzene on (Ar-DAB)PtPh(η^2-C_6H_6)$^+$ by acetonitrile in dichloromethane

A solution of the π-benzene complex (Ar-DAB)PtPh(η^2-C_6H_6)$^+$ **3a** in dichloromethane-d_2 was prepared in situ in an NMR tube by addition of $HBF_4{\cdot}Et_2O$ to a solution of (Ar-DAB)$PtPh_2$ **1a** at -78 °C. Controlled quantities of acetonitrile-d_3 in excess (to ensure pseudo first-order conditions) were added at -78 °C, and the NMR tube was inserted into the pre-cooled NMR probe so that the progress of the ensuing reaction could be monitored by ^{1}H NMR. At the temperatures investigated, smooth release of benzene and the formation of (Ar-DAB)PtPh($NCCD_3$)$^+$ was observed. The rate of the reactions was determined by integration of the Pt-Ph signals in the NMR spectra using the residual proton signals of the solvent as an internal standard. The disappearance of the starting complex exhibited first-order kinetics for at least 3-4 half-lives of the reaction. The pseudo first-order rate constant varied linearly with [acetonitrile-d_3], as illustrated in Figure 10. The near-zero intercept, $(-6 \pm 7) \times 10^{-5}$ s^{-1}, suggests that there is no MeCN-unassisted mechanism operating in parallel with the associative one implied by the data. The average second-order rate constant was determined from these data as $k = (5.70 \pm 0.05) \times 10^{-4}$ M^{-1} s^{-1} at -55 °C.

Importantly, there was no evidence for formation of the Pt(IV) hydrido complex (Ar-DAB)$PtPh_2H(NCCD_3)^+$ in these experiments. This compound, if it were formed, would have been stable under the reaction conditions on the experimental timescale. In a separate experiment, EXSY spectra were recorded of (Ar-DAB)PtPh(η^2-C_6H_6)$^+$ **3a** were recorded in dichloromethane-d_2 in the absence of acetonitrile-d_3 and in the presence of 0.054 M acetonitrile-d_3.[110] In both cases, the EXSY correlation peaks between phenyl and π-benzene signals were seen, as described previously, and with intensities that were independent of the presence (or not) of acetonitrile. These findings provide compelling evidence that the exchange processes seen by EXSY cannot proceed via the intermediacy of (Ar-DAB)$PtPh_2H^+$, which – if formed – should have been efficiently trapped by acetonitrile to furnish the stable, readily observable (N–N)$PtPh_2H(NCCD_3)^+$.

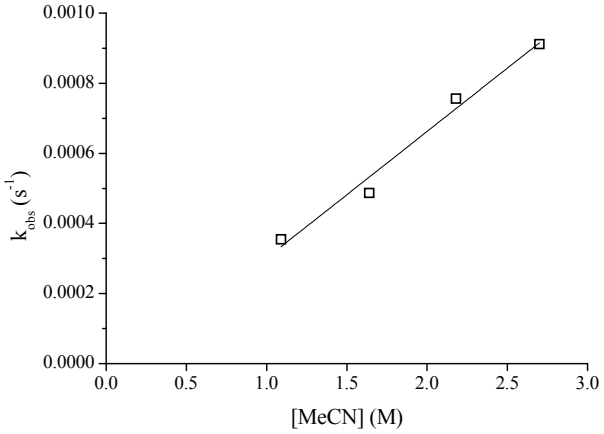

Figure 10. k_{obs} vs $[CD_3CN]$ for the substitution of benzene at (Ar-DAB)PtPh$(C_6H_6)^+$ **3a** in dichloromethane-d_2. Experimental conditions: [Pt] = 0.023 mM, [MeCN] = 5.7 M (30% v/v), T = -55 °C. $HBF_4{\cdot}Et_2O$ was used for in situ protonation of **1a** before addition of CD_3CN.

The temperature dependence of the substitution of benzene by acetonitrile was evaluated in the temperature range -55 to -70 °C. Figure 11 shows a linear Eyring plot of the kinetic data. The derived activation parameters are $\Delta H^{\#} = 39 \pm 2$ kJ mol^{-1} and $\Delta S^{\#} = -126 \pm 11$ J K^{-1} mol^{-1}. The substantially negative entropy of activation and the first-order kinetic behavior of the rate on [MeCN] strongly implies an associative benzene substitution by acetonitrile. This is in agreement with recent DFT calculations which suggest a solvent-induced associative benzene elimination.[102]

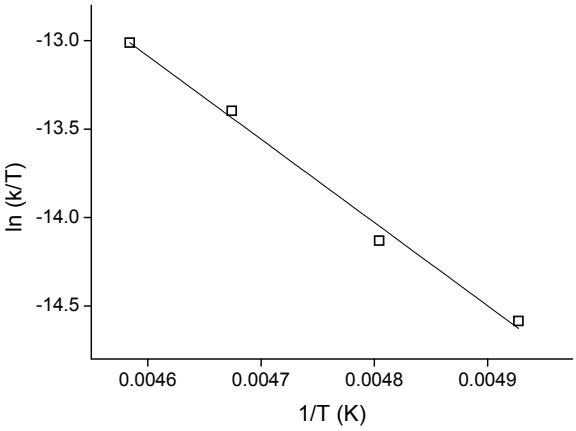

Figure 11. Eyring plot for the kinetic data for the substitution of benzene with acetonitrile at (Ar-DAB)PtPh$(C_6H_6)^+$ **3a** when $HBF_4{\cdot}Et_2O$ was the acid used for the in situ protonation of **1a** before addition of acetonitrile-d_3 to the solution in dichloromethane-d_2. Experimental conditions: [Pt] = 0.023 M, [MeCN] = 2.7 M, $[HBF_4]$ = 0.10 M.

2.3. Discussion

The accumulated kinetic and mechanistic results that have been presented are consistent with the overall reaction mechanism that is shown in Scheme 2 for the protonation of (Ar-DAB)$PtPh_2$ (**A**) and the following benzene-producing reactions. The details of this mechanism will now be the subject of discussion. It will be useful in this context to consult the data in Table 1, which lists rate constants for each step (where available). The data have been determined from the activation parameters described in the Results Section or from data available elsewhere, at the temperatures -78, -40, 0 and +30 °C.

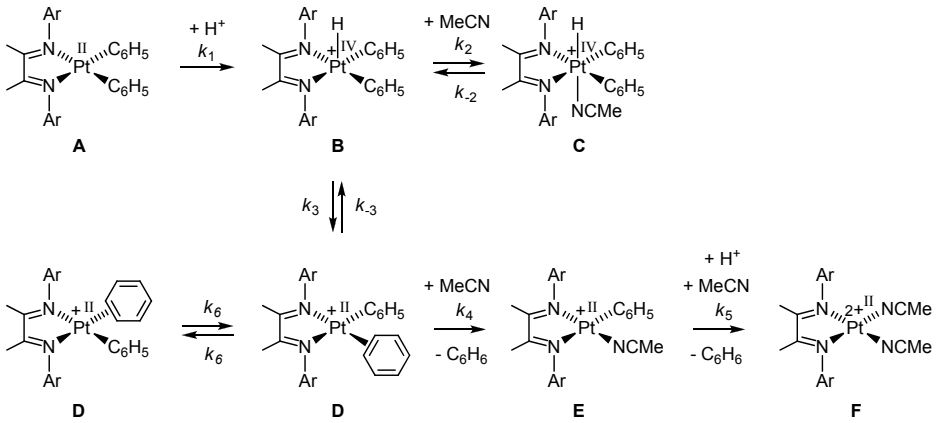

Scheme 2. Proposed mechanistic scheme for the benzene producing reactions under study.

2.3.1 Low-Temperature Protonation of (Ar-DAB)$PtPh_2$.

The protonation of the substrate **A** in dichloromethane/acetonitrile, observed as a fast reaction even at -80 °C, is postulated in Scheme 2 to occur as a two-step process that initially generates the unobserved five-coordinate intermediate (N–N)$PtPh_2H^+$ (**B**) followed by rapid capture of MeCN at the remaining vacant site. A concerted protonation and MeCN coordination cannot be ruled out, as stated in the Results Section. The protonation is slower than that at the analogous (N–N)$PtMe_2$ complex by a factor of ca. 40 at -78 °C under comparable conditions. The difference may be attributed to a combination of the increased steric bulk and decreased donor power of the phenyl ligands vs. the methyl ligands at Pt.

Table 1. Summary of approximate, available first-order or pseudo first-order rate constants (s^{-1}) for the reactions in Scheme 2 at selected temperatures[a]

Temperature	-78 °C	-40 °C	0 °C	+30 °C
$k_1[H^+]$[b]	3.5	75	770	3000
k_{-2}[c]	2.0×10^{-8}	0.00016	0.15	7.5
k_{-3}[d]	$< 5.6 \times 10^{-5}$	< 0.078	< 18	< 430
k_4[MeCN][e]	0.00011	0.0063	0.14	0.85
$k_5[H^+]$[f]	1.0×10^{-9}	1.3×10^{-6}	0.00027	0.0060
k_6[g]	5.6×10^{-5}	0.078	18	430

[a] Data are derived from activation parameters determined in this study unless otherwise noted. [b] Second-order rate constant derived from the low-temperature protonation kinetics multiplied by [HBF_4] taken as 0.0124 M. [c] First-order rate constant derived from the kinetics of benzene elimination from (N–N)$PtPh_2H(NCMe)^+$, assuming rate-determining MeCN dissociation. [d] An upper limit to the value for k_{-3} is given by k_6, see text. [e] Second-order rate constant derived from the benzene substitution kinetics multiplied by [MeCN] taken as 2.7 M. [f] Second-order rate constant derived from the high-temperature protonation kinetics multiplied by [TfOH] taken as 0.13 M. [g] First-order rate constant derived from kinetic data for H/H site-exchange between the phenyl and benzene ligands in (N–N)$Pt(C_6H_5)(\eta^2\text{-}C_6H_6)^+$, see ref [81].

One important question regarding the protonation event is whether the kinetically preferred site of protonation is the metal (rate constant k_{Pt}) or a phenyl ligand (k_{Ph}), see Scheme 3. A similar scheme was the basis for our analysis of the kinetically preferred site of protonation at (diimine)$PtMe_2$ complexes.[79,111] It was concluded that Pt protonation was preferred in that case. In the present context, protonation at Pt produces the five-coordinate intermediate **B**, which will furnish the observed product **C** when trapped by MeCN in the dichloromethane/acetonitrile medium**.** On the other hand, protonation at a phenyl group produces the π-benzene complex **D** which is the observed product in dichloromethane when the protonation is conducted in the absence of MeCN. Despite these observations, protonation at a phenyl group might be kinetically preferred even in the presence of MeCN, provided that the rate of interconversion between **B** and **D**, k_{RC} and k_{OC}, is fast relative to the rates of each of the product forming steps, k_{trap}[MeCN] and k_{subst}[MeCN], both of which are first-order with

respect to [MeCN] (RC denotes "reductive coupling" and OC "oxidative cleavage" as suggested elsewhere[64]). As argued in the case of protonation at (diimine)$PtMe_2$,[79,111] the kinetically preferred site can be assessed provided that a [MeCN]-dependent product distribution is observed (see Chapter 1). The experimental results established that over the [MeCN] range 0.27-8.18 M, more than 90 % of **C** was always produced at -78 °C; traces of **E** were always seen but there was no systematic trend in the **C**/**E** ratio with changes in [MeCN]. A **C**/**E** ratio that appears to be independent of [MeCN] can be explained by two possible scenarios based on Scheme 5: (i) Competing protonation at Pt and Ph with a strong preference for the former ($k_{Pt} > k_{Ph}$), combined with slow rates of interconversion k_{RC} and k_{OC}. The **C**/**E** ratio simply reflects the relative k_{Pt}/k_{Ph} rates. (ii) Protonation to give **B** and/or **D** followed by fast interconversion rates and much slower product-forming steps. The **C**/**E** ratio then depends on the relative k_{trap}/k_{subst} rates and the equilibrium constant for the **B**/**D** interconversion (Curtin-Hammett conditions[112]). The latter explanation can be readily ruled out in our case: The kinetic data in Table 1 clearly show that at -78 °C, an upper limit to the rate of interconversion, determined experimentally from the rates of proton exchange between phenyl and η^2-benzene ligands in (Ar-DAB)PtPh$(\eta^2\text{-}C_6H_6)^+$ complexes (see next paragraph), is orders of magnitude slower than the rate of production of **C** in the protonation reaction. Therefore, **C** cannot be produced via protonation at Ph to give **D** followed by oxidative cleavage to furnish **B**. Consequently, we conclude that the kinetically preferred site of protonation in this system has to be the metal, furnishing the Pt(IV) hydride, rather than a phenyl ligand, to furnish the η^2-benzene complex (however, an *ipso* protonation leading to an unobserved η^1-benzene structure, possibly resembling a Wheland-type intermediate, cannot be ruled out). Similar arguments were used to arrive at the same conclusion in a recent DFT study.[102] The trace quantities of **E** observed at -78 °C might suggest that protonation at Ph to furnish **D** is slightly competitive with the predominant protonation at Pt. On the other hand, the data in Table 1 suggest that substitution of η^2-C_6H_6 by MeCN in **D** should be exceedingly slow compared to the overall rate of protonation at -78 °C, and therefore **E** should not have time to form by this pathway at all on the experimental time scale. We must consider that the traces of **E**, which were observed by ^{1}H NMR but not under UV-vis kinetics conditions (under which traces would be difficult to detect), might be caused by experimental artifacts that are currently beyond our control.

In order that a clear trend be observed in the product distribution when the trapping agent concentration is changed, a relatively delicate balance must exist between the relative rates of the two trapping reactions and the rates of interconversion between the intermediates

that will be trapped. Apparently, the requirements concerning relative rates were met during the protonation of (Ar-DAB)$PtMe_2$ species,[111] but not in the present case. An offset of one of the rates by an order of magnitude or so might be sufficient to prevent the observation of the sought-after trend. We note that in the present case, the steric bulk of the phenyl ligands may retard the trapping by MeCN, but would also similarly affect the rate of associative hydrocarbon substitution. Another significant difference is that benzene is associatively displaced in the present case vs. methane in the former,[111] and that the barriers to reductive cleavage/oxidative coupling tend to be lower for sp^2 C-H bonds. Altogether, it is not obvious to us exactly which of the effects on the relative rates that causes the difference in experimental outcome.

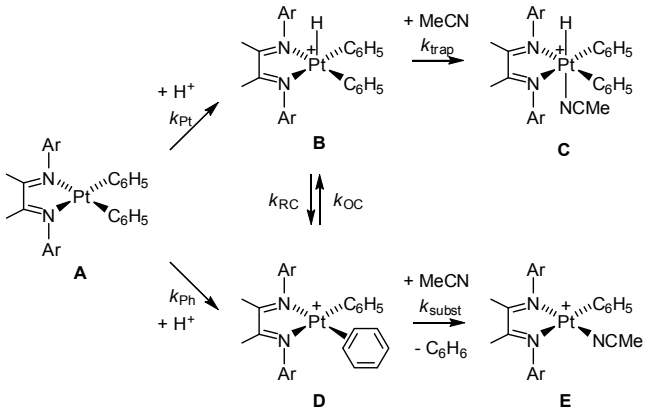

Scheme 3. The two possible sites of protonation at (Ar-DAB)$PtPh_2$.

2.3.2 Reductive Coupling and Oxidative Cleavage.

The kinetics of the proposed reversible interconversion between **B** and **D** in Scheme 3 has been described elsewhere,[81] but some comments need to be made here (see also Chapter 1). It was seen by 2D EXSY ^{1}H NMR spectroscopic experiments on (N–N)PtPh(η^2-C_6H_6)$^+$ **D** in dichloromethane-d_2 that the protons of the C_6H_5 and η^2-C_6H_6 ligands underwent mutual site exchange. This was accompanied by exchange between the two non-equivalent halves of the diimine ligand. The kinetics of these exchange processes were evaluated by quantitative EXSY spectroscopy, and it was found that the diimine-based exchange occurred at the same rate as the C_6H_5/η^2-C_6H_6 exchange, with $\Delta G^{\#}$ ca. 61 kJ mol^{-1} in dichloromethane-d_2 at -40 °C. The underlying exchange mechanism that was originally proposed is the oxidative cleavage depicted in Scheme 4, top path. The five-coordinate species resulting from the oxidative

cleavage of a C-H bond in the benzene ligand is crucial for the proton site exchange as well as for the diimine symmetrization. Since **B** (whether a true intermediate or a transition state in this process) is expected to be a relatively high energy species compared to **D**, the rate constant k_{OC} can be taken as the rate constant for this exchange process. Recent DFT calculations[102] (computed $\Delta G^{\#}$ values at -40 °C) located **B** ca. 73 kJ/mol higher in energy than **D** and they are connected by a 86 kJ/mol barrier when going from **D** to **B**, i.e. the barrier will be merely 13 kJ/mol in the reverse direction. (For these calculations, the polarized continuum model (PCM) was used to include *ether* as the solvent). Interestingly, the DFT results suggested that the C_6H_5/η^2-C_6H_6 exchange process is more likely to occur by a "direct σ-bond metathesis" in which the proton maintains a weak interaction with Pt as it passed along from one phenyl group to the other in the equatorial plane of the complex. We have now established that the EXSY correlation peaks are seen in spectra of $(N–N)PtPh(\eta^2\text{-}C_6H_6)^+$ even in the presence of acetonitrile. This provides strong evidence for the non-involvement of the putative intermediate $(diimine)PtPh_2H^+$ in the exchange process, since it should have immediately formed $(diimine)PtPh_2H(NCCD_3)^+$ by trapping with acetonitrile under the reaction conditions.

The DFT-predicted direct σ-bond metathesis pathway now is an attractive alternative to the oxidative cleavage/reductive coupling pathway for exchange. Such a σ-bond metathesis process appears to nicely explain H/D exchanges between two phenyl groups, via a reasonably looking calculated transition-state structure.[102] (It might be pointed out that the mechanism is not necessarily involved in previously reported, related exchange processes; it appears to us less likely to be involved in exchanges between two methyl groups,[77,111] or between phenyl and methyl groups[60,83]). The computed transition-state free energy for this process, which closely resembles the transition state in what Perutz and Sabo-Etienne[63] have termed a "σ-complex assisted metathesis" (σ-CAM), was 62 kJ mol^{-1}, i.e. ca. 24 kJ mol^{-1} below that for the oxidative cleavage pathway. If these computational results give a true description of the mechanism, then one obvious implication will be that the numerical value that is used for k_{OC} is an *upper limit* to the real value: The EXSY kinetics represent the energetics for reaching the transition-state for the direct exchange process; the transition state for the oxidative cleavage must necessarily be higher in energy and thence the corresponding rate must be even slower – which strengthens the arguments that led to the conclusion in the previous paragraph: Pt is the kinetically preferred site of protonation. We note that kinetic isotope effects obtained by reactions with HX vs. DX acids might shed further light on the

nature of the initial protonation event, as demonstrated in a recent contribution by the Bercaw[113] and Romeo groups,[114] and hope to report on this in a future contribution.

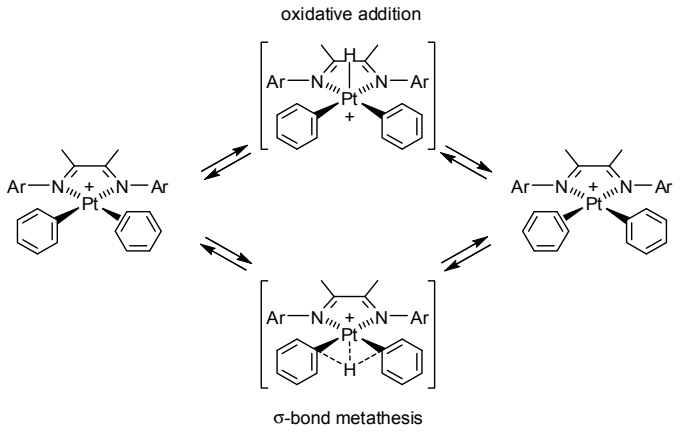

Scheme 4. Oxidative addition (top) and σ-bond metathesis (bottom) pathways for the proton exchange between phenyl and benzene ligands in (Ar-DAB)PtPh(η^2-C_6H_6)$^+$ **3a**.

2.3.3 Elimination of Benzene from (Ar-DAB)PtPh$_2$H(NCMe)$^+$

The six-coordinate Pt(IV) hydride is quite stable on the timescale of all our experiments at -78 °C. When heated, the compound smoothly undergoes benzene elimination to furnish (Ar-DAB)PtPh(NCMe)$^+$ **4a**. The kinetic parameters, notably the rather large $\Delta H^{\#}$ and the substantially positive values for $\Delta S^{\#}$ and $\Delta V^{\#}$, suggest that the rate-limiting step of this reaction must involve MeCN dissociation. The data in Table 1 show that at temperatures well below 0 ºC, MeCN dissociation (k_{-2}) is considerably slower than benzene substitution (k_4[MeCN] and within the framework of Scheme 4 the elimination of benzene from (Ar-DAB)PtPh$_2$H(NCMe)$^+$ to furnish (Ar-DAB)PtPh(NCMe)$^+$ is expected to proceed without the build-up of observable intermediates. At temperatures above 0 ºC, benzene substitution is competitive with or even faster than MeCN dissociation. However, on the assumption that MeCN dissociation is reversible, the accumulation of the putative π-benzene intermediate (Ar-DAB)PtPh(η^2-C_6H_6)$^+$ would be negligible also under these conditions. Thus, the observations are readily reconciled with the notion that benzene elimination is dissociative and takes place without build-up of detectable intermediates. The mechanism is entirely analogous to that observed for the elimination of methane from (Ar-DAB)PtMe$_2$H(NCMe)$^+$.[80] It should be mentioned here that reductive eliminations of X–Y from octahedral $L_4Pt^{IV}(X)(Y)$ compounds are usually found to be dissociative whenever a readily dissociable ligand is

present; whether the overall process occurs in a concerted or stepwise fashion may strongly depend on the nature of the eliminating groups X and Y, as well as of the ancillary ligands L.[38,67,115,116] The five-coordinate species (diimine)$PtPh_2H^+$, a crucial intermediate that is postulated to be in common for the protonation as well as for the benzene reductive elimination processes, has not been directly observed, not even under the rapid-scan conditions utilized here. However, there are a few literature reports on isolable, five-coordinate Pt(IV) alkyl complexes.[38,98,100,101,117-119]

2.3.4 Substitution of Benzene by Acetonitrile at (Ar-DAB)PtPh(η^2-C_6H_6)$^+$

We have reported[81] that (Ar-DAB)PtPh(η^2-C_6H_6)$^+$ complexes are readily available by protonation of (Ar-DAB)$PtPh_2$ complexes in dichloromethane at ca. -78 °C. It was qualitatively seen that the stability of (Ar-DAB)PtPh(η^2-C_6H_6)$^+$ complexes with respect to benzene loss depended highly on the substituents at the *N*-aryl groups of the diimine ligand. Complexes that are 2,6-dimethyl substituted on the *N*-aryl groups slowly start to lose benzene at ca. -40 °C under these conditions, whereas 2,6-unsubstituted analogs start to lose benzene at a substantial rate even at -78 °C. These qualitative stability differences are readily understood if it is assumed that benzene loss occurs by an associative mechanism. Since the N-aryl groups are oriented more or less perpendicularly with respect to the coordination plane of Pt,[81] the N-aryl methyl substituents will serve to sterically protect the Pt center from nucleophilic attack by any incoming ligand that approaches from above or below the coordination plane. Experimental evidence suggests that substitution of methane by acetonitrile in (diimine)PtMe(σ-CH_4)$^+$ complexes,[78] and of toluene by acetonitrile in related (diimine)Pt(*o*/*m*/*p*-tolyl)(η^2-toluene)$^+$ species, are associative in nature. However, the kinetics of these processes has not been investigated in any detail.

The experimental results that have been presented herein leaves no doubt that substitution of benzene by acetonitrile in (Ar-DAB)PtPh(η^2-C_6H_6)$^+$ is an associative process. The first-order dependence of k_{obs} on [MeCN], with the near-zero intercept of the k_{obs} vs. [MeCN] plot in Figure 10, as well as the substantially negative $\Delta S^{\#}$ strongly support this notion. Thus, it appears that hydrocarbon loss from cationic diimine-supported complexes will generally proceed by an associative substitution mechanism in a good donor solvent like acetonitrile. It is noteworthy that addition of MeCN to (Ar-DAB)PtPh(η^2-C_6H_6)$^+$ produces

only (Ar-DAB)PtPh(NCMe)$^+$ and not (Ar-DAB)PtPh$_2$H(NCMe)$^+$, which means that with reference to Scheme 3, it must be required that the rate constant for benzene substitution, k_4[MeCN], is expected to be substantially greater than that for oxidative cleavage, k_{-3}. This is based on the assumption that the trapping reaction k_2 is rapid, which is suggested by the fact that (Ar-DAB)PtPh$_2$H(NCMe)$^+$ is rapidly and cleanly produced from (Ar-DAB)PtPh$_2$ protonation in the presence of MeCN. The data in Table 1 show that the rate of site exchange in (Ar-DAB)PtPh(η^2-C_6H_6)$^+$ far outruns the rate of substitution by MeCN under typical experimental conditions; further evidence for this is provided by the observation of EXSY correlation peaks even in the presence of acetonitrile. This fact provides compelling experimental evidence that site exchange cannot occur by the oxidative cleavage/reductive coupling pathway. The combined data are most consistent with site exchange occurring by a separate pathway, i.e. the concerted σ-bond metathesis pathway indicated in Scheme 4 and suggested by DFT calculations.[102]

2.3.5 Protonation and Benzene Elimination at (Ar-DAB)PtPh(NCMe)$^+$ 4a

The second protonation of (Ar-DAB)PtPh$_2$ **1a** occurs at temperatures near ambient after the Pt(II) cation (Ar-DAB)PtPh(NCMe)$^+$ **4a** has been generated. This protonation is exceedingly slow when $HBF_4{\cdot}Et_2O$ is employed as the acid, but occurs much more rapidly when TfOH is used. This is in accord with the general notion that TfOH is a stronger acid than $HBF_4{\cdot}Et_2O$. The sluggishness of the reaction arises from the combined effect of a high $\Delta H^{\#}$ (resulting from the necessity to protonate an already positively charged metal complex) and a strongly negative $\Delta S^{\#}$. No intermediates have been observed for this reaction – perhaps not too surprising, considering the relatively high temperatures that are required for the protonation. These conditions are expected to lead to the instant elimination of benzene from a formally doubly charged Pt(II) π-benzene complex or a doubly charged Pt(IV) phenyl hydride complex. The kinetic data do not allow us to draw firm conclusions regarding the site of protonation, the involvement (or not) of Pt(IV) hydride species, the involvement (or not) of π-benzene intermediates, or the associative (or dissociative) nature of the benzene elimination or substitution. One difference is particularly striking when the first and second protonation are compared, in addition to the simple fact that the second protonation is much slower than the first: In the first protonation/benzene-forming sequence, the benzene-producing reactions are

rate limiting reactions following a rapid protonation. In the second protonation/benzene-producing sequence, the benzene-producing reactions are rapid reactions following a rate-limiting protonation. This difference might be a consequence of the different temperature regimes of the two reaction sequences: The second protonation occurs at a temperature sufficiently high to dramatically accelerate the high-activation energy (as expressed through $\Delta G^{\#}$) benzene-producing process relative to the lower-activation energy protonation event.

2.4. Summary and concluding remarks

In this chapter, we have described the combined results from NMR and stopped-flow UV-vis spectroscopic measurements on a well-defined sequence of reactions that are initiated by protonation of (Ar-DAB)$PtPh_2$ **1a**. Detailed insight into the kinetics and mechanisms of a cascade of reactions that ultimately leads to the release of two equivalents of benzene has been obtained within the temperature range of -80 to +27 °C. The accumulated experimental data are in agreement with the mechanistic picture that is depicted in Scheme 2. At low temperatures (ca. -80 °C), protonation of (Ar-DAB)$PtPh_2$ with $HBF_4{\cdot}Et_2O$ in dichloromethane/acetonitrile occurs at the metal to furnish an unobserved five-coordinate Pt(IV) complex (Ar-DAB)$PtPh_2H^+$ that is immediately trapped to furnish (Ar-DAB)$PtPh_2H(NCMe)^+$ **2a**. This six-coordinate Pt(IV) hydride is stable under the low-temperature reaction conditions. At higher temperatures, (Ar-DAB)$PtPh_2H(NCMe)^+$ **2a** is kinetically less stable: The energetically costly MeCN dissociation occurs and under these conditions, the following reactions, viz. Ph-H reductive coupling to furnish (Ar-DAB)$PtPh(\eta^2\text{-}C_6H_6)^+$ **3a** and the subsequent associative substitution of acetonitrile for benzene, are quite rapid. Consequently, (Ar-DAB)$PtPh_2H(NCMe)^+$ **2a** produces (Ar-DAB)$PtPh(NCMe)^+$ **4a** without observable intermediates. The next protonation occurs at a reasonable rate only when the stronger acid TfOH is utilized and leads to benzene loss without observable intermediates. The (Ar-DAB)$PtPh(C_6H_6)^+$ **3a** complex can be independently prepared by protonation with $HBF_4{\cdot}Et_2O$ in dichloromethane. Substitution of benzene by acetonitrile at this complex is clearly associative in nature and furnishes exclusively (Ar-DAB)$PtPh(NCMe)^+$ **4a** with no hints of (Ar-DAB)$PtPh_2H(NCMe)^+$ **2a**. This observation provides indirect evidence that the previously reported exchange of protons between the phenyl and benzene ligands in (Ar-DAB)$PtPh(C_6H_6)^+$ probably occurs via a σ-

bond metathesis pathway, also suggested by DFT calculations, rather than by an oxidative cleavage/reductive coupling sequence.

The diimine-Pt system offers rich opportunities to investigate the effects of substituent and other parameters on these and other reactions that are of relevance to C-H bond activation reactions that are of great practical and academic interest. The next objectives addressed in this thesis are the synthesis of new diimine Pt complexes subjected to protonation and the evaluation of the steric and electronic parameters that can be tuned by variation of the diimine ligand.

2.5. Experimental Section

General considerations

The complex (Ar-DAB)$PtPh_2$ **1a** was prepared as described in the literature[81] from $Ph_2Pt(SMe_2)_2$[120] and the diimine.[121] ($Ph_2Pt(SMe_2)_2$ has been reported[122] to exist as mixtures of dimers and trimers).

Pt(II):Pt(IV) ratio vs. [MeCN].

Competitive trapping experiments were conducted by adaptation of already published procedure.[79,111] A solution of (Ar-DAB)$PtPh_2$ (ca. 3 mg, 5 μmol) in CD_2Cl_2 (400 μL) in an NMR tube was cooled to -78 °C and layered with a mixture of $HBF_4{\cdot}Et_2O$ (3 μL) in MeCN-d_3 (x μL) and CD_2Cl_2 (300 − x μL.; x = 10−300 μL). The tube was capped and shaken to mix the reactants immediately before transfer to a pre-cooled NMR probe. A pale yellow solution was immediately obtained. The relative amounts of the Pt(II):Pt(IV) complexes were determined by integration of suitable non-overlapping ^1H NMR signals from the complexes. Thus, the Ar-Me signal at δ 2.13 from one half of the diimine ligand was used for (Ar-DAB)$PtPh(NCCD_3)^+$, whereas the signal at δ 2.41 arising from the methyl groups at the backbone of the diimine ligand were used for (Ar-DAB)$PtPh_2H(NCCD_3)^+$. Characterization of the complexes has been already published.[81] The relative distribution of the two products was unaltered when the tube was kept for 3 h at the same temperature.

NMR Monitoring and Kinetics of Benzene Substitution by MeCN at (Ar-DAB)$PtPh(\eta^2\text{-}C_6H_6)^+$.

The NMR investigation of the benzene substitution kinetics was performed by slight modifications of previously reported procedures.[80,81,111] In an NMR tube, (Ar-DAB)$PtPh_2$ (10 mg, 15 μmol) was dissolved in dichloromethane-d_2 (300 μL), and the tube was cooled to -78 °C on a dry ice/acetone bath. A solution of $HBF_4{\cdot}Et_2O$ (10 μL, 78 μmol) in a mixture of Et_2O-d_{10} (70 μL) and dichloromethane-d_2 (180 μL) was then added, the tube was shaken in the bath, and a ^1H NMR was recorded at -78 °C to ensure that all the starting material was consumed and that (Ar-DAB)$PtPh(\eta^2\text{-}C_6H_6)^+$ had formed (diagnostic signal at δ 6.85, s, 6 H, η^2-C_6H_6). The tube was removed from the NMR probe and returned to the dry ice/acetone bath. A solution of acetonitrile-d_3 (x μL) in dichloromethane (200-x μL) was carefully layered on top of the contents in the NMR tube (x was in the range 40-100 μL, corresponding to acetonitrile concentrations in the range 1.0-2.7 M). The tube was then shaken to ensure complete mixing prior to transfer to the NMR probe and monitoring of the progress of the reaction at pre-determined temperatures. A smooth conversion of (Ar-DAB)$PtPh(\eta^2\text{-}C_6H_6)^+$ to (Ar-DAB)$PtPh(NCCD_3)^+$ (δ 2.37, s, 6 H, Ar-*Me*) and benzene (δ 7.3, s, 6 H) was seen. The kinetic data were obtained by integration of the peak intensity for the phenyl ligand protons (δ 6.0-6.2) of the η^2-benzene complex vs. the residual proton signal of the solvent dichloromethane-d_2 as an internal standard. A plot of ln(relative intensity) vs. time was linear for 3-4 half-lives.

EXSY NMR spectra of (Ar-DAB)$PtPh(\eta^2\text{-}C_6H_6)^+$. In the absence and presence of acetonitrile-d_3.

The sample preparation was identical to those applied to the benzene substitution kinetics experiments described above. The EXSY spectra were recorded at -48 °C without acetonitrile-d_3 or with 0.054 M acetonitrile-d_3. The same experimental parameters were used as described in our previous contribution.[81] The EXSY correlation signals were of indistinguishable intensities in the two experiments.

3. Synthesis, Characterization, and Protonation Reactions of new Ar-BIAN and Ar-BICAT Diimine Platinum Diphenyl Complexes

3.1. Introduction

Since the Bercaw group first reported that a tmeda-Pt(II) complex was capable of activating C-H bonds,[123,124] variously substituted diimine-Pt(II) alkyl and aryl complexes have been intensely investigated to gain insight into the C-H activation mechanism. In this respect, the most commonly studied diimine-ligand systems (Chart 1) are those of the DAB (1,4-diaza-1,3-butadiene) type[60,79-81,83,108,111] and the bpy and bipym systems studied by Puddephatt[125-128] and Periana.[45,129-134] In order to expand the scope of our studies, we have now turned our attention to non-DAB diimine ligands. The closely related Ar-BIAN (Ar-BIAN = bis(arylimino)acenaphthene, see Chart 1) ligand system, pioneered by the Elsevier group,[135-142] has been explored with respect to many catalytic processes, including olefin oligomerization and polymerization[143-147] and olefin/CO copolymerization.[148] The Ar-BIAN system is a highly stable, rigid bidentate spectator ligand with interesting electronic properties.[149,150] Ar-BIAN ligands have been suggested to act as stronger σ-donors toward the metal when compared to related bpy and rather comparable to open chain R-DAB ligands which would be the case if the diimine system in the Ar-BIAN ligand is electronically isolated from and offers no conjugation with the naphthalene backbone.[137] The capacity of this ligand type to support many oxidation states have been amply demonstrated; for example, Pt Ar-BIAN complexes have been reported in oxidation states ranging from Pt(0)[137] via Pt(II)[147] to Pt(IV).[140] Ar-BIAN Pt complexes have found uses in catalytic hydrosilylation of styrene[151] and some complexes have interesting photophysical properties.[152-154] Surprisingly to us, to our knowledge no reports have appeared on the use of Ar-BIAN ligand systems in studies of reactions of relevance to C-H bond activation.

Chart 1

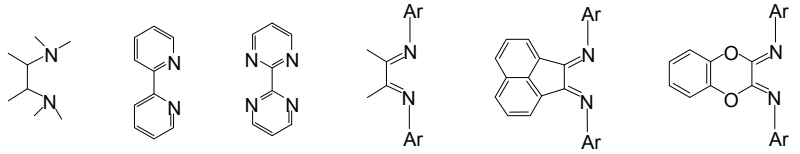

In this chapter, we present the synthesis and spectroscopic and structural characterization of a series of new (diimine)Pt (II) complexes where the diimine is Ar-BIAN with Ar = 2,6-$Me_2C_6H_3$, 2,4,6-$Me_3C_6H_2$, 4-Br-2,6-$Me_3C_6H_2$, 3,5-$Me_2C_6H_3$, 4-MeC_6H_4, and 4-$CF_3C_6H_4$. In addition, we report the novel bis(arylimino) catechole-based ligand system Ar-BICAT, see Chart 1. A qualitative description of the protonation reactions of the corresponding (diimine)$PtPh_2$ complexes is also included and discussed in view of the knowledge of related reactions.

3.2. Results and Discussion

3.2.1 Synthesis and characterization of metal complexes

The air- and moisture-stable platinum complexes **1b-h** (Scheme 1) were prepared in good yields by stirring a solution of $(Me_2S)_2PtPh_2$ and the diimine ligand at ambient temperature by adaptation of published procedures.[81] The complexes were characterized by ^1H, ^{13}C, and ^{195}Pt NMR spectroscopy as well as elemental analysis. Complexes **1b-g** showed ^{195}Pt signals with chemical shifts in the range δ -2770 to -2851; the chemical shift of **1h** appears at δ -3384. Within the series **1b**-**1d**, which are 2,6-dimethyl substituted at Ar and where the substituents within the series change only at the para position of Ar, the ^{195}Pt chemical shift increases (to less negative values) with increasing Hammett σ_p substituent parameters.[155] Similarly, within the series **1e**-**1g**, which are 2,6-unsubstituted and where changes occur at the meta and para positions, there is a trend of increasing chemical shifts with increasing $\Sigma(\sigma_m + \sigma_p)$. Thus, there appears to be a normal substituent electronic effect – higher δ values with increasing electron withdrawing power – of the Ar substituents on the ^{195}Pt NMR chemical shifts in compounds that may be readily compared. Furthermore, the Ar-BIAN and Ar-BICAT ligand systems appear to have a significant effect on the Pt electronic properties, as seen in a comparison of

^{195}Pt chemical shifts for **1b-1h** with those for the corresponding Ar-DAB complexes.[81] The chemical shifts for the Ar-BIAN series are located ca. 280 ppm downfield of the values for the corresponding compounds in the DAB series. This suggests that the Ar-BIAN ligands are more electron withdrawing than the similarly substituted Ar-DAB ligands, which may be attributed to a greater π acceptor capacity for the extended π systems of the BIAN ligands.[156] On the other hand, the ^{195}Pt NMR chemical shift of the Ar-BICAT ligated complex **1h** is far upfield of the corresponding Ar-BIAN and even 300 ppm upfield of the Ar-DAB complexes. The catecholate bridge at the backbone therefore appears to exert a considerable electron donating power towards the metal, transmitted through the diimine ligand core. In summary, approximate chemical shifts for the Pt(II) diphenyl complexes are -2800 for BIAN, -3050 for DAB, and -3380 for BICAT ligand systems.

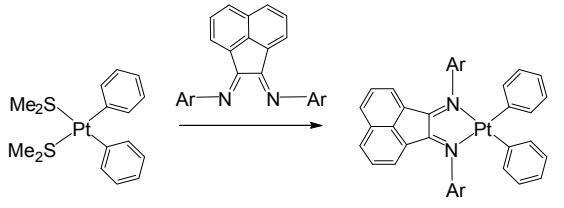

1b-g

Compd	Ar
1b	2,6-$Me_2C_6H_3$
1c	2,4,6-$Me_3C_6H_2$
1d	4-Br-2,6-$Me_2C_6H_2$
1e	3,5-$Me_2C_6H_3$
1f	4-MeC_6H_4
1g	4-$CF_3C_6H_4$

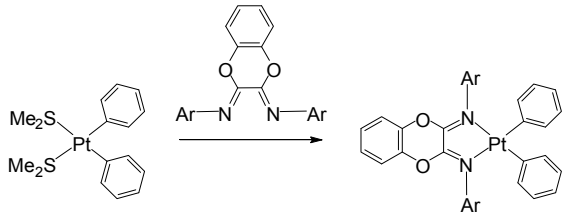

1h

Ar = 4-MeC_6H_4

Scheme 1

Further support for the apparent electronic effect provided by the diimine backbone structure, as inferred from the ^{195}Pt NMR chemical shifts, were obtained from infrared ν(CO) spectra of (diimine)PtPh(CO)$^+$ complexes which were synthesized by protonolysis of the corresponding (diimine)$PtPh_2$ complexes in trifluoroethanol under a CO atmosphere. This is an adaptation of a published procedure for generation of (Ar-DAB)PtMe(CO)$^+$ complexes (see also Experimental section).[83] The IR ν(CO) spectra of the Ar-BIAN, Ar-DAB, and Ar-BICAT complexes with Ar = 4-MeC_6H_4 exhibited CO stretching bands at 2115.6, 2113.8, and 2113.2 cm^{-1}, respectively. Whereas the differences are small, these data do indeed support the notion that the electronic effect of the Pt centre is altered by tuning of the diimine backbone

structure. The combined IR and ^{195}Pt NMR data allow us to confidently assert that the BICAT system is a better electron donor than the DAB system, whereas the BIAN system is the poorest donor of the three. We note that the published ν(CO) data for (ArN=CH-CH=NAr)PtMe(CO)$^+$ are ca. 4-5 cm^{-1} higher than those for the corresponding (ArN=CMe-CMe=NAr)PtMe(CO)$^+$ complexes.[83]

3.2.2 Low-temperature protonation of (N–N)PtPh$_2$ in the presence of acetonitrile

In situ protonation of **1b-h** was performed in NMR tubes at -78 °C with $HBF_4{\cdot}Et_2O$ (see Experimental Section). Protonation in the presence of acetonitrile-d_3 in dichloromethane-d_2 led to the immediate formation of the hexacoordinated Pt(IV) hydrides (N–N)PtPh$_2$H(NCCD$_3$)$^+$ (**2b-h**) (Scheme 6). The ^{1}H NMR spectra of these hexacoordinated Pt(IV) hydrides exhibit characteristic Pt-*H* singlets at δ ca. –21 with the expected ^{195}Pt satellites, ^1J(^{195}Pt-H) of ca. 1600 Hz. The ^{1}H NMR spectra show that the two halves of the diimine ligands are symmetry equivalent. We infer that the hydride and MeCN ligands occupy the two apical, mutually trans, coordination sites. For the Ar-BIAN complexes, the signals that arise from ortho and meta Ar-H and Ar-Me groups (when sufficiently resolved) have split into two sets of signals of equal intensity. Such duplication is not seen for any other signals. This phenomenon is most likely due to restricted rotation around the N-C(aryl) bond, where the rotational barrier is imposed by the nearby ortho protons at the BIAN skeleton. This renders the aryl hydrogens or methyl groups located at the "top" (hydride side, Scheme 6) and "bottom" (MeCN side) of the square plane chemically non-equivalent. Such a hindrance to rotation was also observed with Ar-DAB complexes.[81] In the case of the Ar-BICAT complex **2h**, such "top-bottom" non-equivalence was not observed, and the ^{1}H NMR signals appeared more broadened – possibly indicating somewhat slowed rotation at -78 ºC. This suggests less severe steric repulsions between the *N*-aryl methyl protons and the catechole backbone.

As is commonly seen, Pt(IV) hydrides require stabilization[128] by an additional axial ligand, in our case, acetonitrile. When the NMR samples were heated, **2g-h** gradually eliminated benzene starting at ca. -40 °C to furnish the corresponding Pt(II) acetonitrile complexes **4b-h** (Scheme 2), for which the spectroscopic data reveal that the "top-bottom" symmetry has been restored. These complexes have been independently synthesized (vide infra).

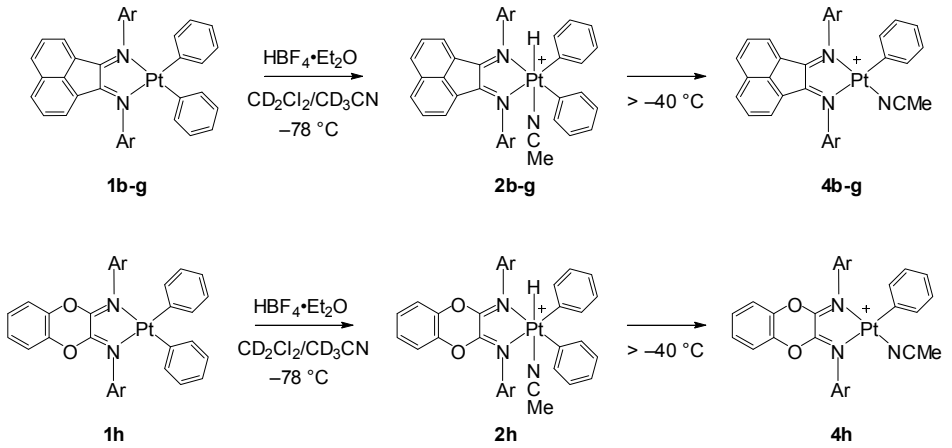

Scheme 2

Similar behavior involving protonation at the metal and subsequent hydrocarbon elimination has been reported for (Ar-DAB)$PtMe_2$[77,79,80,111] and (Ar-DAB)$PtPh_2$[81,157] complexes. The formation of **2b-h** is fully consistent with protonation at Pt to give a coordinately unsaturated, five-coordinate Pt(IV) hydride intermediate that is trapped by acetonitrile, in agreement with mechanistic studies on the mentioned diimine-Pt dimethyl and diphenyl complexes.[80,157]

3.2.3 Low-temperature protonation of (N–N)$PtPh_2$ in the absence of acetonitrile

Protonation of **1b-h** with $HBF_4{\cdot}Et_2O$ in dichloromethane-d_2 in the presence of Et_2O-d_{10} (see Experimental section) leads to the quantitative formation of the Pt(II) π-benzene complexes (N–N)$Pt(C_6H_5)(\eta^2\text{-}C_6H_6)^+$ (**3b-h**, Scheme 3) at sub-ambient temperatures. The ^{1}H NMR spectra of these complexes exhibit a characteristic singlet arising from the η^2-C_6H_6 ligand at ca. δ 7.1 (**3b-g**) or 6.9 (**3h**); the lower chemical shift value of the latter may again reflect the better donor capacity of the BICAT system when compared to BIAN. These signals exhibit a somewhat broadened base, which sometimes can be resolved to reveal broadened ^{195}Pt satellites where the broadening is presumed to arise from spin relaxation caused by chemical shift anisotropy.[158-160] Compounds **1b-d** underwent facile protonation at -30 °C, in the sense that the reaction was complete by the time that an NMR spectrum could be recorded. At this temperature the products **3b-d** are only partially stable, as slow liberation of benzene is seen. At temperatures of -50 °C and below, the protonations of the Ar-BIAN complexes **1b-d** (which are 2,6-Me_2 substituted at Ar) were surprisingly slow (30 min or more was required for complete reaction), compared to the corresponding Ar-DAB complexes (complete reaction

by the time NMR spectra could be recorded).[81] The slower protonation of these Ar-BIAN complexes than of analogously substituted Ar-DAB complexes with comparable steric requirements may be a result of the poorer electron donating power of the Ar-BIAN system, as inferred from IR and ^{195}Pt NMR data in a previous paragraph. By contrast, compounds **1e-g** (2,6-unsubstituted at Ar) were immediately protonated even at -70 °C, and the corresponding benzene complexes **3e-g** started to slowly lose benzene already at -50 °C. The differences in reactivity between the **b-d** and **e-g** series presumably arise from the steric influence of the substituents at Ar in the Ar-BIAN ligands. Since the Ar groups are expected to be more or less perpendicularly oriented with respect to the Pt coordination plane, the 2,6-Me_2 substituents will cause a congestion of the space immediately above and below the coordination plane. Thus, protonation by the external acid will be inhibited in these complexes. On the other hand, the η^2-benzene complexes will be stabilized by the 2,6-dimethyl groups because the displacement of benzene (and other hydrocarbons) from these and related diimine-Pt complexes has been demonstrated to be associative reactions.[78,82,157]

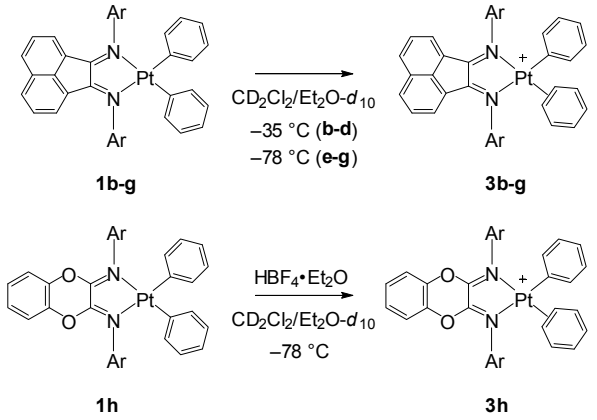

Scheme 3

It has been demonstrated that the kinetically preferred site of protonation is the Pt centre for (Ar-DAB)$PtMe_2$ complexes.[79,111] We have recently presented experimental evidence that this is also the case for (Ar-DAB)$PtPh_2$ analogs,[157] a scenario that had already been predicted by DFT calculations.[102] The distinct difference in protonation rates between **1b-d** and **1e-g** may indirectly support the notion of a metal-centered protonation followed by a rapid C(phenyl)/H reductive coupling to furnish the π-benzene ligand: A metal-based protonation in which the acid approaches from above or below the coordination plane should be considerably inhibited by the 2,6-Me_2-substituted aryl groups. On the other hand, a ligand-

centered protonation might be less dependent on the nature of these substituents, especially if the putative approach of the acid towards the phenyl ligand occurs more or less in the coordination plane.

In the case of BICAT complex, protonation to furnish **3h** is immediate at -78 °C. Monitoring of the complex showed no degradation after more than 1 h at that temperature. Decomposition and liberation of benzene was observed from ca. -60 °C, indicating that the BICAT ligand appears to activate the neutral complex toward protonation (as might be expected for a better donor ligand), and the π-benzene complex toward benzene loss, when compared to the BIAN systems.

3.2.4 Protonation of 1b-h in the presence of acetonitrile at ambient temperature

Treatment of the (N–N)$PtPh_2$ complexes **1b-h** with triflic acid (TfOH) or $HBF_4{\cdot}Et_2O$ in acetonitrile at ambient temperature led to rapid conversion to the corresponding monophenyl solvento cations (N–N)$PtPh(NCMe)^+$ (**4b-h**, Scheme 2). The BF_4^- salts of **4b-h** were isolated and characterized spectroscopically as well as by elemental analysis and, in some cases, by X-ray diffraction (vide infra). The C_{2v} symmetry of the precursors **1b-h** was clearly broken in **4b-h** as evidenced by the two sets of signals arising from the two halves of the diimine ligands. The coordinated acetonitrile ligands in the isolated compounds **4b-h** were seen as NMR singlets at δ 2.06-2.21; for complexes **4b** and **4h**, a $^4J(^{195}Pt\text{-}H)$ coupling of 10.3 and 13.9 Hz respectively were seen in this signal. Species **4** are presumed to form by protonation at Pt with concomitant elimination of benzene, as reported for Ar-DAB analogs.[81,157]

Quantitative production of benzene was seen when the protonation reactions were monitored by NMR (done for **1b**, **f**, and **h**). Complexes **4** were also generated by addition of acetonitrile to solutions of pre-formed π-benzene complexes (N–N)$Pt(C_6H_5)(\pi\text{-}C_6H_6)^+$ **3** (done for **3b**, **f**, and **h**). Substitution of benzene by acetonitrile occurred within ca. 15 min to an extent of ca. 10% already at -70 °C for **3b** and **3f**, and even at -78 ºC for **3h**. These are temperatures at which the π-benzene species are stable in the absence of acetonitrile, clearly consistent with the notion that the substitution of benzene by acetonitrile occurs associatively.

3.2.5 Protonation of 1b-g in the presence of acetonitrile at elevated temperatures

Treatment of the (Ar-BIAN)$PtPh_2$ complexes **1b-g** with triflic acid (TfOH) in acetonitrile at 50 °C overnight led to clean conversion to the corresponding dicationic Pt(II) species (Ar-BIAN)$Pt(NCMe)_2^{2+}$ (**7b-g**, Scheme 4) which were characterized spectroscopically and, in part, by elemental analysis. The triflate salt of **7c** was in addition characterized by X-ray crystallography (vide infra).

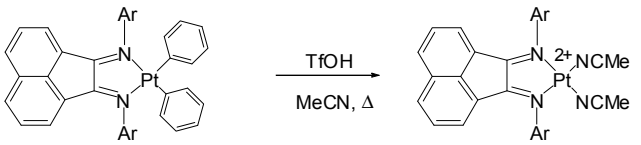

1b-g **7b-g**

Scheme 4

Double protonation of diimine Pt dimethyl complexes to furnish related dicationic species has been reported previously to occur when (Ar-DAB)$PtMe_2$ complexes are treated with TfOH or BF_3 isn trifluoroethanol.[108] This appears to be the first structurally characterized (diimine)$Pt(NCMe)_2^{2+}$ complex. We recently have reported that an analogous double protonation of an (Ar-DAB)$PtPh_2$ complex occurs with TfOH, but not with HBF_4, in MeCN at temperatures above ambient.

The C_{2v} symmetry of the precursor **1b-g** was clearly preserved as evidenced by the observation of one set of signals arising for the two halves of the diimine ligands. The coordinated acetonitrile ligands in the isolated compounds **7b-c** and **7e-f** appeared as singlets at δ 2.24-2.37 with no discernible $^4J(^{195}Pt\text{-}H)$ couplings. Compounds **7d** and **7g** were characterized in situ due to decomposition during attempted purification. We surmise that the Pt(II) species **7** are produced by two successive protonation/benzene elimination sequences but have made no attempts at investigating the finer details of the underlying reaction mechanism.

3.2.6 X-ray crystal structures

Crystals of **1b**, **1c**, **1f**, **1g**, **4b**, **4c**, **7b**, and **7c** were subjected to structure determinations by X-ray crystallography. Selected crystallographic data for these complexes are listed in Table 1. Selected bond distances and angles are summarized in Table 2. Figure 1 shows ORTEP drawings of all solid-state structures.

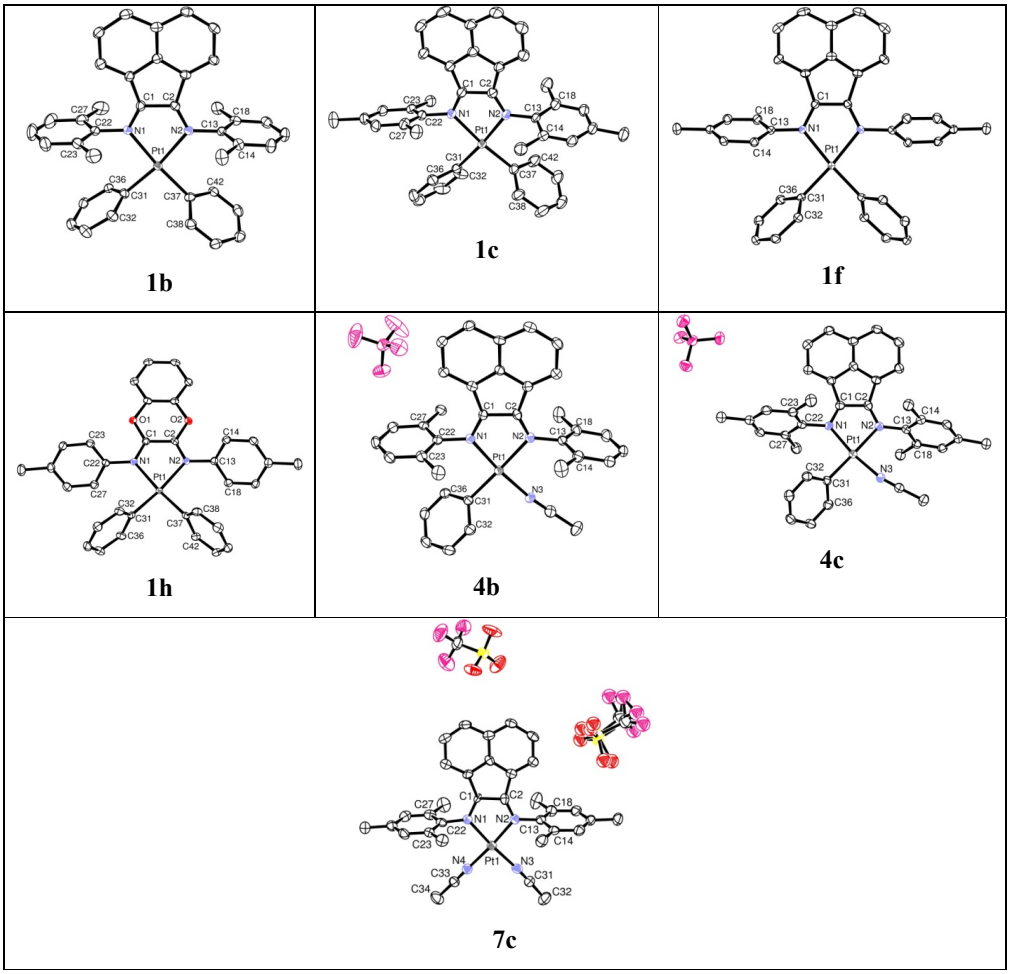

Figure 1. ORTEP drawings of (N–N)Pt^{II} complexes **1b**, **1c**, **1f**, **1g**, **4b**, **4c**, **7b**, and **7c**. 50% probability ellipsoids are shown (hydrogen atoms are removed for clarity. In **7c** there are two molecules in the asymmetric unit, but only one is shown for clarity).

Certain key features are common to all structurally characterized compounds. They all have the square-planar environment that is expected around Pt(II). The deviations from the least squares planes defined by the central Pt atom and the four Pt-bonded atoms are in the range of 0.0-0.057 Å for Pt and 0.001-0.052 Å for the attached C or N atoms (further details on the metric parameters can be found in the electronic Supporting Information). The sum of the four cis L-Pt-L' angles around platinum is 360 ± 0.3° for all compounds. The acenapthene backbone lies in the coordination plane defined by Pt, N1 and N2. The backbone plane of the

BICAT ligand as defined by the catechole ring is only slightly bent from the coordination plane by a 7.6° angle. The rather slight deviation from coplanarity suggests that electronic communication between the backbone skeleton and the diimine-metal structure may occur through the ligand π system.

Some interesting differences may be found, to be discussed in the following paragraph, when comparisons are made between neutral, monocationic, and dicationic species on one side, and between BIAN, BICAT, and DAB ligated systems of same charge on the other.

The Pt-N(diimine) bond distances average 2.120 Å for the three neutral Ar-BIAN complexes **1b**, **1c**, and **1f**. The corresponding chelate bite angles average 77.7º. In the monocationic complexes **4b** and **4c** the Pt-N(diimine) distances average 2.064 Å whereas the bite angles are 79.2º. Finally, in the dicationic complex **7c**, the average Pt-N(diimine) distance is 2.009 Å whereas the bite angle is 80.8º. Thus, Pt-N(diimine) bonds are, as might be expected, shortened when the positive charge increases, and this bond shortening has the consequence of slightly increasing the ligand bite angle. The replacement of a phenyl ligand by MeCN might also contribute to the bite angle increase. For the previously reported[81] (Ar-DAB)$PtPh_2$ and (Ar-DAB)$PtPh(NCMe)^+$ systems, a similar trend towards Pt-N(diimine) bond shortening (from 2.103 Å to 2.053 Å) and chelate bite angle opening (from 75.8 to 77.7º) is also seen when the neutral and charged systems are compared. The average Pt-C(phenyl) bond distances in neutral Ar-BIAN complexes **1b**, **1c**, and **1f** (2.003 Å) are slightly shorter than in the two cationic counterparts **4b** and **4c** (2.011 Å); a modest change in the same direction was seen in the Ar-DAB systems.[81] When the three ligand systems Ar-BIAN, Ar-BICAT, and Ar-DAB are compared for (diimine)$PtPh_2$ compounds, it is noteworthy that the Pt-N(diimine) bond distances decrease from Ar-BICAT (2.146) Å) via Ar-BIAN (2.120 Å) to Ar-DAB (2.103 Å). The average Pt-C(phenyl) bond distances show less variation but tend to decrease in the opposite order, i.e. from Ar-DAB (2.011 Å) via Ar-BIAN (2.003 Å) to Ar-BICAT (1.990 Å). Although variations in metric parameters are modest, the data may suggest that the Ar-BICAT system has a somewhat weaker trans influence than the Ar-BIAN and Ar-DAB systems. There appears to be no significant differences in the C=N and C-C bond distances of the ligand backbone when the neutral complexes of Ar-BIAN, Ar-DAB, and Ar-BICAT ligands are compared. In the neutral Ar-BIAN complexes **1b**-**1f**, the N-Pt-N bite angle is rather constant at 77.62-77.86º but undergoes a slight decrease to 76.75º in Ar-BICAT complex **1h** and a further decrease to 75.47-75.88º in the previously published[81] Ar-DAB complexes.

In the cationic compounds **4b** and **4c**, the Pt-N(acetonitrile) distances (1.967 Å) are shorter than the average Pt-N(diimine) distances (2.064 Å) by ca. 0.1 Å. The Pt-N1 bond distances trans to MeCN (2.014(3) Å) are significantly shorter than the Pt-N2 bond distances trans to phenyl (2.113 Å) by ca. 0.1 Å, clearly as a result of the greater trans influence of the phenyl compared to the acetonitrile ligand. In the dicationic complex **7c**, the average Pt-N(acetonitrile) distance of 1.997 Å is slightly longer than in the monocationic species **4b** and **4c**. It remains to be seen whether these changes in bond distances and angles correlate with relative chemical reactivities that are under investigation in our group.

The phenyl ligands and the *N*-aryl groups of the diimines are twisted away from planarity with the Pt coordination plane, as inferred from the torsion angles in Table 2. The aryl groups are twisted out of the coordination plane by 83° and 77-82°, respectively, in complexes **1b** and **1c** which are 2,6-dimethyl-substituted at the aryl. The corresponding twist angles are 64.5º and by 51-54° in complexes **1f** and **1h**, respectively, which are not 2,6-dimethyl-substituted. The torsion angles of the phenyl groups with respect to the coordination plane span 59-78° in compounds **1b** and **1c** and 61-86° in **1f** and **1h**. These differences reflect the increased steric demands of the 2,6-dimethyl-substituted systems and appear to be a common feature for *N*,*N*'-diaryl-substituted (N–N)PtX_2 complexes where similar trends in dihedral angles have been reported.[81,82,84,85,138,146,147,156,161-164] This emphasizes the steric hindrance imposed by the 2,6-dimethyl substituted *N*-aryl groups: The perpendicular orientation of these *N*-aryl groups with respect to the coordination plane causes the methyl groups to sterically block the access to Pt from above and below the coordination plane. This has a pronounced effect on the qualitative protonation rates and on the stabilities of the Pt(II) π-benzene complexes, as discussed earlier.

Table 1. Crystallographic Data for **1b**, **1c**, **1f**, **1g**, **4b**, **4c**, **7b**, and **7c**

compound	**1b**	**1c**	**1f**	**1h**	**4b**	**4c**	**7c**
Formula	$C_{40}H_{34}N_2Pt$	$C_{42}H_{38}N_2Pt$	$C_{38}H_{30}N_2Pt{\cdot}2(CH_2Cl_2)$	$C_{34}H_{28}N_2O_2Pt{\cdot}1.5(CH_2Cl_2)$	$C_{36}H_{32}N_3PtBF_4{\cdot}2(CH_2Cl_2)$	$C_{38}H_{36}N_3PtBF_4{\cdot}(CH_2Cl_2)$	$C_{34}H_{28}N_4Pt{\cdot}2(CF_3SO_3)^-$
formula weight	737.8	765.87	879.62	819.10	958.43	901.55	985.84
colour	Green	Black	Black	Red	Red	Red	Red
crystal system	Triclinic	Monoclinic	Monoclinic	Monoclinic	Triclinic	Monoclinic	Monoclinic
Space group	*P -1*	*$P2_1/n$*	*C2/c*	*C2/c*	*P -1*	*$P2_1/c$*	*C2/c*
a (Å)	7.7564(15)	10.9971(6)	16.250(6)	26.9288(10)	12.470(4)	16.7874(18)	45.443(7)
b (Å)	9.6428(18)	24.7328(15)	23.643(9)	16.3437(6)	13.713(4)	13.0774(14)	15.064(2)
c (Å)	21.685(4)	12.5147(7)	9.052(3)	18.4914(13)	13.834(4)	17.1024(18)	23.998(4)
α	85.280(3)	90	90	90	64.476(3)	90	90
β	79.733(3)	95.378(2)	93.499(4)	128.35	88.788(3)	92.5320(10)	110.685(2)
γ	87.308(3)	90	90	90	67.244(3)	90	90
V ($Å^3$)	1589.7(5)	3388.9(3)	3471(2)	6382.7(6))	1938.2(10)	3750.9(7)	15369(4)
Z	2	4	4	8	2	4	16
T (K)	105	105	105	103	103	105	105
F(000)	732	1528	1736	3224	944	1784	7742
Radiation	Mo Kα (0.71073)Å	Mo Kα (0.71073)Å	Mo Kα (0.71073)Å	Mo Kα (0.71073)Å	Mo Kα (0.71073)Å	Mo Kα (0.71073)Å	Mo Kα (0.71073)Å
θ range (°)	1.9 to 28.4	1.7 to 28.3	1.52 to 27.56	1.57 to 28.74	1.66 to 28.60	1.96 to 27.13	1.60 to 27.12
Reflection measured	14164	27077	14136	27916	17664	30983	64440
Unique reflection	7260	8357	3985	7718	8986	8269	16927
No. of data/restraint/param.	6484/0/388	6140/0/406	3595/0/214	6291/0/395	7672/0/460	6175/0/451	13564/472/961
Goodness of fit, *F*	1.0775	1.1030	1.0330	1.1257	1.1055	1.0015	1.221
R_1, *w* R_2 [I>3 σ (I)]	0.027, 0.03	0.020, 0.022	0.0208, 0.0225	0.0162, 0.0169	0.0286, 0.0296	0.0263, 0.0289	0.0545*, 0.1481*
Largest diff. peak (e $Å^{-3}$)	1.47, -1.26	1.33, -0.95	1.06, -0.77	0.80, -0.50	1.07, -0.97	2.07, -0.88	5.956, -1.177

*(Refined on F^2). Values are for R_1, *w* R_2 [I>2 σ (I)]

Table 2. Selected bond distances and angles for **1b**, **1c**, **1f**, **1g**, **4b**, **4c**, **7b**, and **7c**

Compound	**1b**	**1c**	**1f**	**1h**	**4b**	**4c**	**7c**
Bond distances							
Pt1 N1	2.115(2)	2.122(2)	2.1180(19)	2.1427(17)	2.014(3)	2.014(3)	2.027(5)
Pt1 N2	2.138(2)	2.107(2)	-	2.1492(17)	2.111(3)	2.115(3)	1.997(5)
Pt1 N3	-	-	-	-	1.969(3)	1.965(3)	1.997(7)
Pt1 N4	-	-	-	-	-	-	1.983(6)
Pt1 C31	2.002(3)	1.994(3)	2.001(2)	1.991 (2)	2.010(3)	2.011(4)	-
Pt1 C37	2.020(3)	1.998(3)	-	1.988 (2)	-	-	-
N1 C1	1.287(4)	1.282(3)	1.290(3)	1.280(3)	1.300(4)	1.301(5)	1.308(4)
N2 C2	1.291(4)	1.288(3)	-	1.279(3)	1.286(4)	1.286(5)	1.281(4)
C1 C2	1.489(4)	1.487(4)	-	1.478(3)	1.488(4)	1.490(5)	1.494(4)
C1 C1	-	-	1.482(4)	-	-	-	-
Bond angles							
N1 Pt1 N2	77.86(10)	77.62(8)	77.68(11)	76.75(7)	79.76(11)	80.08(12)	80.76(19)
N1 Pt1 C31	93.04(11)	97.13(9)	97.40(9)	97.85(7)	97.05(12)	97.89(14)	-
N2 Pt1 C37	95.54(11)	95.73(9)	-	97.93(7)	-	-	-
C31 Pt1 C37	93.50(12)	89.52(10)	87.53(13)	87.38(8)	-	-	-
Pt1 N1 C1	114.3(2)	113.89(17)	114.06(15)	114.12(14)	114.5((2)	114.1(3)	113.3(4)
Pt1 N2 C2	113.0(2)	114.47(18)	-	113.75(13)	112.3(2)	112.1(2)	114.3(4)
C1 N1 C22	118.5(2)	118.8(2)	-	120.30(18)	118.5(3)	117.0(3)	122.2(5)
C2 N2 C13	118.9(2)	120.2(2)	-	120.17(17)	121.7(3)	122.5(3)	118.2(5)
C13 N1 C1	-	-	118.46(19)	-	-	-	-
N1 Pt1 N3	-	-	-	-	172.51(12)	171.33(13)	174.6(2)
N2 Pt1 N3	-	-	-	-	93.11(12)	91.81(13)	95.3(2)
N3 Pt1 C31	-	-	-	-	89.93(13)	90.36(14)	-
							-
Torsion angles							
C1 N1 C22 C27	87.5(4)	104.1(3)	-	130.8(3)	82.3(5)	100.5(4)	75.7(8)
C2 N2 C13 C18	-84.3(4)	-84.4(3)	-	-135.7(3)	-93.9(5)	-105.0(4)	-80.0(9)
C1 N1 C13 C18	-	-	63.8(3)	-	-	-	-
C36 C31 Pt1 N1	71.5(2)	120.9(2)	58.7(2)	90.8(2)	52.9(3)	127.2(3)	-
C42 C37 Pt1 N2	-53.4(3)	-72.1(3)	-	-95.2(2)	-	-	-

3.3. Mechanistic issues

Scheme 5 summarizes the current view of the mechanisms that operate for protonation-induced benzene eliminations from (diimine)$PtPh_2$ complexes.[157]

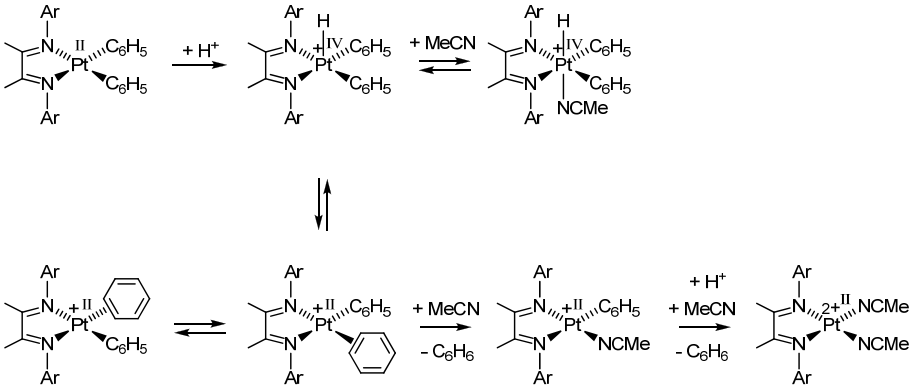

Scheme 5

We have previously reported that (Ar-DAB)$PtMe_2$ complexes undergo protonation with the metal centre as the kinetically preferred site of attack.[111] Recent DFT calculations have indicated that this holds true for protonation of (Ar-DAB)$PtPh_2$ complexes as well,[102] a conclusion that has been supported by recent kinetic studies in our group.[157] In the present contribution, the observed formation of hexacoordinated Pt(IV) hydrides (Ar-BIAN)$PtPh_2H(NCMe)^+$ and (Ar-BICAT)$Ph_2H(NCMe)^+$ by protonation of square-planar Pt(II) precursors are in agreement with a metal-centered protonation, although ambiguity exists because a rapid protonation at a phenyl ligand followed by immediate intramolecular proton transfer to the metal cannot be disregarded by this simple observation. Recently, this alternative has been independently argued against on the basis of kinetic arguments derived from DFT results[102] as well as experimental work.[157]

The π-benzene complexes **3b-d**, sterically shielded at Pt by the 2,6-Me_2 substituents at the *N*-aryl groups, are formed at ca. -30 °C by protonation with HBF_4 in dichloromethane. On the other hand, formation of the corresponding complexes **3e-h**, sterically considerably less shielded, occurs at much lower temperatures, around -60 °C. The considerable difference in protonation rates between **1b-d** and **1e-h** supports the notion of a metal-centered protonation followed by a rapid C(phenyl)/H reductive coupling to furnish the π-benzene ligand: A metal-

based protonation in which the acid approaches from above or below the coordination plane should be considerably inhibited by the 2,6-Me_2-substituted aryl groups; a great difference between **1b-d** and **1e-h** results. On the other hand, a ligand-centered protonation might be less dependent on the nature of these substituents, especially if the putative approach of the acid towards the phenyl ligand occurs more or less in the coordination plane – and the expected difference between **1b-d** and **1e-h** would be less striking.

In our recent mechanistic study of the protonation of (Ar-DAB)$PtPh_2$ (Ar = 2,6-$Me_2C_6H_4$),[157] one issue that was discussed and could not be straightforwardly established was whether the protonation of the neutral Pt(II) complex in the presence of acetonitrile to give (Ar-DAB)$PtPh_2H(NCMe)^+$ was a stepwise process, involving initial protonation followed by rapid capture of the putative 5-coordinate intermediate (Ar-DAB)$PtPh_2H^+$ by acetonitrile, or a concerted process, in which protonation was assisted by a simultaneous acetonitrile coordination. The same question is relevant in the context of protonation of the (Ar-BIAN)$PtPh_2$ complexes described in the present contribution. We note that the series of complexes **1b-1d** that are sterically protected by the 2,6-dimethyl substituted *N*-aryl groups are protonated rather slowly in dichloromethane, and temperatures as high as ca. -30 ºC are required for protonation to furnish the corresponding π-benzene complexes **3b-d** at reasonable rates (NMR monitoring of the reactions). On the other hand, in dichloromethane containing acetonitrile, protonation to yield the hexacoordinate hydrides **2b-d** proceeded rapidly even at -70 ºC. The considerable difference in rates of protonation under these different conditions is certainly consistent with an acetonitrile-assisted protonation event, i.e. a scenario that bypasses the 5-coordinate species as discrete intermediates. However, alternative explanations are also present (even disregarding the possibility of solvent medium effects on the kinetics and thermodynamics of the proton transfer). For example, assume that the 5-coordinate *does* form rapidly under both conditions, but in a relatively unfavorable pre-equilibrium proton transfer (which means that the 5-coordinate will not build up in detectable quantities). The 5-coordinate now has two options that are relevant within the frame of this discussion: One option is to undergo trapping by acetonitrile; this reaction involves no bond cleavages and might be expected to have a fairly low activation barrier. The other option is for the 5-coordinate to undergo the C(phenyl)/H reductive coupling that furnishes the π-benzene complex; this reaction involves cleavage of a Pt-H bond and might have a higher activation barrier. The relative rates of product appearance under the two conditions (solvent, temperature) in this scenario reflects the relative rates of trapping vs. C/H coupling rather than protonation kinetic per se. It might at first glance be argued that among the Ar-BIAN and Ar-

DAB systems, the former is a more likely candidate for a concerted pathway because this ligand is the poorer donor of the two: This would tend to enhance the need for electronic saturation, achievable by acetonitrile coordination. Yet, the same ligand property would also enhance the tendency toward reductive C(phenyl)/H reductive coupling. Thus, the question of whether protonation/acetonitrile coordination is a stepwise or concerted process still remains unanswered.

The π-benzene complex **3b** appears to be thermally more robust in the absence of acetonitrile than the Pt(IV) hydridodiphenyl complex **2b** in the presence of acetonitrile. Whereas **3b** decomposes by benzene elimination at ca. -30 °C, **4b** undergoes benzene elimination at -50 °C without observation of the more robust **3b** as an intermediate. The addition of acetonitrile to a solution of **3b** leads to benzene substitution already at -70 °C by what is believed to be an associative process.[60,81,82,102,157] It is likely that the π-benzene complex is an intermediate in the elimination of benzene from **4b**. Acetonitrile dissociation from **4b** is expected to have a reasonably high activation barrier. We have recently reported that benzene elimination from (Ar-DAB)$PtPh_2H(NCMe)^+$ (Ar = 2,6-$Me_2C_6H_4$) proceeds with rate-limiting acetonitrile dissociation with $\Delta H^{\#}$ ca. 88 kJ mol^{-1}.[157] The final step in the reductive elimination, benzene substitution from the cationic π-benzene complex, occurs associatively, and this is a relatively facile process in the presence of acetonitrile. This scenario agrees qualitatively with findings by Templeton and co-workers, mentioned in Chapter 1.[165]

3.4. Conclusions

A series of new diimine platinum diphenyl complexes have been synthesized and subjected to protonation reactions that are of relevance for our on-going investigation of mechanistic aspects of Pt-mediated C-H activation reactions which in the past has focused on Ar-DAB supporting ligands. Thus, the well known Ar-BIAN diimine structures have been used, and a novel Ar-BICAT diimine structure has been synthesized. Spectroscopic features of the Ar-BIAN, Ar-BICAT, and Ar-DAB systems have been compared and suggest that the donor capacity of the ligands decrease in the order Ar-BICAT > Ar-DAB > Ar-BIAN. Furthermore, crystallographic data suggest that the trans influence of the ligands increases in the order Ar-BICAT > Ar-BIAN > Ar-DAB. (N–N)$PtPh_2$ complexes based on the Ar-BIAN and Ar-BICAT ligands were subjected to protonation reactions, as an extension of recently

reported work on the kinetics of an (Ar-DAB)$PtPh_2$ complex.[157] Very approximate assessments of the rates of protonation and the ensuing reactions lead to some tentative conclusions regarding the influence of the ligands on the reactivity patterns. First of all, the behavior of all the systems were quite similar in that the entire sequence of reactions proceeded in two well-defined protonation/benzene elimination steps, nicely separated in onset temperatures, independently of the diimine structure. Spectroscopic data suggest that variations of the diimine backbone, i.e. BIAN vs. DAB vs. BICAT, constitutes a more powerful way to tune the electronic properties of the ligand system than variations of the *N*-aryl substituents within a given backbone series. However, regardless of the backbone structure, the rate of protonation appears to be primarily controlled by steric factors, best modulated by the presence, or not, of ortho substituents at the *N*-aryl groups.

3.5. Experimental section

3.5.1 General considerations

In signal assignments, the terms Ar$H_{o,m,p}$ denotes protons in the *o*, *m*, *p* positions of the diimine *N*-aryl substituents (relative to N-attached carbon), Ph$H_{o,m,p}$ denotes the *o*, *m*, *p* protons of the Pt-phenyl ligands, and An$H_{o,m,p}$ denotes protons in the *o*, *m*, *p* positions of the BIAN skeleton (relative to attachment point of the 5-membered ring). IR spectra were recorded on a Perkin Elmer Spectrum One spectrometer. Elemental analyses were performed by Mikro Kemi AB, Uppsala, Sweden. Mass spectra were recorded on a Waters Micromass Q-TOF2W instrument. MS data are given as *m/z* values.

3.5.2 X-ray crystallographic structure determinations

Crystals of **1b**, **1c**, **1f**, **1g**, **4b-c**, **7b**, and **7c** were grown from dichloromethane/pentane. The crystals were mounted on glass fiber with perfluoropolyether, and the data were collected at 105 K on a Siemens 1K SMART CCD diffractometer using graphite-monochromated Mo Kα radiation. Data collection method: ω-scan, range 0.3°, crystal to detector distance 5 cm. Data reduction and cell determination were carried out with the SAINT and XPREP programs.[166] Absorption corrections were applied by the use of the SADABS program.[167] All

the structures were solved using the Sir92[168] or Sir97[169] programs and refined on *F* using the program Crystals.[170] The non-hydrogen atoms were refined with anisotropic thermal parameters; the H atoms were all located in a difference map, but those attached to carbon atoms were repositioned geometrically. The H atoms were initially refined with soft restraints on the bond lengths and angles to regularize their geometry (C-H in the range 0.93-98 Å) and isotropic ADPs (U(H) in the range 1.2-1.5 × U_{equiv} of the adjacent atom), after which they were refined with riding constraints.

3.5.3 Synthetic procedures

The Ar-BIAN ligands,[138,161,171] the Ar-BICAT precursor[172] Ar'N=C(Cl)-C(Cl)=NAr' with Ar' = 4-MeC_6H_4, and $Ph_2Pt(SMe_2)_2$[120] were prepared according to published procedures.

Ar-BICAT with Ar = 4-MeC_6H_4. To a solution of pyrocatechol (277 mg, 2.51 mmol) in THF (20 mL) was added NaH (181 mg, 7.6 mmol). After 45 min and the end of gas evolution, the resulting solution was added dropwise to a solution of Ar'N=C(Cl)-C(Cl)=NAr' (640 mg, 2.10 mmol) in THF (40 mL), upon which a progressive green coloration appeared. The mixture was stirred overnight at room temperature. Solid ammonium chloride (400 mg, 7.5 mmol) was added and the mixture was stirred for an additional 15 min. After filtration, the solution was concentrated, and the resulting solid was stirred in pentane for 1 h. The extracts were evaporated to give a white solid (450 mg, 63 %) that was sufficiently pure (ca. 95% by ^{1}H NMR) for the following coordination at Pt. The ligand itself revealed difficult to purify due to decomposition on silica gel (attempted purification of the ligand by chromatography on silica, filtration through celite, or extraction were unsuccessful). ^{1}H NMR (200 MHz, CD_2Cl_2) δ 7.24 (br, 8 H, Ar$H_{o,m}$), 7.10-7.07 (m, AA'BB' pattern, 4 H, catechole-*H*), 2.39 (s, 6 H, Ar*Me*). ^{13}C {^{1}H} NMR (75 MHz, CD_2Cl_2) δ 139.4, 135.9, 129.7, 124.9, 123.7, 116.8, 98.9, 21.2. EI-MS *m/z* 342 (62, M^+), 327 (22), 225 (100).

General procedure for preparation of (Ar-BIAN)$PtPh_2$ (1b-g) and (Ar-BICAT)$PtPh_2$ (1h). The complexes (diimine)$PtPh_2$ were prepared from $Ph_2Pt(SMe_2)_2$ and the appropriate diimine ligand by adapting a literature procedure.[81] A mixture of $Ph_2Pt(SMe_2)_2$ (ca. 300 mg, 63 mmol) and the diimine (ca. 250 mg, 63 mmol) was stirred overnight at room temperature in toluene (15 mL). The solution was concentrated and dichloromethane (ca. 15

mL) was added. The solution was filtered, and concentrated again. The resulting solid was washed with pentane and dried in air to afford the desired complex as a deep green solid in 63-92% yields.

(2,6-$Me_2C_6H_3$-BIAN)$PtPh_2$ (1b). From $Ph_2Pt(SMe_2)_2$ (300 mg, 0.63 mmol) and the corresponding diimine (246 mg, 0.63 mmol); yield, 380 mg (82 %); green microcrystals. ^{1}H NMR (200 MHz, CD_2Cl_2): δ 8.21 (d, *J* = 8.0 Hz, 2 H, AnH_p), 7.40 (dd, *J* = 7.2, 7.1 Hz,, *J* = 7.2 Hz, 2 H, AnH_m), 7.08 (br, 6 H, Ar$H_{m,p}$), 7.03 (d, *J* = 6.6 Hz; $^3J(^{195}$Pt-H) = 54.2 Hz, 4 H, PhH_o), 6.79 (d, *J* = 7.3 Hz, 2 H, AnH_o), 6.62-6.45 (m, 6 H, Ph$H_{m,p}$), 2.30 (s, 12 H, Ar*Me*); ^{13}C{ NMR (75 MHz, CD_2Cl_2) δ 145.3, 137.6, 130.0, 128.4, 126.9, 125.8, 122.6, 121.5, 98.9, 98.8, 17.8; ^{195}Pt{^{1}H} NMR (107 MHz, CD_2Cl_2) δ -2770. Anal. Calcd for $C_{40}H_{34}N_2Pt$: C, 65.12; H, 4.64; N, 3.80. Found: C, 64.92; H, 4.54; N, 3.84.

(2,4,6-$Me_3C_6H_2$-BIAN)$PtPh_2$ (1c). From $Ph_2Pt(SMe_2)_2$ (500 mg, 1.05 mmol) and the corresponding diimine (438 mg, 1.05 mmol); yield, 705 mg (87 %); green microcrystals. ^{1}H NMR (300 MHz, CD_2Cl_2) δ 8.20 (d, *J* = 8.4 Hz, 2 H, AnH_p), 7.40 (dd, *J* = 7.4, 7.3 Hz, 2 H, AnH_m), 7.01 (dd, *J* = 7.2, 1.4 Hz, ^3J (^{195}Pt-H) = 66.6 Hz, 4 H, PhH_o), 6.86 (br s, 4 H, ArH_m), 6.82 (d, *J* = 7.2 Hz, 2 H, AnH_o), 6.59 (br t, *J* = 7.2 Hz, 4 H, PhH_m), 6.50 (tt, *J* = 7.0, 1.4 Hz, 2 H, PhH_p), 2.32 (s, 6 H, ArMe_p), 2.23 (s, 12 H, ArMe_o); ^{13}C{^{1}H} (125 MHz, CD_2Cl_2) δ 171.5, 143.0, 137.8, 136.6, 132.5, 130.0, 129.9, 129.0, 128.8, 125.7, 122.6, 121.5, 21.0, 17.7; ^{195}Pt{^{1}H} NMR (107 MHz, CD_2Cl_2) δ -2777. Anal. Calcd for $C_{42}H_{40}N_2Pt$: C, 65.70; H, 5.25; N, 3.65. Found: C, 65.25; H, 5.0; N, 3.75.

(4-Br-2,6-$Me_2C_6H_2$-BIAN)$PtPh_2$ (1d). From $Ph_2Pt(SMe_2)_2$ (300 mg, 0.63 mmol) and the corresponding diimine (344 mg, 0.63 mmol); yield, 443 mg (78 %); green microcrystals. ^{1}H NMR (300 MHz, CD_2Cl_2) δ (d, *J* = 8.2 Hz, 2 H, AnH_p), 7.46 (dd, *J* = 8.3, 7.3 Hz, 2 H, AnH_m), 7.22 (br s, 4 H, ArH_m), 7.01 (dd, *J* = 7.5, 3.3 Hz, ^3J (^{195}Pt-H) = 70.8 Hz, 4 H, PhH_o), 6.96 (d, 2 H, *J* = 7.1 Hz, AnH_o), 6.64 (br t, *J* = 7.0 Hz, 4 H, PhH_m), 6.56 (tt, *J* = 7.2, 2.4 Hz, 2 H, PhH_p), 2.27 (s, 12 H, Ar*Me*); ^{13}C{^{1}H} NMR (75 MHz, CD_2Cl_2) δ 171.5, 144.3, 141.3, 137.4, 132.7, 131.6, 131.1, 130.5, 128.7, 126.1, 122.8, 121.9, 119.9, 17.7; ^{195}Pt{^{1}H} NMR (107 MHz, CD_2Cl_2) δ -2750. Anal. Calcd for $C_{40}H_{34}Br_2N_2Pt$: C, 53.52; H, 3.82; N, 3.12; Found: C, 53.30; H, 3.65; N, 3.20.

(3,5-$Me_2C_6H_3$-BIAN)$PtPh_2$ (1e). From $Ph_2Pt(SMe_2)_2$ (300 mg, 0.63 mmol) and the corresponding diimine (246 mg, 0.63 mmol); yield, 422 mg (91 %); green microcrystals. ^{1}H NMR (300 MHz, CD_2Cl_2) δ 8.18 (d, *J* = 7.7 Hz, 2 H, AnH_p), 7.42 (dd, *J* = 7.2, 7.2 Hz, 2 H, AnH_m), 7.23 (d, *J* = 7.2 Hz, 2 H, AnH_o), 6.97 (dd, *J* = 8.1, 1.4 Hz, $^3J(^{195}$Pt-H) = 71.8 Hz, 4 H,

PhH_o), 6.87 (br s, 2 H, ArH_p), 6.70 (br s, 4 H, ArH_o), 6.65 (br t, J = 7.5 Hz, 4 H, PhH_m), 6.53 (tt, J = 7.2, 1.5 Hz, 2 H, PhH_p), 2.21 (s, 12 H, Ar*Me*); $^{13}C\{^1H\}$ NMR (75 MHz, CD_2Cl_2) δ 138.9, 137.8, 129.9, 129.4, 128.8, 126.1, 123.8, 121.7, 120.3, 21.2; $^{195}Pt\{^1H\}$ NMR (107 MHz, CD_2Cl_2) δ -2849. Anal. Calcd for $C_{40}H_{34}N_2Pt$: C, 65.12; H, 4.64; N, 3.80. Found: C, 64.85; H, 4.70; N, 3.90.

(4-MeC_6H_4-BIAN)PtPh_2 (1f). From $Ph_2Pt(SMe_2)_2$ (264 mg, 0.56 mmol) and the corresponding diimine (200 mg, 0.56 mmol); yield, 270 mg (68 %); green microcrystals. ^1H NMR (300 MHz, CD_2Cl_2) δ 8.18 (d, J = 8.2 Hz, 2 H, AnH_p), 7.40 (t, J = 7.2 Hz, 2 H, AnH_m), 7.12 (app d, J = 7.8 Hz, 6 H, Ar*H* and AnH_o), 6.98 (d, J = 8.3 Hz, 4 H, Ar*H*), 6.92 (dd, J = 8.3, 1.3 Hz, $^3J(^{195}Pt\text{-}H)$ = 40.1 Hz, 4 H, PhH_o), 6.62 (br t, J = 6.9 Hz, 4 H, PhH_m), 6.54 (tt, J = 7.3, 1.4 Hz, 2 H, PhH_p), 2.39 (s, 6 H, Ar*Me*); $^{13}C\{^1H\}$ NMR (75 MHz, CD_2Cl_2) δ 138.2, 137.5, 129.9, 129.5, 129.4, 126.2, 123.8, 122.3, 121.6, 21.2; $^{195}Pt\{^1H\}$ NMR (107 MHz, CD_2Cl_2) δ -2851. Anal. Calcd for $C_{38}H_{32}N_2Pt$: C, 64.12; H, 4.53; N, 3.94. Found: C, 64.00; H, 4.20; N, 4.00.

(4-$CF_3C_6H_4$-BIAN)PtPh_2 (1g). From $Ph_2Pt(SMe_2)_2$ (370 mg, 0.78 mmol) and the corresponding diimine (365 mg, 0.78 mmol). The product was purified by chromatography on silica with dichloromethane-pentane (1:1). Yield, 370 mg (92 %); green microcrystals. ^1H NMR (200 MHz, CD_2Cl_2) δ 8.24 (d, J = 8.1 Hz, 2 H, AnH_p), 7.54 (d, J = 8.3 Hz, 4 H, ArH_m), 7.44 (d, J = 7.2, 7.2 Hz, 2 H, AnH_m), 7.20 (app d, J = 7.5 Hz, 6 H, AnH_o and ArH_o), 6.86 (dd, J = 8.0, 1.6 Hz, $^3J(^{195}Pt\text{-}H)$ = 64.7 Hz, 4 H, PhH_o), 6.67-6.55 (m, 6 H, Ph$H_{m,p}$); $^{13}C\{^1H\}$ NMR (75 MHz, CD_2Cl_2) δ 141.4, 137.7, 130.8, 129.7, 128.0, 126.5, 126.3, 124.0, 123.0, 122.1; ^{19}F NMR (188 MHz, CD_2Cl_2) δ -62.57; $^{195}Pt\{^1H\}$ NMR (107 MHz, CD_2Cl_2) δ -2782. Anal. Calcd for $C_{38}H_{24}F_6N_2Pt$: C, 55.82; H, 2.96; N, 3.43. Found: C, 55.7; H, 3.00; N, 3.50.

(4-MeC_6H_4-BICAT)PtPh_2 (1h). The diimine (350 mg, 1 mmol) was added to a toluene suspension of $Ph_2Pt(SMe_2)_2$ (485 mg, 1 mmol) and stirred overnight under inert atmosphere. Filtration and concentration gave a red mixture that was purified by chromatography on silica with dichloromethane-pentane (1:1). Yield, 488 mg (69 %); red microcrystals. ^1H NMR (300 MHz, CD_2Cl_2) δ 7.19 and 7.11 (two m, AA'BB' pattern, 2 H each, catechole-*H*), 6.98 (br d, J = 8.3 Hz, 4 H, Ar*H*), 6.92-6.86 (m, 8 H, Ar*H* and PhH_o), 6.57-6.53 (m, 6 H, Ph$H_{m,p}$), 2.30 (s, 3 H, Ar*Me*); ^{13}C NMR (75 MHz, CD_2Cl_2) δ 140.9, 138.3, 138.2, 138.0, 137.4, 128.7, 126.7, 126.2, 124.0, 121.5, 117.4, 21.1; $^{195}Pt\{^1H\}$ NMR (107 MHz, CD_2Cl_2) δ -3384. Anal. Calcd for $C_{34}H_{28}N_2O_2Pt{\cdot}H_2O$: C, 57.54; H, 4.26; N, 3.96. Found: C, 57.65; H, 4.17; N, 4.10.

General procedure for in situ generation of (N–N)PtPh$_2$H(NCCD$_3$)$^+$ (2b-h) as their BF$_4^-$ salts. The appropriate (N–N)PtPh$_2$ complex **1** (ca. 4 mg, 5 μmol) was dissolved in CD_2Cl_2 (400 μL) and kept under inert atmosphere at -78 °C in an NMR tube. A pre-made mixture of $HBF_4{\cdot}Et_2O$ (5 μL, ca. 40 μmol) in CD_3CN (100 μL) and CD_2Cl_2 (200 μL) was then carefully layered on top of the solution of **1** in CD_2Cl_2 and the tube with contents was maintained at -78 °C in a dry ice/acetone bath without mixing of the layers. This procedure was used to minimize premature protonation of the Pt complex **1**. The tube was shaken to mix the layers immediately before it was transferred to the pre-cooled NMR probe at the desired temperature. The low-temperature ^{1}H NMR spectra indicated clean conversion of compounds **1** into the corresponding Pt(IV) hydrides **2**. No traces of the Pt(II) species (N-N)PtPh(NCCD$_3$)$^+$ (**4**) were seen.

(2,6-Me$_2$C$_6$H$_3$-BIAN)PtPh$_2$H(NCCD$_3$)$^+$BF$_4^-$ (2b·BF$_4^-$). ^{1}H NMR (500 MHz, CD_2Cl_2, -78 °C) δ 8.24 (d, *J* = 8.3 Hz, 2 H, An*H*$_p$), 7.56 (t, *J* = 7.8 Hz, 2 H, An*H*$_m$), 7.19 (t, *J* = 7.6 Hz, 2 H, Ar*H*$_p$), 7.13 (d, *J* = 7.5 Hz, 2 H, Ar*H*$_m$), 7.06 (d, *J* = 7.3 Hz, 2 H, Ar*H*$_m$), 6.89-6.60 (m, 8 H, Ph*H*$_{o,p}$ and An*H*$_o$), 6.61 (t, *J* = 7.6 Hz, 4 H, Ph*H*$_m$), 2.19 (s, 6 H, Ar*Me*), 2.00 (s, 6 H, Ar*Me*), -20.89 (s, $^1J(^{195}$Pt-H) = 1598 Hz, 1 H, Pt*H*).

(2,4,6-Me$_3$C$_6$H$_2$-BIAN)PtPh$_2$H(NCCD$_3$)$^+$BF$_4^-$ (2c·BF$_4^-$). ^{1}H NMR (500 MHz, CD_2Cl_2, -78 °C) δ 8.23 (d, *J* = 8.2 Hz, 2 H, An*H*$_p$), 7.55 (t, *J* = 7.9 Hz, 2 H, An*H*$_m$), 6.86 (s, 2 H, Ar*H*$_m$), 6.80 (s, 2 H, Ar*H*$_m$), 6.80-6.68 (m, 8 H, An*H*$_o$, Ph*H*$_{o,p}$), 6.62 (br t, *J* = 7.5 Hz, 4 H, Ph*H*$_m$), 2.28 (s, 6 H, Ar*Me*), 2.12 (s, 6 H, Ar*Me*), 1.93 (s, 6 H, Ar*Me*), -20.99 (s, $^1J(^{195}$Pt-H) = 1605 Hz, 1 H, Pt*H*).

(4-Br-2,6-Me$_2$C$_6$H$_2$-BIAN)PtPh$_2$H(NCCD$_3$)$^+$BF$_4^-$ (2d·BF$_4^-$). ^{1}H NMR (500 MHz, CD_2Cl_2, -78 °C) δ 8.28 (d, *J* = 8.3 Hz, 2 H, An*H*$_p$), 7.61 (t, *J* = 7.8 Hz, 2 H, An*H*$_m$), 7.31 (s, 2 H, Ar*H*$_m$), 7.22 (s, 2 H, Ar*H*$_m$), 6.92 (d, *J* = 7.4 Hz, 2 H, An*H*$_o$), 6.84-6.70 (m, 6 H, Ph*H*$_{o,p}$), 6.66 (br t, ^3J = 7.4 Hz, 4 H, Ph*H*$_m$), 2.18 (s, 6 H, Ar*Me*), 1.97 (s, 6 H, Ar*Me*), -20.90 (s, $^1J(^{195}$Pt-H) = 1593 Hz, 1 H, Pt-*H*).

(3,5-Me$_2$C$_6$H$_3$-BIAN)PtPh$_2$H(NCCD$_3$)$^+$BF$_4^-$ (2e·BF$_4^-$). ^{1}H NMR (500 MHz, CD_2Cl_2, -78 °C) δ 8.22 (d, *J* = 8.3 Hz, 2 H, An*H*$_p$), 7.58 (t, *J* = 7.9 Hz, 2 H, An*H*$_m$), 7.27 (d, *J* = 7.3 Hz, 2 H, An*H*$_o$), 7.00-6.83 (m, 6 H, Ph*H*$_o$ and Ar*H*$_o$), 6.75 (br t, *J* = 7.2 Hz, 2 H, Ph*H*$_p$), 6.69-6.64 (m, 6 H, Ph*H*$_m$ and Ar*H*$_o$), 6.51 (s, 2 H, Ar*H*$_p$), 2.18 (s, 6 H, Ar*Me*), 2.10 (s, 6 H, Ar*Me*), -21.46 (s, $^1J(^{195}$Pt-H) = 1608 Hz, 1 H, Pt*H*).

(4-MeC$_6$H$_4$-BIAN)PtPh$_2$H(NCCD$_3$)$^+$BF$_4^-$ (2f·BF$_4^-$). ^{1}H NMR (500 MHz, CD_2Cl_2, -78 °C) δ 8.22 (d, *J* = 8.3 Hz, 2 H, An*H*$_p$), 7.56 (t, *J* = 7.9 Hz, 2 H, An*H*$_m$), 7.14-7.09 (m, 6 H,

Ar*H* and AnH_o), 6.95 (d, *J* = 7.9 Hz, 2 H, Ar*H*), 6.93- 6.84 (m, 6 H, Ar*H* and PhH_o), 6.76 (t, *J* = 7.3 Hz, 2 H, PhH_p), 6.62 (t, *J* = 7.5 Hz, 4 H, PhH_m), 2.33 (s, 6 H, Ar*Me*), -21.37 (s, $^1J(^{195}$Pt-H) = 1608 Hz, 1 H, Pt*H*).

(4-$CF_3C_6H_4$-BIAN)$PtPh_2H(NCCD_3)^+BF_4^-$ (2g·BF_4^-). ^{1}H NMR (500 MHz, CD_2Cl_2, -78 °C) δ 8.27 (d, *J* = 8.3 Hz, 2 H, AnH_p), 7.62 (d, *J* = 8.5 Hz, 2 H, Ar*H*), 7.60 (t, *J* = 7.9 Hz, 2 H,AnH_m), 7.55 (d, *J* = 8.3 Hz, 2 H, Ar*H*), 7.35 (d, *J* = 7.9 Hz, 2 H, Ar*H*), 7.17 (d, *J* = 7.3 Hz, 2 H, AnH_o), 7.10 (d, *J* = 8.0 Hz, 2 H, Ar*H*), 6.84 (d, *J* = 7.5 Hz, $^3J(^{195}$Pt-H) = 60.3 Hz, 4 H, PhH_o), 6.75 (br t, *J* = 7.3 Hz, 2 H, PhH_p), 6.60 (br t, *J* = 7.4 Hz, 4 H, PhH_m), -21.15 (s, $^1J(^{195}$Pt-H) = 1592 Hz, 1 H, Pt*H*).

(4-MeC_6H_4-BICAT)$PtPh_2H(NCCD_3)^+BF_4^-$ (2h·BF_4^-). ^{1}H NMR (500 MHz, CD_2Cl_2, -78 ºC) δ 7.21-7.19 (m, 2 H, catechole-*H*), 7.11-7.09 (m, 2 H, catechole-*H*), 6.95 (br d, *J* = 7.9 Hz, 4 H, Ar*H*), 6.82-6.79 (m, 8 H, Ar*H* and PhH_o), 6.74 (br t, *J* = 7.5 Hz, 2 H, PhH_p), 6.59 (br t, *J* = 7.9 Hz, 4 H, PhH_m), 2.23 (s, 6 H, Ar*Me*), -21.61 (s, $^1J(^{195}$Pt-H) = 1594 Hz, 1 H, Pt*H*).

General procedure for the synthesis of (N–N)$PtPh(NCMe)^+$ (4b-h) as their BF_4^- salts. HBF_4·Et_2O (22 μL, 0.16 mmol) was added dropwise to a stirred solution of (N–N)$PtPh_2$ (ca. 100 mg, depending on the diimine, 0.14 mmol) in acetonitrile at 0 °C under an argon atmosphere. The solution was stirred and gradually warmed to ambient temperature. After 1 h the solvent was removed under vacuum, and the resulting red-orange solid was washed several times with ether. The product was recrystallized from a dichloromethane solution layered with ether.

(2,6-$Me_2C_6H_3$-BIAN)$PtPh(NCMe)^+BF_4^-$ (4b·BF_4^-). From **1b** (113 mg, 0.15 mmol). Yield, 88 mg (73 %). ^{1}H NMR (300 MHz, CD_2Cl_2) δ 8.35 (d, *J* = 7.1 Hz, 1 H, AnH_p), 8.33 (d, *J* = 7.1 Hz, 1 H, AnH_p), 7.64 (dd, *J* = 8.3 Hz, *J* = 8.3 Hz, 1 H, AnH_m), 7.54 (dd, *J* = 8.3 Hz, *J* = 8.3 Hz, 1 H, AnH_m), 7.44 (br, 3 H, Ar*H*), 7.22 (t, *J* = 8.3 Hz, 1 H, ArH_p), 7.16 (d, *J* = 7.0 Hz, 1 H, AnH_o), 7.09 (d, *J* = 7.7 Hz, 2 H, ArH_m), 6.89-6.87 (m, 2 H, PhH_o), 6.74-6.71 (m, 3 H, Ph$H_{m,p}$), 6.69 (d, *J* = 7.2 Hz, 1 H, AnH_o), 2.50 (s, 6 H, Ar*Me*), 2.24 (s, 6 H, Ar*Me*), 2.06 (s, ^4J(Pt-H) = 10.3 Hz, 3 H, NC*Me*); ^{13}C{^{1}H} NMR (75 MHz, CD_2Cl_2) δ 148.2, 142.2, 135.1, 133.7, 133.0, 132.2, 130.5, 130.4, 140.0, 129.6, 129.4, 129.1, 127.0, 125.6, 125.5, 125.2, 124.9, 18.0, 17.9, 3.2; ^{19}F NMR (188 MHz, CD_2Cl_2) δ -153.02, -153.07 ($^{10}BF_4^-$ and $^{11}BF_4^-$); ^{195}Pt NMR (107 MHz, CD_2Cl_2) δ -3170. Elem. Anal. Calc. for $C_{36}H_{32}BF_4N_3Pt$: C, 54.8; H, 4.1; N, 5.3. Found: C, 54.0; H, 4.3; N, 5.3. ESI MS *m/z*: 701.1 (M^+).

(2,4,6-$Me_3C_6H_2$-BIAN)$PtPh(NCMe)^+BF_4^-$ (4c·BF_4^-). From **1c** (100 mg, 0.13 mmol). Yield, 90 mg (85 %). ^{1}H NMR (300 MHz, CD_2Cl_2) δ 8.35 (d, *J* = 7.9 Hz, 1 H, AnH_p), 8.33 (d,

J = 7.6 Hz, 1 H, AnH_p), 7.64 (dd, *J* = 7.4, 7.3 Hz, 1 H, AnH_m), 7.54 (dd, *J* = 7.5, 7.2 Hz, 1 H, AnH_m), 7.24 (br s, 2 H, ArH_m), 7.18 (d, *J* = 7.2 Hz, 1 H, AnH_o), 6.89 (br s, 2H, ArH_m), 6.89-6.85 (m, 2 H, PhH_o), 6.75-6.72(m, 4 H, AnH_o and Ph$H_{m,p}$), 2.47 (s, 3 H, ArMe_p), 2.45 (s, 6 H, ArMe_o), 2.30 (s, 3 H, ArMe_p), 2.16 (s, 6 H, ArMe_o), 2.07 (s, 3 H, NC*Me*); $^{13}C\{^1H\}$ NMR (75 MHz, CD_2Cl_2) δ 178.9, 148.0, 140.2, 139.9, 139.4, 139.1, 135.3, 133.5, 132.8, 130.4, 130.3, 130.1, 129.9, 129.6, 128.8, 126.9, 125.7, 125.5, 124.9, 21.2, 21.1, 17.9, 17.2, 3.2; ^{19}F NMR (188 MHz, CD_2Cl_2) δ -153.11, -153.16 ($^{10}BF_4^-$ and $^{11}BF_4^-$); ^{195}Pt NMR (107 MHz, CD_2Cl_2) δ −3164. Anal. Calcd for $C_{38}H_{36}BF_4N_3Pt$: C, 55.9; H, 4.4; N, 5.2. Found: C, 55.0; H, 4.5; N, 5.0. ESI MS *m/z* 729.1 (M^+).

(4-Br-2,6-$Me_2C_6H_2$-BIAN)PtPh(NCMe)$^+BF_4^-$ (4d·BF_4^-). From **1d** (100 mg, 0.11 mmol). Yield, 71 mg (68 %). ^1H NMR (300 MHz, CD_2Cl_2) δ 8.41 (d, *J* = 8.4 Hz, 1 H, AnH_p), 8.38 (d, *J* = 8.4 Hz, 1 H, AnH_p), 7.69 (dd, *J* = 8.3, 8.3 Hz, 1 H, AnH_m), 7.62 (br s, 2 H, ArH_m), 7.60 (dd, *J* = 8.3, 8.3 Hz, 1 H, AnH_m), 7.24 (br s, 2 H, ArH_m), 7.21 (d, *J* = 7.1 Hz, 1 H, AnH_o), 6.86-6.77 (m, 6 H, AnH_o and Ph$H_{o,m,p}$), 2.49 (s, 6 H, Ar*Me*), 2.21 (s, 6 H, Ar*Me*), 2.19 (br s, 3 H, NC*Me*); $^{13}C\{^1H\}$ NMR (75 MHz, CD_2Cl_2) δ 178.9, 172.7, 148.4, 141.5, 134.9, 134.2, 133.5, 132.4, 132.3, 132.1, 131.5, 130.6, 130.5, 127.3, 125.6, 125.2, 125.1, 124.9, 122.6, 122.2, 17.9, 17.8, 3.5; ^{19}F NMR (188 MHz, CD_2Cl_2) δ -152.61, -152.65 ($^{10}BF_4^-$ and $^{11}BF_4^-$); ^{195}Pt NMR (107 MHz, CD_2Cl_2) δ -3177. Anal. Calcd for $C_{36}H_{30}BBr_2F_4N_3Pt$: C, 45.7; H, 3.2; N, 4.4. Found: C, 44.7; H, 3.2; N, 4.2. ESI MS *m/z*: 857.9, 859.9 (M^+).

(3,5-$Me_2C_6H_3$-BIAN)PtPh(NCMe)$^+BF_4^-$ (4e·BF_4^-). From **1e** (100 mg, 0.14 mmol. Yield, 82 mg (76 %). ^1H NMR (300 MHz, CD_2Cl_2) δ 8.30 (d, *J* = 8.2 Hz, 1 H, AnH_p), 8.28 (d, *J* = 8.1 Hz, 1 H, AnH_p), 7.62 (dd, *J* = 7.4, 8.2 Hz, 1 H, AnH_m), 7.52 (dd, *J* = 7.5, 8.3 Hz, 1 H, AnH_m), 7.47 (d, *J* = 7.1 Hz, 1 H, AnH_o), 7.24 (br s, 1 H, ArH_p), 7.15 (br s, 2 H, ArH_o), 7.02 (d, *J* = 7.1 Hz, 1 H, AnH_o), 6.93 (br s, 1 H, ArH_p), 6.89-6.86 (m, 2 H, PhH_o), 6.77-6.71 (m, 3 H, Ph$H_{m,p}$), 6.61 (br s, 2 H, ArH_o), 2.50 (s, 6 H, Ar*Me*), 2.20 (s, 6 H, Ar*Me*), 2.19 (s, 3 H, NC*Me*); $^{13}C\{^1H\}$ NMR (75 MHz, CD_2Cl_2) δ 144.4, 140.8, 139.9, 135.5, 133.0, 132.5, 131.2, 130.5, 129.7, 126.3, 125.6, 124.7, 120.5, 119.2, 21.5, 21.1, 3.7; ^{19}F NMR (188 MHz, CD_2Cl_2) δ -153.04, -153.10 ($^{10}BF_4^-$ and $^{11}BF_4^-$); ^{195}Pt NMR (107 MHz, CD_2Cl_2) δ -3216. Anal. Calcd for $C_{36}H_{32}BF_4N_3Pt$: C, 54.8; H, 4.1; N, 5.3. Found: C, 53.8; H, 4.3; N, 5.7. ESI MS *m/z*: 701.1 (M^+).

(4-MeC_6H_4-BIAN)PtPh(NCMe)$^+BF_4^-$ (4f·BF_4^-). From **1f** (100 mg, 0.14 mmol). Yield, 58 mg (54 %). ^1H NMR (300 MHz, CD_2Cl_2) δ 8.30 (d, *J* = 8.2 Hz, 1 H, AnH_p), 8.28 (d, *J* = 7.8 Hz, 1 H, AnH_p), 7.62 (t, *J* = 7.8 Hz, 1 H, AnH_m), 7.57- 7.45 (m, 6 H, An$H_{o,m}$ and

Ar*H*), 7.11 (d, *J* = 8.0 Hz, 2 H, Ar*H*), 6.93-6.85 (m, 5 H, Ar*H*, AnH_o and PhH_o), 6.74-6.72 (m, 3 H, Ph$H_{m,p}$), 2.57 (s, 3 H, Ar*Me*), 2.36 (s, 3 H, Ar*Me*), 2.20 (br s, 3 H, NC*Me*); $^{13}C\{^1H\}$ NMR (75 MHz, CD_2Cl_2) δ 178.6, 171.4, 147.9, 142.4, 142.0, 140.5, 139.7, 135.8, 133.1, 132.5, 132.2, 130.9, 130.7, 130.2, 129.6, 127.2, 126.2, 125.9, 125.5, 125.1, 124.5, 122.8, 121.9, 21.4, 21.6, 3.8; ^{19}F NMR (188 MHz, CD_2Cl_2) δ -152.88, -152.93 ($^{10}BF_4^-$ and $^{11}BF_4^-$); ^{195}Pt NMR (107 MHz, CD_2Cl_2) δ -3216. Anal. Calcd for $C_{34}H_{28}BF_4N_3Pt$: C, 53.7; H, 3.7; N, 5.5. Found: C, 51.3; H, 3.8; N, 5.1. ESI MS *m/z*: 673.1 (M^+).

(4-$CF_3C_6H_4$-BIAN)PtPh(NCMe)$^+BF_4^-$ (4g·BF_4^-). From **1g** (100 mg, 0.12 mmol). Yield, 60 mg (56 %). ^1H NMR (300 MHz, CD_2Cl_2) δ 8.34 (d, *J* = 6.8 Hz, 1 H, AnH_p), 8.32 (d, *J* = 7.0 Hz, 1 H, AnH_p), 8.06 (d, *J* = 8.4 Hz, 2 H, Ar*H*), 7.82 (d, *J* = 6.2 Hz, 2 H, Ar*H*), 7.64 (dd, *J* = 7.5, 8.2 Hz, 1 H, AnH_m), 7.58-7.51 (m, 3 H, AnH_m and Ar*H*), 7.39 (d, *J* = 7.3 Hz, 1 H, AnH_o), 7.24 (d, *J* = 8.3 Hz, 2 H, Ar*H*), 6.92 (d, *J* = 8.3 Hz, 1 H, AnH_o), 6.86-6.84 (m, 2 H, PhH_o), 6.72-6.70 (m, 3 H, Ph$H_{m,p}$), 2.21 (s, 3 H, NC*Me*); $^{13}C\{^1H\}$ NMR (75 MHz, CD_2Cl_2) δ 135.5, 133.7, 133.1, 132.3, 129.9, 127.9, 127.6, 127.0, 126.3, 125.9, 125.6, 124.8, 124.0, 123.0, 3.8; ^{19}F NMR (188 MHz, CD_2Cl_2) δ -62.65 (s, Ar-CF_3), -63.02 (s, Ar-CF_3), -152.35 and -152.40 ($^{10}BF_4^-$ and $^{11}BF_4^-$); ^{195}Pt NMR (107 MHz, CD_2Cl_2) δ -3240. Anal. Calcd for $C_{34}H_{22}BF_{10}N_3Pt$: C, 47.0; H, 2.6; N, 4.8. Found: C, 46.2; H, 2.7; N, 4.9; ESI MS *m/z*: 781.0 (M^+).

(4-MeC_6H_4-BICAT)PtPh(NCMe)$^+BF_4^-$ (4h·BF_4^-). From **1h** (100 mg, 0.15 mmol). Yield, 89 mg (83 %). ^1H NMR (200 MHz, CD_2Cl_2) δ 7.43 (br, 4 H, Ar*H*), 7.31-7.20 (m, 3 H, catechole-*H*), 7.14-7.08 (m, 1 H, catechole-*H*), 6.95 (br d, *J* = 7.9 Hz, 2 H, Ar*H*), 6.87 (br d, *J* = 8.1 Hz, 2 H, Ar*H*), 6.83-6.78 (m, 2 H, PhH_o), 6.69-6.63 (m, 3 H, Ph$H_{m,p}$), 2.47 (s, 3 H, Ar*Me*), 2.26 (s, 3 H, Ar*Me*), 2.08 (s, $^4J(^{195}Pt\text{-}NCMe)$ = 13.9 Hz, 3 H, NC*Me*); ^{19}F NMR (188 MHz, CD_2Cl_2) δ -152.15, 152.20 ($^{10}BF_4^-$ and $^{11}BF_4^-$); ESI MS *m/z*: 655.2 (M^+).

General procedure for in situ generation of (N–N)PtPh(η^2-C_6H_6)$^+$ (3b-h) as their BF_4^- salts. The appropriate (N-N)$PtPh_2$ complex (ca. 5 mg, 7 μmol) was dissolved in CD_2Cl_2 (400 μL) and kept under an inert atmosphere at -78 °C in an NMR tube. A pre-made mixture of $HBF_4{\cdot}Et_2O$ (5-10 μL) in Et_2O-d_{10} (80 μL) and CD_2Cl_2, for a total volume of 300 μL, was then carefully layered on top of the solution of **1** in CD_2Cl_2 and the tube with contents was maintained at -78 °C in a dry ice/acetone bath without mixing of the layers. This procedure was used to minimize premature protonation of the Pt complex **1**. The tube was shaken to mix the layers immediately before it was transferred to the pre-cooled NMR probe at the desired

temperature. The low-temperature ^{1}H NMR spectra indicated clean conversion of compounds **1b-h** into the corresponding Pt(II) phenyl π-benzene complexes **3b-h**.

(2,6-Me$_2$C$_6$H$_3$-BIAN)PtPh(η^2-C$_6$H$_6$)$^+$BF$_4^-$ (3b·BF$_4^-$). ^{1}H NMR (500 MHz, CD_2Cl_2, -35 °C) δ 8.29 (d, J = 8.3 Hz, 1 H, AnH_p), 8.24 (d, J = 8.4 Hz, 1 H, AnH_p), 7.51 (t, J = 7.9 Hz, 1 H, AnH_m), 7.46 (t, J = 7.9 Hz, 1 H, AnH_m), 7.40-7.37 (m, 3 H, ArH), 7.07 (s, 6 H, C_6H_6), 7.02 (t, J = 7.6 Hz, 1 H, ArH_p), 6.92 (d, J = 6.7 Hz, 2 H, ArH_m), 6.74 (br d, J = 7.0 Hz, 2 H, PhH_o), 6.52-6.36 (m, 5 H, AnH_o and Ph$H_{m,p}$), 2.29 (s, 6 H, Ar*Me*), 2.20 (s, 6 H, Ar*Me*).

(2,4,6-Me$_3$C$_6$H$_2$-BIAN)PtPh(η^2-C$_6$H$_6$)$^+$BF$_4^-$ (3c·BF$_4^-$). ^{1}H NMR (500 MHz, CD_2Cl_2, -35 °C) δ 8.28 (d, J = 8.3 Hz, 1 H, AnH_p), 8.23 (d, J = 8.4 Hz, 1 H, AnH_p), 7.55 (t, 1 H, J = 8.2 Hz, AnH_m), 7.46 (t, J = 8.1 Hz, 1 H, AnH_m), 7.16 (s, 2 H, ArH_m), 7.05 (s, 6 H, C_6H_6), 6.68 (br s, 4 H, ArH_m and PhH_o), 6.57 (d, J = 8.2 Hz, 1 H, AnH_o), 6.46-6.38 (m, 4 H, AnH_o and Ph$H_{m,p}$), 2.42 (s, 3 H, ArMe_p), 2.25 (s, 6 H, ArMe_o), 2.14 (s, 3 H, ArMe_p), 2.12 (s, 6 H, ArMe_o).

(4-Br-2,6-Me$_2$C$_6$H$_2$-BIAN)PtPh(η^2-C$_6$H$_6$)$^+$BF$_4^-$ (3d·BF$_4^-$). ^{1}H NMR (500 MHz, CD_2Cl_2, -35 °C) δ 8.33 (d, J = 8.4 Hz, 1 H, AnH_p), 8.28 (d, J = 8.4 Hz, 1 H, AnH_p), 7.58-7.49 (m, 4 H, AnH_m and ArH_m), 7.10 (s, 6 H, C_6H_6), 7.06 (s, 2 H, ArH_m), 6.74 (br , 2 H, PhH_o), 6.62 (d, J = 6.4 Hz, 1 H, AnH_o), 6.57-6.55 (m, 2 H, AnH_o and PhH_p), 6.49 (br t, 2 H, J = 7.1 Hz, PhH_m), 2.24 (s, 6 H, Ar*Me*), 2.17 (s, 6 H, Ar*Me*).

(3,5-Me$_2$C$_6$H$_3$-BIAN)PtPh(η^2-C$_6$H$_6$)$^+$BF$_4^-$ (3e·BF$_4^-$). ^{1}H NMR (500 MHz, CD_2Cl_2, -55 °C) δ 8.27 (d, J = 7.3 Hz, 1 H, AnH_p), 8.23 (d, J = 7.4 Hz, 1 H, AnH_p), 7.55 (t, J = 7.5 Hz, 1 H, AnH_m), 7.46 (t, J = 7.7 Hz, 1 H, AnH_m), 7.18 (s, 1 H, ArH_p), 7.12 (s, 6 H, C_6H_6), 7.08 (s, 2 H, ArH_o), 6.77 (d, J = 9.4 Hz, 1 H, AnH_o), 6.71 (s, 1 H, ArH_p), 6.64 (d, J = 7.7 Hz, 1 H, AnH_o), 6.40 (s, 2 H, ArH_o), 6.30-6.22 (m, 5 H, Ph$H_{o,m,p}$), 2.44 (s, 6 H, Ar*Me*), 2.06 (s, 6 H, Ar*Me*).

(4-MeC$_6$H$_4$-BIAN)PtPh(η^2-C$_6$H$_6$)$^+$BF$_4^-$ (3f·BF$_4^-$). ^{1}H NMR (500 MHz, CD_2Cl_2, -78 °C) δ 8.25 (d, J = 8.3 Hz, 1 H, AnH_p), 8.21 (d, J = 8.4 Hz, 1 H, AnH_p), 7.54-7.49 (m, 3 H, AnH_m and 2 ArH), 7.45-7.38 (m, 3 H, AnH_m and ArH), 7.09 (br s, 6 H, C_6H_6), 6.89 (d, J = 8.1 Hz, 2 H, ArH), 6.73-6.71 (m, 3 H, AnH_o and ArH), 6.42 (d, J = 7.4 Hz, 1 H, AnH_o), 6.30-6.26 (m, 3 H, Ph$H_{o,p}$), 6.19 (br t, J = 7.2 Hz, 2 H, PhH_m), 2.46 (s, 3 H, Ar*Me*), 2.18 (s, 3 H, Ar*Me*).

(4-CF$_3$C$_6$H$_4$-BIAN)Pt(η^2-C$_6$H$_6$)Ph]$^+$BF$_4^-$ (3g·BF$_4^-$). ^{1}H NMR (500 MHz, CD_2Cl_2, -55 °C) δ 8.31 (d, J = 8.3 Hz, 1 H, AnH_p), 8.28 (d, J = 9.0 Hz, 1 H, AnH_p), 8.02 (d, J = 7.3 Hz, 2 H, ArH), 7.79 (d, J = 8.3 Hz, 2 H, ArH), 7.56 (t, J = 7.3 Hz, 1 H, AnH_m), 7.47 (t, J = 7.3 Hz, 1 H, AnH_m), 7.36 (d, J = 7.3 Hz, 2 H, ArH), 7.10-7.08 (m, 8 H, C_6H_6 and 2 ArH), 6.72 (d, J =

7.7 Hz, 1 H, AnH_o), 6.57 (d, J = 7.7 Hz, 1 H, AnH_o), 6.31-6.29 (m, 3 H, Ph$H_{o,p}$), 6.19 (t, J = 7.2 Hz, 2 H, PhH_m).

(4-MeC$_6$H$_4$-BICAT)Pt(η^2-C$_6$H$_6$)Ph$^+$BF$_4^-$ (3h·BF$_4^-$). ^{1}H NMR (500 MHz, CD_2Cl_2, -78 ºC) δ 7.36-7.32 (m, 4 H, Ar*H*), 7.22-7.17 (m, 2 H, catechole-*H*), 7.11 (br d, J = 7.8 Hz, 1 H, catechole-*H*), 7.04 (br d, J = 7.9 Hz, 1 H, catechole-*H*), 6.90 (br s, 6 H, C$_6$*H*$_6$), 6.72 (d, J = 8.1 Hz, 2 H, Ar*H*), 6.66 (d, J = 7.2 Hz, 2 H, Ar*H*), 6.25-6.21 (m, 3 H, Ph$H_{o,p}$), 6.08 (br t, J = 7.0 Hz, 2 H, PhH_m), 2.34 (s, 3 H, Ar*Me*), 2.07 (s, 3 H, Ar*Me*).

General procedure for synthesis of (N–N)Pt(NCMe)$_2^{2+}$ (7b-h) as their TfO$^-$ salts. TfOH (ca. 150 μL, 1 mmol) was added dropwise to a stirred solution of (N–N)$PtPh_2$ (ca. 100 mg, 0.10 mmol) in acetonitrile (3 mL) under argon atmosphere. The solution was heated to 50 °C and stirred overnight. The solvent was removed under vacuum, producing an orange solid which was washed several times with ether.

(2,6-Me$_2$C$_6$H$_3$-BIAN)Pt(NCMe)$_2^{2+}$(TfO$^-$)$_2$ (7b·(TfO$^-$)$_2$). From **1b** (80 mg, 0.10 mmol) and TfOH (40 μL, 0.46 mmol). Yield, 78 mg (75 %). ^{1}H NMR (300 MHz, CD_2Cl_2) δ 8.44 (d, J = 8.3 Hz, 2 H, AnH_p), 7.71 (dd, J = 7.4, 7.5 Hz, 2 H, AnH_m), 7.58-7.44 (m, 6 H, Ar$H_{m,p}$), 7.04 (d, J = 7.3 Hz, 2 H, AnH_o), 2.50 (s, 12 H, Ar*Me*), 2.24 (s, 6 H, NC*Me*); ^{13}C{^{1}H} NMR (125 MHz, CD_2Cl_2) δ 136.2, 131.6, 131.1, 130.5, 127.4, 18.0, 3.0; ^{19}F NMR (188 MHz, CD_2Cl_2) δ -78.83; ^{195}Pt NMR (107 MHz, CD_2Cl_2) δ -2391. Anal. Calcd for $C_{34}H_{30}F_6N_4O_6PtS_2$: C, 42.4; H, 3.1; N, 5.8. Found: C, 43.7; H, 3.6; N, 6.2. ESI MS *m/z*: 332.6 (M^{2+}), 312.0 (M^{2+}- MeCN).

(2,4,6-Me$_3$C$_6$H$_2$-BIAN)Pt(NCMe)$_2^{2+}$(TfO$^-$)$_2$ (7c·(TfO$^-$)$_2$). From **1c** (100 mg, 0.13 mmol) and TfOH (40 μL, 0.46 mmol). Yield, 102 mg (79 %). ^{1}H NMR (300 MHz, CD_2Cl_2) δ 8.44 (d, J = 8.2 Hz, 2 H, AnH_p), 7.70 (dd, J = 7.8, 7.7 Hz, 2 H, AnH_m), 7.24 (br s, 4 H, ArH_m), 7.08 (d, J = 7.3 Hz, 2 H, AnH_o), 2.46 (br s, 12 H, ArMe_o), 2.45 (s, 6 H, ArMe_p), 2.34 (s, 6 H, NC*Me*);; ^{13}C{^{1}H} NMR (75 MHz, CD_2Cl_2) δ 182.1, 152.4, 145.8, 141.9, 138.7, 135.8, 132.3, 130.8, 130.5, 127.1, 122.7, 21.3, 18.0, 3.6; ^{19}F NMR (188 MHz, CD_2Cl_2) δ -78.85; ^{195}Pt NMR (107 MHz, CD_2Cl_2) δ -2391. Anal. Calcd for $C_{36}H_{34}F_6N_4O_6PtS_2$: C, 43.6; H, 3.5; N, 5.7. Found: C, 43.3; H, 3.5; N, 5.3. ESI MS *m/z*: 346.6 (M^{2+}), 326.0 (M^{2+}- MeCN).

(4-Br-2,6-Me$_2$C$_6$H$_2$-BIAN)Pt(NCCD$_3$)$_2^{2+}$(TfO$^-$)$_2$ (7d·(TfO$^-$)$_2$). On top of a solution of **1c** (8 mg, 9 μmol) in dichloromethane-d_2 (400 μL) was layered 50 μL of dichloromethane-d_2. Then a premixed solution of TfOH (3 μL, 0.035 mmol)) in acetonitrile-d_3 (200 μL) was added, and the tube was shaken and kept overnight at 50 °C at which point a bright orange solution was obtained. ^{1}H NMR (300 MHz, CD_2Cl_2) δ 8.43 (d, J = 8.1 Hz, 2 H, AnH_p), 7.70

(dd, J = 8.2, 8.2 Hz, 2 H, AnH_m), 7.59 (br s, 4 H, ArH_m), 7.07 (d, J = 7.3 Hz, 2 H, AnH_o), 2.46 (s, 12 H, Ar*Me*).

(3,5-$Me_2C_6H_3$-BIAN)Pt(NCMe)$_2^{2+}$(TfO$^-$)$_2$ (7e·(TfO$^-$)$_2$). From **1e** (100 mg, 0.13 mmol) and TfOH (40 μL, 0.47 mmol). Yield, 85 mg (65 %). ^{1}H NMR (300 MHz, CD_2Cl_2) δ 8.23 (d, J = 8.2 Hz, 2 H, AnH_p), 7.62 (dd, J = 8.2, 8.1 Hz, 2 H, AnH_m), 7.40 (br s, 4 H, ArH_o), 7.30 (br s, 2 H, ArH_p), 7.17 (d, J = 7.3 Hz, 2 H, AnH_o), 2.48 (s, 12 H, Ar*Me*), 2.37 (s, 6 H, NC*Me*); ^{13}C{^{1}H} NMR (75 MHz, CD_2Cl_2) δ 141.4, 134.4, 132.7, 128.9, 127.2, 120.2, 21.4, 3.8; ^{19}F NMR (188 MHz, CD_2Cl_2) δ -78.8; ^{195}Pt NMR (107 MHz, CD_2Cl_2) δ -2397. Anal. Calcd for $C_{34}H_{30}F_6N_4O_6PtS_2$: C, 42.4; H, 3.1; N, 5.8. Found: C, 41.3; H, 3.2; N, 5.4. ESI MS *m/z*: 346.6 (M^{2+}), 326.0 (M^{2+}- MeCN).

(4-MeC_6H_4-BIAN)Pt(NCMe)$_2^{2+}$(TfO$^-$)$_2$ (7f·(TfO$^-$)$_2$). From **1f** (100 mg, 0.14 mmol) and TfOH (50 μL, 0.56 mmol). Yield, 80 mg (61 %). ^{1}H NMR (300 MHz, CD_2Cl_2) δ 8.35 (d, J = 8.1 Hz, 2 H, AnH_p), 7.65 (dd, J = 7.5, 7.3 Hz, 2 H, AnH_m), 7.54 (br, 8 H, Ar*H*), 7.21 (d, J = 7.3 Hz, 2 H, AnH_o), 2.54 (s, 6 H, Ar*Me*), 2.29 (s, 6 H, NC*Me*); ^{13}C{^{1}H} NMR (75 MHz, CD_2Cl_2) δ 141.1, 134.5, 134.1, 131.3, 129.8, 127.1, 123.0, 21.6, 3.9; ^{19}F NMR (188 MHz, CD_2Cl_2) δ -78.7; ^{195}Pt NMR (107 MHz, CD_2Cl_2) δ -2407. Anal. Calcd for $C_{32}H_{26}F_6N_4O_6PtS_2$: C, 41.1; H, 2.8; N, 6.0. Found: C, 39.4; H, 2.9; N, 5.4. ESI MS *m/z*: 318.5 (M^{2+}), 298.0 (M^{2+}-MeCN).

(4-$CF_3C_6H_4$-BIAN)Pt(NCCD$_3$)$_2^{2+}$(TfO$^-$)$_2$ (7g·(TfO$^-$)$_2$). On top of a solution of **1g** (8 mg, 0.01 mmol) in dichloromethane-d_2 (400 μL) was layered 50 μL of dichloromethane-d_2. Then a premixed solution of TfOH (3 μL, 0.035 mmol)) in acetonitrile-d_3 (200 μL) was added, and the tube was shaken and kept overnight at 50 °C at which point a bright orange solution was obtained ^{1}H NMR (200 MHz, CD_2Cl_2) δ 8.37 (d, J = 8.2 Hz, 2 H, AnH_p), 8.02 (dd, J = 9.4, 9.3 Hz, 8 H, Ar*H*), 7.65 (dd, J = 6.8, 7.9 Hz, 2 H, AnH_m), 7.10 (d, J = 7.4 Hz, 2 H, AnH_o); ^{19}F NMR (188 MHz, CD_2Cl_2) δ -62.48 (s, ArCF_3), -78.66 (s, OTf).

General procedure for the preparation and characterization of (diimine)Pt(CO)Ph$^+$BF$_4^-$. (4-MeC_6H_4-DAB)$PtPh_2$ was prepared according to the published procedure.[83] These compounds were prepared solely for IR and ^{1}H NMR characterization by adaptation of a published procedure.[83] $HBF_4{\cdot}Et_2O$ (3-6 μL, 0.02-0.04 mmol) was added to a solution of (diimine)$PtPh_2$ complex (15-30 mg, 0.02-0.04 mmol) in trifluoroethanol (2 mL). After 18 h under a CO atmosphere, the solution was concentrated to give an oily residue. Part of the product was dissolved in CD_2Cl_2 for NMR characterization whereas another part was dissolved in CH_2Cl_2 for IR characterization.

(4-MeC$_6$H$_4$-DAB)Pt(CO)Ph$^+$BF$_4^-$. ^{1}H NMR (200 MHz, CD_2Cl_2) δ 7.39 (d, *J* = 8.1 Hz, 2 H, Ar*H*), 7.25 (d, *J* = 8.5 Hz, 2 H, Ar*H*), 6.92-6.86 (m, 4 H, Ar*H*, PhH_o), 6.86-6.72 (m, 3 H, Ar*H*, PhH_p), 6.63-6.59 (m, 2 H, PhH_m), 2.46 (s, 3 H, DAB*Me*), 2.44 (s, 3 H, DAB*Me*), 2.38 (s, 3 H, Ar*Me*), 2.21 (s, 3 H, Ar*Me*); IR (CH_2Cl_2) ν(CO) 2113.8 cm^{-1}.

(4-MeC$_6$H$_4$-BIAN)Pt(CO)Ph$^+$BF$_4^-$.5f ^{1}H NMR (200 MHz, CD_2Cl_2) δ 8.29 (br d, *J* = 8.2 Hz, 2 H, AnH_p), 7.68 (t, *J* = 7.4 Hz, 2 H, AnH_m), 7.61 (d, *J* = 7.6 Hz, 1 H, AnH_o), 7.55 (br, 4 H, Ar*H*), 7.51 (d, *J* = 7.8 Hz, 1 H, AnH_o), 7.09 (d, *J* = 8.6 Hz, 2 H, Ar*H*), 7.08-7.02 (m, 2 H, PhH_o), 6.99-6.80 (m, 3 H, Ph$H_{m,p}$), 6.84 (d, *J* = 7.6 Hz, 2 H, Ar*H*), 2.56 (s, 3 H, Ar*Me*), 2.35 (s, 3 H, Ar*Me*); IR (CH_2Cl_2) ν(CO) 2115.6 cm^{-1}.

(4-MeC$_6$H$_4$-BICAT)Pt(CO)Ph$^+$BF$_4^-$. 5h ^{1}H NMR (200 MHz, CD_2Cl_2) δ 7.54 (br d, *J* = 8.4 Hz, 2 H, Ar*H*), 7.39 (br d, *J* = 8.3 Hz, 2 Ar*H*), 7.35-7.25 (m, 3 H, catechole-*H*), 7.19-7.16 (m, 1 H, catechole-*H*), 7.05-7.00 (m, 2 H, PhH_o), 6.95-6.75 (m, 7 H, ArH and Ph$H_{m,p}$), 2.47 (s, 3 H, Ar*Me*), 2.25 (s, 3 H, Ar*Me*); IR (CH_2Cl_2) ν(CO) 2113.2 cm^{-1}.

4. Steric and electronic effect investigation on the protonolysis reaction mechanism at a series of (N-N)$PtPh_2$ complexes by complementary ^{1}H NMR and UV-Vis spectroscopy

4.1. Introduction

In order to gain further insight into the (diimine)$PtPh_2$ protonolysis reaction mechanism we decided to investigate the electronic and steric influence on the process by variation of the diimine ligand (Chart 1). Previous observations revealed poor electronic influence on such system by variation of the *N*-aryl group of the diimine.[83] However, tuning of the backbone structure seemed to provide significant electronic influence on the metal centre as previously discussed in Chapter 3. We anticipated that a more electron rich metal centre would stabilize the π-benzene complex and facilitate the study of its chemistry. (π-benzene Pt(II) complex decompose by associative substitution in acetonitrile containing solvent mixtures at low temperature).[81] Electron-rich (N-N)PtPh(π-benzene)$^+$ complex may also facilitate a C-H oxidative addition pathway over σ-CAM during the benzene/phenyl proton exchange. Thus, we successfully substituted the flexible dimethyl substituted diimine backbone (Ar-DAB) by two more rigid diimine backbone ligands, a poorly electron-donating acenaphtene backbone diimine ligand (Ar-BIAN **b-f**), and a strong electron donating catecholate backbone diimine ligand (Ar-BICAT **h)**. To assert more rigorously the electronic and steric influence of the *N*-Aryl group, the present chapter also includes a series of Ar-BIAN ligands.

Chart 1

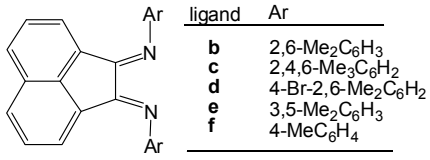

ligand	Ar
b	2,6-$Me_2C_6H_3$
c	2,4,6-$Me_3C_6H_2$
d	4-Br-2,6-$Me_2C_6H_2$
e	3,5-$Me_2C_6H_3$
f	4-MeC_6H_4

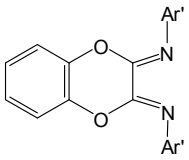

ligand	Ar'
h	4-MeC_6H_4

In this chapter the kinetic investigation results of these processes, *i.e.* protonation followed by benzene elimination are described, Scheme 1. The temperature, concentration, and solvent dependence support the previously envisaged protonolysis mechanism involved. Electronic and steric effect of the diimine are discussed and rationalized.

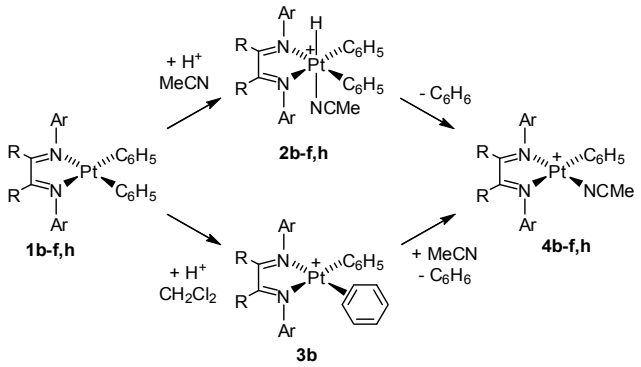

Scheme 1. Succession of mechanistic events investigated here, resulting from the protonation reaction of (N-N)$PtPh_2$ complexes **1b-f,h**

4.2. Results and discussion

4.2.1 Low-temperature protonation of (N-N)$PtPh_2$ in the presence of acetonitrile

Upon protonation in coordinating solvent mixtures of acetonitrile in dichloromethane, (N-N)$PtPh_2$ complexes (**1b-f, h**) all react to give (N-N)$PtPh_2H(NCMe)^+$ (**2b-f, h**) according to Scheme 2 as discussed in Chapter 3.[102,157]

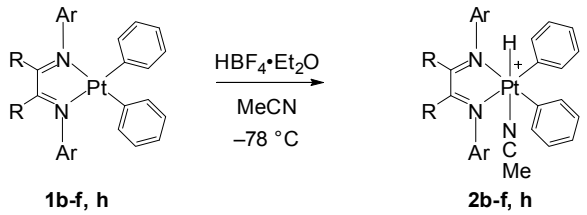

Scheme 2. Low temperature protonation reaction in the presence of acetonitrile

This first reaction step was monitored between -80 °C and -50 °C by time-resolved UV-vis stopped-flow spectroscopy. The acid and the acetonitrile concentrations were systematically changed at -80 °C, always in excess in order to ensure pseudo-first-order conditions. Under such conditions, the protonation always resulted in a drastic UV-vis spectral change over the whole wavelength window. All the complexes showed distinctive decrease in absorbance at

high wavelength (ca 350 - 600 nm) and additionally present clear isobestic point located between 306-320 nm from **1b-f** and at 375 nm from **1h**. Consequently an absorbance increase is observed below the corresponding isobestic point for each complex. However technical issues with the light transmittance when passing through the micro-cuvette immersed in a cold silicon oil bath made the observation of such low wavelength isobestic point not systematic (**1b**) and the kinetic data were, when needed, extracted by reduction to the "clean" portion of the spectra (always above ca 400 nm). A typical example of the time dependent UV-vis spectra is presented in Figure 1 that was fitted to a pseudo-first-order exponential decay.

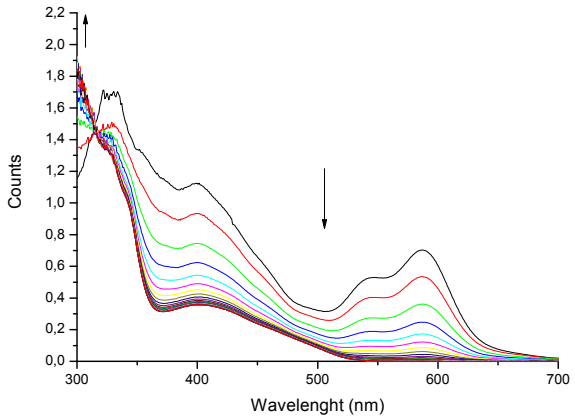

Figure 1. UV-vis time-resolved spectra for the protonation of (Ar-BIAN)$PtPh_2$ **1b** in dichloromethane at -80°C. Experimental conditions: [Pt] 0.125 mM, [$HBF_4.Et_2O$] = 1.17 mM, [MeCN] = 5.74 M. Total duration of the experiment 2 seconds

The resulting pseudo-first-order kinetics were independent in [MeCN] (done for **1b** at 0.95 and 5.74 M, and **1d**: 0.95-5.74M. Lower acetonitrile concentration could not be used due to poor solubility of the acid in dichloromethane. The acid concentration dependence for complex **1b** (1.17 – 25 mM) of the pseudo-first-order rate constant at -80 °C in a 5.74 M acetonitrile solution is presented Figure 2.

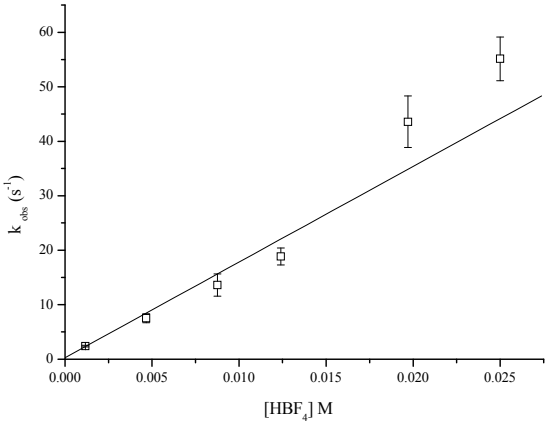

Figure 2. Acid concentration dependence on the protonation of (Ar-BIAN)$PtPh_2$ **1b** at -80 °C. Experimental conditions: [Pt] = 0.125 mM, 5.74 M solution of acetonitrile in dichloromethane.

A zero intercept with the *y* axis is seen (within experimental error) and consequently we conclude that no acid independent process is involved in the kinetics of this reaction. The protonation step follows a second-order kinetic rate law. From the slope of the linear plot of k_{obs} versus [HBF_4.Et_2O] the rate constant was calculated as k (-80 °C) = 2298 ± 192 M^{-1} s^{-1} for complex **1b**. The corresponding rate constants for complexes **1c-d** are reported in Table 1.

Efforts to collect kinetic data revealed more difficult when no methyl substituent in the 2,6 position of the *N*-Aryl groups were present (**1e-f** and **1h**). In these cases, the protonation was extremely fast and less than 150 ms were required to notice complete consumption of the starting material, even at -80 °C, which precluded the collection of kinetic data. We attribute the great rate difference between **1b-d** and **1e, f, h** to the steric shielding caused by the 2,6-Me_2 substituents that block the access to the Pt centre. This is in agreement with crystallographic data that emphasized the steric hindrance around the metal brought by the methyl group in the ortho positions of the *N*-Aryl group.[173]

Temperature dependent kinetic measurements were obtained by recording the time dependent spectra of the protonation of **1b** with a 25 mM acid solution in 30 % [MeCN] (v/v; 5.74 M) in the temperature range of -80 °C to -56 °C. The Eyring plot in Figure 3 shows an excellent linear fit, and the resulting activation parameters are $\Delta H^{\#}$ = 30.2 ± 0.5 $kJmol^{-1}$ and $\Delta S^{\#}$ = -29.8 ± 2.3 $JK^{-1}mol^{-1}$ for complex **1b**.

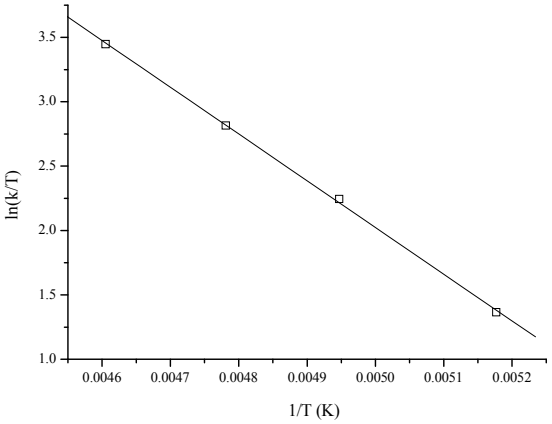

Figure 3. Eyring plot for the protonation reaction of (Ar-BIAN)$PtPh_2$ complex **1b**. Experimental conditions: [Pt] = 0.125 mM, 5.74 M acetonitrile solution in dichloromethane, and 25 mM of [$HBF_4.Et_2O$].

Analogues data were collected for the reaction of complexes **1c-d**. The essentials kinetic data extracted can be found in Table 1.

Based on the rather similar values of $\Delta H^{\#}$ (28- 33 $kJmol^{-1}$) and substantially negative $\Delta S^{\#}$ (-25 to -30 $Jmol^{-1}K^{-1}$) for the protonation of **1b-d**, we conclude that all complexes react in a similar associative manner under the studied conditions. This is in agreement with previously mentioned observation on closely related diimine (Ar-DAB)$PtPh_2$ system (Table1).[173]

The electronic influence on the kinetics of that first protonation reaction can be discussed and rationalized by the analysis of Table 1 which summarizes the data presented herein for all three Ar-BIAN complexes **1b-d** that are sterically protected at the metal by the 2,6-Me_2 substitution pattern of the *N*-Aryl group, as well as the Ar-DAB diimine system.

Table 1. Kinetic data for the low temperature protonation of (N-N)$PtPh_2$ **1b-d** in acetonitrile solvent mixtures.

Entry	**(N-N)$PtPh_2$**	**k ($M^{-1}s^{-1}$) at -80 °C**	**$\Delta H^{\#}$ ($kJmol^{-1}$)**	**$\Delta S^{\#}$ ($JK^{-1}mol^{-1}$)**
1[157]	**(Ar-DAB)$PtPh_2$**	350 ± 7	29 ± 2	-46 ± 10
2	**1b**	2298 ± 192	30.2 ± 0.5	-29.8 ± 2.3
3	**1c**	3375 ± 870	28.7 ± 0.4	-27.1 ± 1.9
4	**1d**	486 ± 42	32.3 ± 0.7	-24.7 ± 3.3

Entries **2-4** show that the rate increases with increasing donor ability of the *N*-aryl groups respectively H, Me and Br substituted in the para position. Enhanced electron donation increases the electron density at the metal, which results in a faster rate of protonation.

We have seen in Chapter 3 that the electron-density of the metal was best modulated when the backbone of the diimine ligand was altered, as opposite to *N*-aryl substitution variations. We showed that the Ar-DAB ligand was a better donor ligand than the Ar-BIAN investigated here. The slower protonation rate of the complexes **1b-d** as compared to Ar-DAB is therefore understood as resulting from steric factors. It was reported that torsion angles between the diimine backbone and the *N*-aryl groups of the Ar-DAB ligand metal complex spanned between 90° and 101°,[81] whereas in the case of the Ar-BIAN complex **1b** they spanned between 88° and 84°.[173] This reveals that the Ar-DAB diimine backbone tends to flip further through the metal the *N*-Aryl groups than the Ar-BIAN backbone, providing a better steric shielding of the metal. Additional evidence for a steric interaction between the backbone and the *N*-aryl groups was seen by low temperature ^{1}H NMR characterisation of the hexacoordinated (N-N)$PtPh_2HNCMe^+$ complexes **2b-f.** A top-bottom symmetry, with a split of the NMR signals of the up/down *N*-aryl signals was observed. Such splitting was not observed in the case of Ar-BICAT complex **2h** where the steric interaction between the *N*-aryl groups and the catecholate backbone was deduced as not present. Consequently, we assume that the ortho protons of the rigid Ar-BIAN diimine backbone provide a weaker steric repulsion of the *N*-aryl groups, than the flexible and voluminous dimethyl diimine backbone of the Ar-DAB complex. These steric interactions influence the steric environment at the metal, and are responsible for the faster protonation kinetics reported here with the Ar-BIAN diimine ligands.

4.2.2 Protonation in poorly coordinating solvent mixtures of ether in dichloromethane

In absence of acetonitrile the (N-N)$PtPh_2$ complexes **1b-f,h** all react by protonation to form (N-N)$PtPh(\eta^2\text{-}C_6H_6)$ **3**, Scheme 3, at different temperatures depending largely on the substitution pattern of the *N*-Aryl groups. Sterically protected metal complexes **1b-d** react promptly with the acid at *ca* -35 °C whereas non sterically hindered metal complexes **1e-f, h** react at *ca* -78 °C.

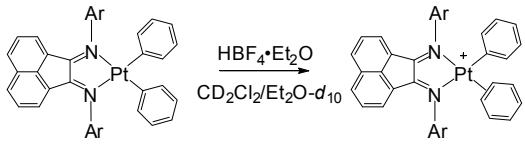

1b **3b**

Scheme 3. Protonation of (N-N)$PtPh_2$ with $HBF_4.Et_2O$ in dichloromethane-d_2

The kinetics of this reaction was studied for complex **1b** by low temperature ^1H NMR. In order to assure a homogeneous solution of the acid in dichloromethane, a solution of acid was prepared by dissolution in a small amount of Et_2O-d_{10} (10 %, v/v) before addition to the dichloromethane solution of complex (see experimental section). The consumption of complex **1b** was monitored by integration of a triplet centered at δ 6.56 attributed to the meta protons of the phenyl ligands. Evidence for the formation of the benzene complex is seen by the appearance of a large broaden peak at ca δ 7.07 attributed to the η^2-C_6H_6 ligand (top spectrum, Figure 4). Supporting evidence is provided by the breaking of symmetry in the complex that is apparent in the NMR spectra (Figure 4) and by the disappearance of, as an illustrating example, a doublet at δ 8.2 attributed to the para protons of the Ar-BIAN backbone (bottom spectra), which gave rise to two doublets at δ 8.28 and 8.22.

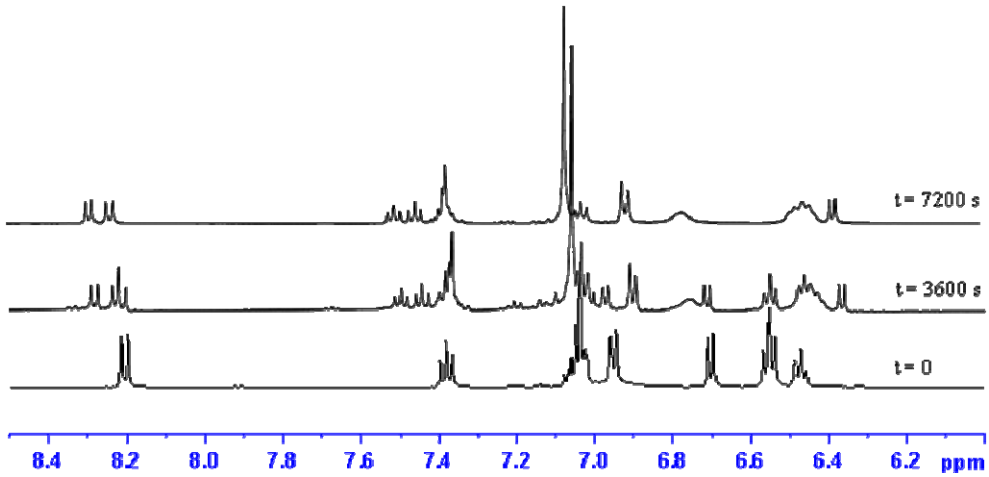

Figure 4. Selected region of ^1H NMR spectra during protonation experiment of **1b** with $HBF_4.Et_2O$ in dichloromethane-d_2 solution, at -60 °C. Total duration of the experiment: *ca*. 2h30

A strong acid concentration dependence was seen on the rate of the protonation in this weakly coordinating solvent mixture that we were not able to quantitatively measure. The temperature dependence of this process was monitored between -45 °C and -60 °C, and the pseudo-first-

order rate constants were extracted from the exponential decay of the integrated value for selected ^{1}H NMR peaks versus time, after normalization of the integrals using the solvent peak as an internal standard. The resulting activation parameters extracted from the Eyring plot (Figure 5) were determined as $\Delta H^{\#} = 39.2 \pm 1.3$ kJmol^{-1} and $\Delta S^{\#} = -121.5 \pm 5.9$ JK^{-1}mol^{-1}.

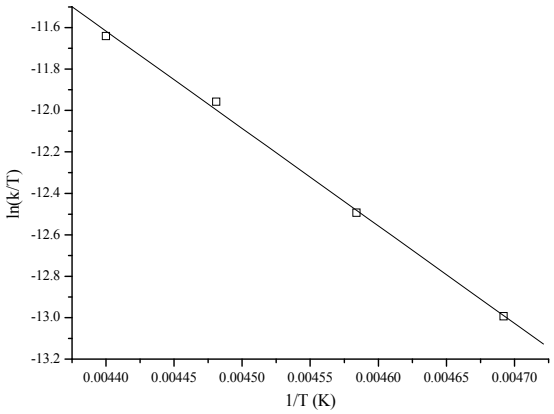

Figure 5. Temperature dependence of the protonation of complex **1b** with $HBF_4.Et_2O$ in dichloromethane-d_2. Experimental conditions: [Pt] = 0.014 M, [$HBF_4.Et_2O$] = 0.104 M

The result represents the first experimental kinetic data obtained for that specific protonation step in ether-dichloromethane solvent mixture. This represents a great input in the understanding of the protonation induced benzene releasing reaction investigated in our group, and the mechanistic information we can deduce will be further addressed in the discussion section.

It is difficult to assert the electronic influence of the backbone structure on the protonation kinetics in the absence of acetonitrile because, as previously mentioned no data were reported in the case of a Ar-DAB diimine system. Furthermore the protonation event of the Ar-BICAT complex **1h** was also complete before a ^{1}H NMR spectrum could be acquired. In that case this is most probably due to the absence of steric hindrance around the metal centre.

4.2.3 Study of the benzene elimination from (N-N)PtPh$_2$H(NCMe)$^+$ 2b-f, h at higher temperature

At temperatures above -30 °C, the protonation reactions for all the (N-N)$PtPh_2$ complexes **1b-f, h** are immediate in dichloromethane containing acetonitrile solvent mixtures as observed

under ^{1}H NMR and UV-vis experimental conditions. The following benzene elimination was monitored by UV-vis spectroscopy. The (N-N)PtPh$_2$H(NCMe)$^+$ **2b-f, h** complexes undergo a smooth release of benzene to form (N-N)PtPh(NCMe)$^+$ **4b-f, h**, Scheme 4, as detected by ^{1}H NMR. Observations, even as transient species, of Pt π-benzene intermediates **3** have not been reported under UV-vis conditions. In the following we describe the detailed kinetic investigation of this process in near ambient temperature conditions. The stopped-flow technique allowed the mixing and instant protonation of the Pt complexes, as deduced by the immediate disappearance of the UV-vis signature of the neutral complexes. The following, slower benzene elimination reactions could then be monitored and effects of [HBF_4], [MeCN], and temperature are reported in the following.

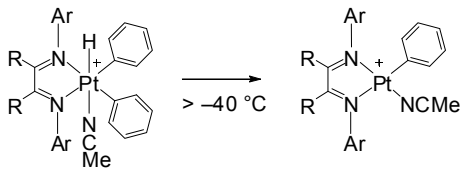

2b-f, h **4b-f, h**

Scheme 4. Elimination of benzene reaction from (N-N)PtPh$_2$H(NCMe)$^+$ **2b-f, h**

A time-resolved UV-vis spectrum for complex **2b** is presented Figure 6, and reveals the presence of an isobestic point at 311 nm which suggests a smooth process without accumulation of intermediates. The spectral changes can nicely be fitted to a single exponential decay, implying pseudo-first-order kinetics. The kinetic measurements were done by monitoring the absorbance *vs* time evolution over the whole spectral range.

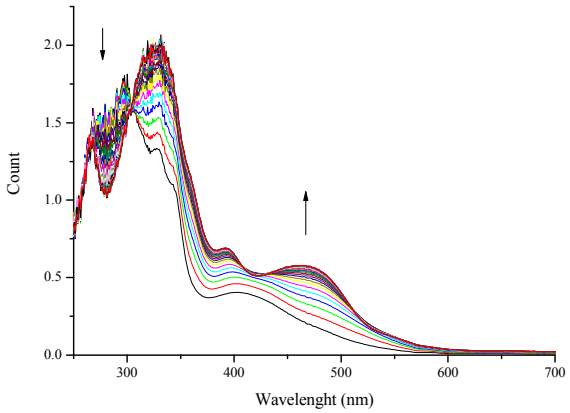

Figure 6: UV-vis spectral evolution during benzene elimination from in situ generated (N-N)$PtPh_2H(NCMe)^+$ **2b** (Scheme 6) with $HBF_4.Et_2O$, in a 5.74 M solution of acetonitrile in dichloromethane at -15 °C. Total duration of the experiment *ca.* 120 seconds

The acid concentration dependence on the reaction was investigated at constant [MeCN] in dichloromethane solution with $HBF_4.Et_2O$ for complexes **2b**, **2c** and **2h**. In none of these cases the kinetics showed any significant acid concentration dependence.

The effect of the acetonitrile concentration on the reaction rate was also investigated over the 0.93-5.74 M concentration range at a given temperature depending on the complex studied. For all complexes, the reaction rate decreased with increasing acetonitrile concentration as illustrated for complex **2c**, Figure 7.

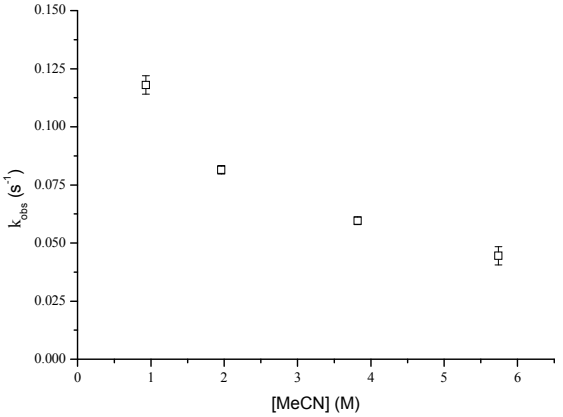

Figure 7. k_{obs} (s^{-1}) as a function of acetonitrile concentration during monitoring of the benzene elimination reaction from **2c**. Experimental conditions: 0.125 mM [Pt], 9.3 mM [HBF_4], T = -10 °C

The analysis of this experimental observation, not seen previously with related diimine Pt complexes,[173] will be further addressed in the discussion section.

4.2.4 Benzene substitution reaction from π-benzene complex 3b

Once the (Ar-BIAN)PtPh(η^2-C_6H_6)$^+$ **3b** complex is formed in situ, it is possible to monitor the benzene substitution reaction occurring upon controlled addition of acetonitrile by ^{1}H NMR. The clean liberation of benzene and the formation of (N-N)PtPh(NCMe)$^+$ **4b**, Scheme 5, is observed.[80,157] This mechanistic step, postulated as intermediate during the benzene elimination from **2b-f, h** to **4b-f, h**, was not observed under time-resolved UV-vis spectroscopy experimental conditions. ^{1}H NMR spectroscopy was used to investigate the [MeCN] and temperature influences on that reaction.

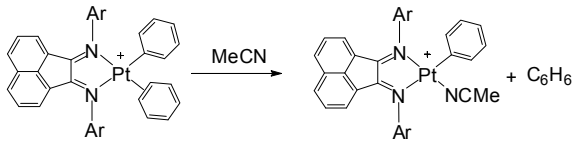

3b **4b**

Scheme 5. Substitution of benzene after generation of (N-N)PtPh(η^2-C_6H_6)$^+$ **3b** from protonation of complex **1b** in dichloromethane-d_2 solution.

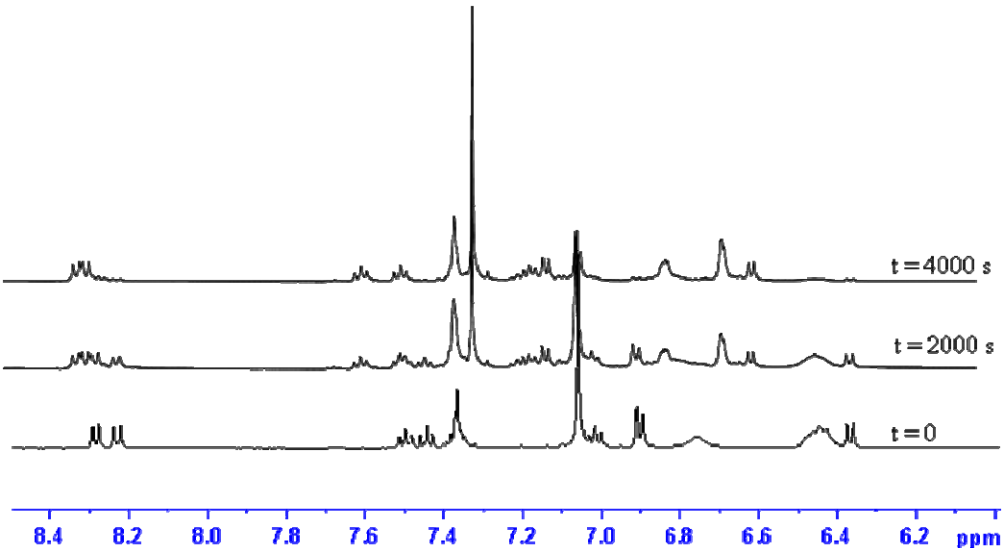

Figure 9. Selected region of the ^{1}H NMR spectra during benzene substitution at (N-N)PtPh(η^{2}-C_6H_6)$^{+}$ **3b** by addition of acetonitrile at -70 °C, Scheme 7.

^{1}H NMR monitoring of the reaction, Scheme 5, was performed by integration of selected NMR signals of complex **3b** (bottom spectrum, Figure 9) centred at δ 6.35 and δ 6.45 after normalisation of the integrated values with the solvent signal. These two signals, attributed to the meta and para protons of the phenyl ligand from **3b** and the ortho protons signals of the Ar-BIAN backbone, were overlapping each other but were distinctively separated from the product NMR signals, as seen Figure 9, top spectrum. The integration values *vs* time curve was nicely fitted to a single exponential decay.

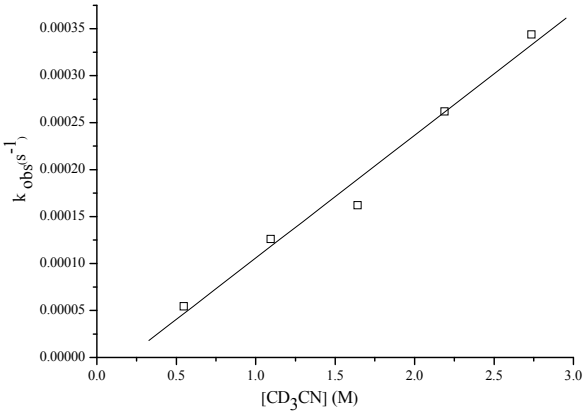

Figure 10. Acetonitrile concentration dependence on the rate of benzene substitution from pre-formed (N-N)PtPh(η^2-C_6H_6)$^+$ complex **3b**. Experimental conditions [Pt] = 0.014 M, [$HBF_4 \cdot Et_2O$] = 0.104 M, T = -70 °C.

The pseudo-first-order rate constant showed a linear acetonitrile concentration dependence (0.55 - 2.74 M) and the reaction rate constant was determined as $k_{(subst)} = 1.31\ 10^{-4} \pm 0.11\ M^{-1}s^{-1}$ at -70 °C (Figure 10). The almost zero intercept ($-2.5 \pm 2.0\ 10^{-5}\ s^{-1}$) strongly points toward the absence of a parallel acetonitrile independent process.

Importantly no traces of (N-N)$PtPh_2H(NCMe)^+$ were detected by ^{1}H NMR spectroscopy, upon addition of the acetonitrile to (N-N)PtPh(η^2-C_6H_6)$^+$. This confirms similar observation at (Ar-DAB)Pt diimine complex.[173] This is of importance since observable equilibria between Pt(II) π-benzene and Pt(IV) hydrido phenyl complexes upon addition of acetonitrile have been reported, as mentioned in Chapter 1.[157]

The temperature dependence of the substitution reaction rate was determined between -55 °C and -70 °C, and provided a good linear Eyring plot from which the activation parameters were extracted as $\Delta H^{\#}$ = 40.0 ± 0.2 kJmol^{-1} and $\Delta S^{\#}$ = -119.4 ± 1.1 JK^{-1}mol^{-1}. Those data are in agreement with an associative mechanism of substitution, which is commonly seen for substitution reactions at cationic Pt(II) metal centre. [98,99,174]

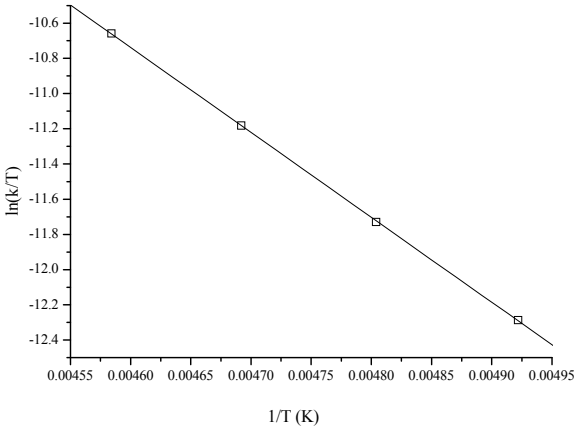

Figure 11. Temperature dependence of the benzene substitution by acetonitrile from (N-N)PtPh(η^2-C_6H_6)$^+$ **3b**. Experimental conditions [Pt] = 0.014 M, [$HBF_4 \cdot Et_2O$] = 0.104 M, [MeCN] = 2.7 M.

4.3. Suggested mechanism and diimine electronic and steric influence on the processes investigated

The kinetic data presented previously agreed largely with our already published mechanistic proposal for the protonation of (N–N)$PtPh_2$ (**A**) and the following benzene-releasing reactions. However, the results presented give new insight in this mechanism and allow the discussion of the steric and electronic factors influencing it. The mechanism presented in Scheme 6, and the data accumulated herein will be discussed in the following.

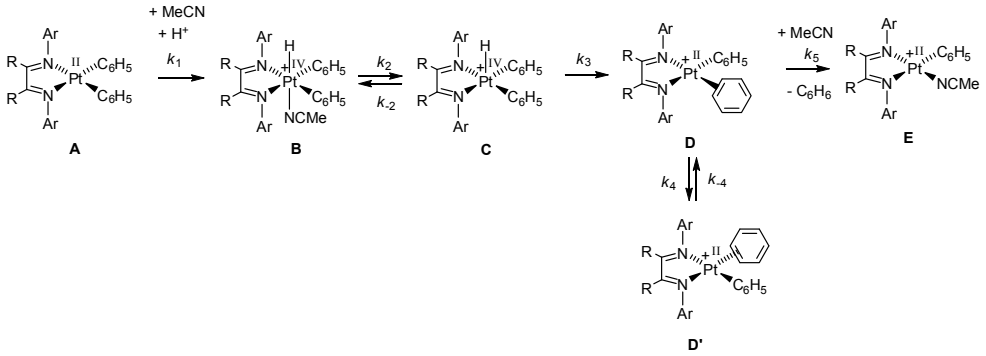

Scheme 6. Proposed mechanism for the protonation induced benzene releasing reaction investigated

4.3.1 Protonation

The data accumulated here emphasize the factors influencing the protonation in acetonitrile containing solvent mixtures. Protonation reactions have been monitored by UV-vis spectroscopy when the diimine ligand presented a 2,6-Me_2 substitution pattern on the *N*-Aryl groups in acetonitrile containing solvent mixtures. When this substitution pattern is absent, we were not able to acquire kinetic data since the protonation was too fast, even at -80 °C. We have already discussed the crystallographic data that revealed the steric hindrance around the metal resulting from the 2,6-Me_2 *N*-aryl substitution. This represents supporting evidence for the notion of a metal centre kinetic site of protonation at (diimine)$PtPh_2$ complexes. Whatever the conditions used, the experimental data support the hypothesis of a metal site of protonation, even though no pentacoordinate (N-N)$PtPh_2H^+$ **C** species have been detected yet. We also have been able to characterize the steric influence induced by the diimine backbone substitution pattern on the protonation event as Ar-DAB complex showed slower protonation kinetics than the less electron rich Ar-BIAN complexes (see Table 1). We have been able to characterize the sensitivity of the protonation kinetics to the electron-tuning of the complex brought by variation in the para position of the 2,6-Me_2 *N*-aryl groups. In the Ar-BIAN series (**b-f**), a better electron-donor ligand translates in faster kinetics of protonation. Although this may appear intuitive, this is the first experimental characterization of that effect. The positive $\Delta H^{\#}$ (ca 28-33 kJ mol^{-1}) and negative $\Delta S^{\#}$ (-28 to -33 J K^{-1} mol^{-1}), are in agreement with the associative nature of the process investigated.

In poorly coordinating solvent mixtures of ether in dichloromethane, the activation parameters determined for the protonation step with complex **1b** are $\Delta H^{\#}$ ca 39 kJ mol^{-1} and $\Delta S^{\#}$ ca -122 J K^{-1} mol^{-1}. This is the first experimental determination of the protonation activation parameters

under such conditions. One may assume that the lower $\Delta H^{\#}$ determined (30 kJ mol^{-1}) between the two protonation event conditions is indicative for a concerted protonation mechanism in the presence of acetonitrile, as opposite to a stepwise scenario where protonation at the metal is followed by a rapid coordination of acetonitrile. The latter is assumed because no acetonitrile concentration dependence on the protonation kinetics of diimine Pt dimethyl or diphenyl complexes has been reported.[157,175] However the high acetonitrile excess relative to the diimine complex present during the experimentations makes this observation not conclusive. One may argue that under the conditions used, the acetonitrile concentration saturation regime was reached and explain that no dependence was observed. Alternatively, the significant but rather small $\Delta H^{\#}$ difference (*ca* 10 kJ mol^{-1}) may as well be due to solvent effect, from going to an (30 % v/v) acetonitrile to (10 % v/v) ether solvent mixture in dichloromethane (the acid being not soluble in pure dichloromethane), the former with higher dielectric constant being more prompt to dissociate the acid. This will affect both the $\Delta H^{\#}$ and $\Delta S^{\#}$ of the reaction. Thus, the $\Delta H^{\#}$ differences measured in two solvent mixtures appear not conclusive, and the mechanistic uncertainty of a concerted or a stepwise protonation event is not resolved.

Another alternative explanation for the $\Delta H^{\#}$ differences observed exists. Assuming a metal centre protonation, as already discussed, and a stepwise scenario, the protonation of the diimine complex **A** lead to the formation of a pentacoordinate Pt(IV) hydride intermediate **C**. We have measured a $\Delta H^{\#}$ of 30 kJ mol^{-1} for that step in acetonitrile containing solution of dichloromethane. This step is followed by a reductive coupling to form (N-N)PtPh(C_6H_6)$^+$, **D**. The additional 9 kJ mol^{-1} may result from the activation energy of the reductive coupling going from **C** to **D**, which sum up to the $\Delta H^{\#}$ 39 kJ mol^{-1} measured in poorly coordinating solvent mixtures where protonation of **A** leads to **D**. DFT investigations[80,157] calculated a $\Delta H^{\#}$ of ca 13 kJ mol^{-1} for the reductive coupling step from **C** to **D** on a related (Ar-DAB)$PtPh_2$. As demonstrated elsewhere,[102] the Ar-BIAN is a poorer electron donor to the metal than the Ar-DAB analogue. The reductive coupling step is then expected to proceed with lower activation energy. The experimental data presented here appear to agree.

4.3.2 Benzene elimination

The hexacoordinate Pt(IV) hydrides **B** are quite stable on the timescale of all our experiments at -80 °C. When heated, the compounds undergo benzene elimination to furnish (N–N)PtPh(NCMe)$^+$ **E**. Reductive X-Y eliminations from octahedral $L_2Pt^{IV}(X)(Y)$ compounds

are usually considered to be dissociative if a readily dissociable ligand is present; whether the overall process occurs in a concerted or stepwise fashion is strongly dependent on the nature of X, Y, and the supporting ligands L.[173] The previous mechanistic proposal with (Ar-DAB)$PtMe_2H(NCMe)^+$ or (Ar-DAB)$PtPh_2H(NCMe)^+$ complexes suggested that this reaction involves a rate limiting MeCN dissociation, based notably on the rather large $\Delta H^{\#}$, substantially positive values for $\Delta S^{\#}$, and the absence of acetonitrile dependence on the kinetics.[38,67,115,116] This was rather surprising since an inverse [Py] dependence (Py = pyridine) has been reported,[80,157] when examining the reductive elimination at (dppe)$PtMe_3Py$, leading to ethane and (dppe)PtMePy for which an initial pyridine dissociation followed by rate determining reductive elimination of ethane was determined. In our case, where an inhibition of the kinetics is characterized at high acetonitrile concentration, the expression of the rate law k_{obs} for benzene reductive elimination can be determined using the steady state approximation by (1), in reference to Scheme 8.

$$k_{obs} = \frac{k_2 k_3}{k_{-2}[MeCN] + k_3} \quad (1)$$

The inverse dependence reported can be linearised by (2).

$$\frac{1}{k_{obs}} = \frac{[MeCN]}{K k_3} + \frac{1}{k_2} \text{ with } K = \frac{k_2}{k_{-2}} \quad (2)$$

This means, in the case of $k_3 << k_{-2}$[MeCN] (3), an inverse [MeCN] dependence will be seen, with a zero intercept with the *y* axis of the plot of $1/k_{obs}$ as a function of [MeCN], and the rate determining step will be the phenyl/proton reductive coupling. Conversely, if $k_3 >> k_{-2}$[MeCN] no [MeCN] dependence is to be expected and the rate law expression reduces to $k_{obs} = k_2$, corresponding to a rate determining acetonitrile dissociation. A third case will arise if $k_3 \approx k_{-2}$[MeCN]. In this case both terms k_{-2}[MeCN] and k_3 are kinetically significant and will contribute to the rate law.

The plot of $1/k_{obs}$ as a function of the [MeCN], reported Figure 12 for complex **2c**, provides a good linear relationship. k_2 was extracted from the *y* axis intercept as $1/k_2$ and calculated as 0.045 s^{-1} for **2c** at -10 °C. Similar graphics for complexes **2b** and **2d-e, h** were obtained. The kinetic data extracted can be found in Table 2.

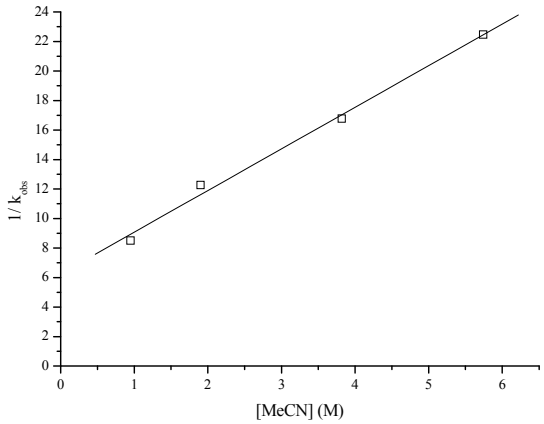

Figure 12. $1/k_{obs}$ (s^{-1}) as a function of acetonitrile concentration variation during monitoring of the benzene elimination reaction from **2c**. Experimental conditions: 0.125 mM [Pt], 9.3 mM [$HBF_4.Et_2O$], T = -10 °C

Temperature dependent kinetic measurements were obtained by recording the time-resolved UV-vis spectra evolution during elimination of benzene with a 12.5 mM acid solution in 30 % MeCN (v/v; 5.74 M) at a temperature range varying between -15 °C and +15 °C, for complex **2b**.

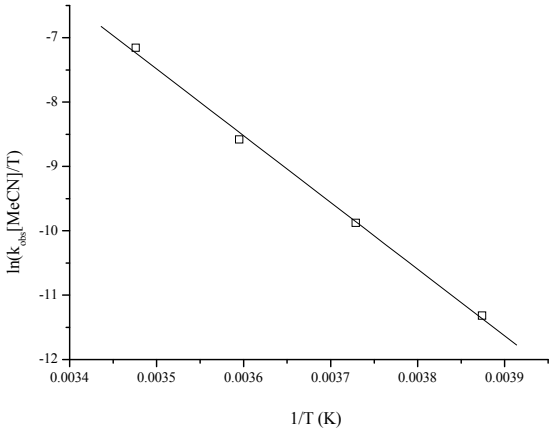

Figure 13. Temperature dependence for the acetonitrile dissociation reaction after rapid protonation of **1b** with $HBF_4.Et_2O$. Experimental conditions: [Pt] = 0.125 mM, [MeCN] = 5.74 M, and [HBF_4] = 12.4 mM

Supposing a rate limiting reductive coupling, the activation parameters were calculated from the Eyring plot extracted as $\ln(k_{obs}[MeCN])$ as a function of (1/T), Figure 13.[74] The excellent linear fit obtained, allowed the determination of $\Delta H^{\#} = 86 \pm 3$ kJ mol^{-1} and $\Delta S^{\#} = 71 \pm 12$ J K^{-1} mol^{-1} for complex **2b**. The activation parameters determined in a similar way for all complexes are reported Table 2.

The rate law, as expressed previously, reveals that several elementary steps contribute significantly to the rate determining step. The activation parameters determined by the Eyring plot combine each of these terms, associated with each process occurring for the benzene releasing reaction. As a results $\Delta H^{\#} = \Delta H^{\#}_{(2)} + \Delta H^{\#}_{(3)}$, and $\Delta S^{\#} = \Delta S^{\#}_{(2)} + \Delta S^{\#}_{(3)}$, where $_{(2)}$ and $_{(3)}$ correspond to the acetonitrile dissociation and the reductive coupling steps respectively, Scheme 8. The activation parameters interpretation is therefore complicated and we will limit our conclusion to the observed large positive value of $\Delta H^{\#}$ and $\Delta S^{\#}$ supportive for the overall dissociative character of the process investigated.

Table 2. Kinetic data for the benzene elimination mechanism from $(N\text{-}N)PtPh_2H(NCMe)^+$ **2b-f, h**

Entry	**$(N\text{-}N)PtPh_2H(NCMe)^+$**	**k_{obs} (s^{-1})[a]**	**k_2 (s^{-1})**	**Temperature**	**$\Delta H^{\#}$ (kJmol^{-1})**	**$\Delta S^{\#}$ (JK^{-1}mol^{-1})**
1	**Ar-DAB**	0.312	0.312	5°C	82 ± 2	62 ± 6
2	**2b**	0.3	1.71	5 °C	86.3 ± 3.2	71.4 ± 11.5
3	**2c**	0.045	0.16	-10 °C	87.1 ± 0.4	74.7 ± 1.6
4	**2d**	0.031	0.11	-10 °C	85.2 ± 2.5	65.1 ± 8.9
5	**2e**	1.11	3.81	20 °C	86.7 ± 1	66.3 ± 3.7
6	**2f**	0.92	3.24	20 °C	87.3 ± 1	66.9 ± 3.5
7	**2h**	0.014	0.048	-10 °C	87.0 ± 2.3	65.6 ± 8.2

[a] [MeCN] = 5.74 M

Table 2 confirms that for all complexes studied here $k_2 > k_{obs}$, *i.e.* acetonitrile dissociation is not rate determining. The rate differences between k_2 and k_{obs} are small (factor of 3 to 5) which support the notion that for all complexes the acetonitrile dissociation and the reductive coupling proceed at close rate, *i.e.* there is no true rate determining step. It will then be interesting to evaluate the kinetic isotope effect that is expected when protonation is performed with deuterated acid. This will reinforced our mechanistic proposal where the metal-hydrogen bond is broken during the reductive coupling step.

As seen by comparison of entry **3** and **4** (Table 2) where the Ar-BIAN ligands only differ by the substitution pattern of the *N*-Aryl groups, there is almost no variation of k_2 at a given temperature between the two complexes. The same olds true comparing entry **5** and **6**.This suggests that electronic factors, provided by the *N*-aryl groups have little influence on the acetonitrile dissociation. The acetonitrile dissociation from complex **2b**, entry **2**, appears to proceed faster than the Ar-DAB ligand complex, entry **1**. These two complexes differ only by the backbone substitution pattern as mentioned earlier. As a poorer electron donor ligand, complex **2b** would be expected to behave in the opposite way based on electronic considerations. It seems that steric factor induced by the backbone structure influence the reactivity of the complex, as seen during protonation experiments.

We have demonstrated the strong influence of the diimine backbone on the relative rates of reductive coupling (k_3) and acetonitrile dissociation (k_2). It appears that in the case of (Ar-DAB)Pt complexes the acetonitrile dissociation is rate determining, and in the studied Ar-BIAN and Ar-BICAT cases here, the reductive coupling and the acetonitrile dissociation both contribute to the rate law. At first it may appear surprising that both the less and more electron-donating diimine systems (Ar-BIAN and Ar-BICAT, respectively), compared to the Ar-DAB have the same effect. Two opposite effects translate in the same direction. Based on the electronic and steric effects discussed, we assume that the relatively electron-poor Ar-BIAN diimine ligand allows (3) by decreasing k_{-2}[MeCN] and increasing k_3. In a different way we assume that the good electron-donating Ar-BICAT ligand system influence the overall rate by decreasing k_3 because a reductive coupling will be disfavored with a better electron donor ligand. It appears that the Ar- DAB ligand complexes present an intermediate case where an highly unstable pentacoordinated Pt(IV) hydride is rapidly reduced to form the π-benzene complex. Ar-DAB diimine ligand system, as electronically intermediate to the discussed diimine system here, provides a specific electronic and steric environment at the Pt metal centre that allowed the kinetic characterization of the acetonitrile dissociation, as previously envisaged, and not of the reductive coupling.

4.3.3 Benzene substitution

Substitution at Pt(II) metal complex is commonly an associative process even though some example of a dissociative mechanism have been reported at $Pt(II)R_2L_2$ complexes (R= Me or Ph and L = dmso, R_2S, or phosphine).[176] Remarkably it was also shown that alkene

substitution at Pd^0(Ar-BIAN)(alkene) complexes could occur by associative as well as dissociative mechanism depending on the substitution pattern on the *N*-Aryl substituent. The reaction was associative in nature for complexes bearing phenyl or tolyl-BIAN ligand but dissociative at 2,6-i-$Pr_2C_6H_3$-BIAN.[177-184] In the case of substitution reactions at Pt(II)(η^2-C_6H_6), we have already mentioned for Ar-DAB complexes that this reaction proceeds associatively.[137] In the current study, we also characterized the associative character of the benzene substitution for the Ar-BIAN complex **4b**.

An important aspect, produced here, is the supporting evidence for the σ-bond metathesis nature of the mechanism for the benzene/phenyl proton exchange. If an oxidative cleavage pathway was favored, the addition at low temperature of acetonitrile to a Pt(II)(η^2-C_6H_6) complex might led to the observation of (N-N)$PtPh_2H(NCMe)^+$. In the case of Ar-BICAT diimine ligand this would have been favored relative to the Ar-DAB or Ar-BIAN diimine ligands because of electronic consideration that would tend to facilitate such oxidative addition pathway for relatively electron-rich metal complex.

4.4. Summary and concluding remarks

Two complementary spectroscopic techniques, NMR and stopped-flow UV-vis spectroscopy, were used to gain detailed insight into the kinetics and mechanism of a well-defined successive protonation and benzene releasing reactions at series of (diimine)$PtPh_2$ complexes of importance for C-H activation investigation. Modulation of the electronic and steric properties of the complex by variation of the diimine ligand can be exerted by varying both the backbone and the *N*-Aryl substituents of the diimine. It appears that the steric hindrance provided by the *N*-aryl substitution is significantly affecting the kinetics of the protonations studied. Steric factors induced by the diimine backbone structure appeared also significant, both in regards of the protonation and of the benzene elimination mechanisms. Electronic factors modulated by variation of the diimine backbone and by the *N*-aryl substitution appeared also significant.

The accumulated experimental data are in agreement with the mechanistic picture depicted in Scheme 8. At low temperatures (ca. -80 °C), protonation of (N–N)$PtPh_2$ with $HBF_4{\cdot}Et_2O$ in dichloromethane/acetonitrile occurs at the metal to furnish (N–N)$PtPh_2H(NCMe)^+$. Steric control exerted by the substitution pattern of the diimine ligand clearly suggests that the metal center is the site of protonation. For the first time activation parameters for the protonation

reaction of (diimine)$PtPh_2$ complexes yielding to (diimine)$PtPh(\eta^2\text{-}C_6H_6)^+$ are presented. They tend to support the mechanistic proposal for a metal center protonation followed by reductive coupling, although ambiguities remain. At higher temperatures, (diimine)$PtPh_2H(NCMe)^+$ progressively eliminate benzene. Kinetic investigation revealed for the first time an acetonitrile inhibition behavior of the process, which contrast with early reports on (Ar-DAB)$PtPh_2$ and (Ar-DAB)$PtMe_2$ complexes. It appears that in all cases reported here, the acetonitrile dissociation and the reductive coupling which furnish a (diimine)$PtPh(\eta^2\text{-}C_6H_6)^+$ intermediate proceed at close rate as no rate limiting step could be determined. The following benzene substitution induced by addition of acetonitrile proceeds at faster rate, and we present supporting evidence for the associative nature of this process.

5. UV-vis stopped-flow investigation of the protonolysis reaction of (Ar-BIAN)$PtPh_2$ complexes 1b and 1e in ether dichloromethane solvent mixtures.

5.1. Introduction

We have previously addressed the protonolysis reaction mechanism of (N-N)$PtPh_2$, in solvent mixtures of acetonitrile in dichloromethane.[157] Protonation of (N-N)$PtPh_2$ led to (N-N)$PtPh_2H(NCMe)^+$ via a pentacoordinated Pt(IV) hydride stabilized by acetonitrile coordination at low temperature. This intermediate is unstable and upon warming, the liberation of benzene is observed. We have presented evidence that the mechanism of the benzene elimination proceeded by acetonitrile dissociation, followed by reductive coupling to yield to a (N–N)$PtPh(\eta^2\text{-}C_6H_6)^+$ intermediate. The formation of (N–N)$PtPh(\eta^2\text{-}C_6H_6)^+$ has independently been observed by low temperature protonation in ether-dichloromethane solutions. An associative substitution of benzene by acetonitrile mechanism, already apparent at -70 ˚C by ^{1}H NMR, to form (N-N)$PtPh(NCMe)^+$ has been characterized as predicted by theoretical calculation.[102,157,185] Different parameters may however alter the mechanism of the substitution. Among them are solvent[102] and counter anion effects,[186] nucleophilicity of the incoming reagent, steric effects,[187,188] and the electronic properties of the metal.[137] Dissociative substitutions have long been seen as exception, but such cases are reported.[177-184,189]

In this chapter, we present the concentration, temperature and pressure dependent kinetic parameters of the protonolysis reaction mechanism of (N-N)$PtPh_2$ complexes **1b** and **1e** (Chart 1) in ether-dichloromethane solvent mixtures as a result of a time-resolved UV-vis stopped-flow investigation.

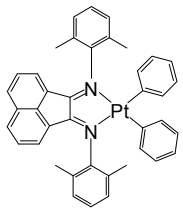

1b

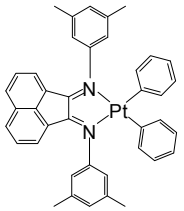

1e

Chart 1

5.2. Results

5.2.1 Protonation and benzene substitution reactions from (Ar-BIAN)$PtPh_2$ 1e

The protonation reaction of (Ar-BIAN)$PtPh_2$ **1e** with $HBF_4.Et_2O$ in ether-dichloromethane solvent mixtures has previously been reported and resulted in the formation of (Ar-BIAN)Pt(Ph)(η^2-C_6H_6)$^+$ **3e**.[177-184] Ether is used to assure the good solubility of the acid in dichloromethane. The reaction could not be monitored by ^{1}H NMR since the reaction was completed at -78 °C before a spectrum could be recorded. The π-benzene complex is thermally unstable and decomposes by liberation of benzene at ca -50 °C.[173] The identity of the product complex has not been resolved but a reasonable candidate is (Ar-BIAN)Pt(Ph)(solv)$^+$ **6e** where solv is a coordinated solvent molecule of dichloromethane-d_2 or Et_2O-d_{10} , or water. It was reported that in the presence of acetonitrile, the π-benzene complex reacted by associative substitution to give (Ar-BIAN)PtPh(NCMe)$^+$ **4e**.[173] We decided to take advantage of the faster time scale of experiment accessible by UV-vis stopped-flow techniques as compared to NMR, to monitor the reactions.

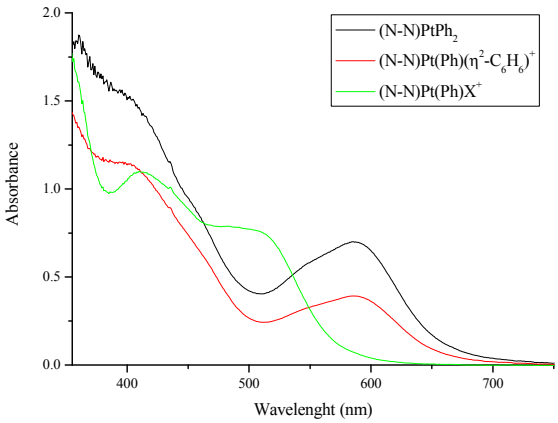

Figure 1: Discernable species involved upon protonation of (Ar -BIAN)$PtPh_2$, **1e** with $HBF_4.Et_2O$ Time scale of event 12 seconds, temperature -20 °C

UV-vis monitoring of the reaction of (Ar -BIAN)$PtPh_2$ **1e** with $HBF_4.Et_2O$ solution between -40 °C and -10 °C results in the detection of three species as illustrated Figure 1. The first UV-vis spectrum is identical to the independently recorded spectrum of the neural complex. As

seen Figure 2 where the reaction was monitored at -40 °C, two steps were detected. The first step results in a rapid absorbance decay of ca 0.20 units at 590 nm over 350 ms. A second step was deduced from the slower absorbance decay observed of ca 0.10 units over 25 s. The absorbance decay is observed until 0.05 units at 590 nm over more than 10 minutes at -40 °C.

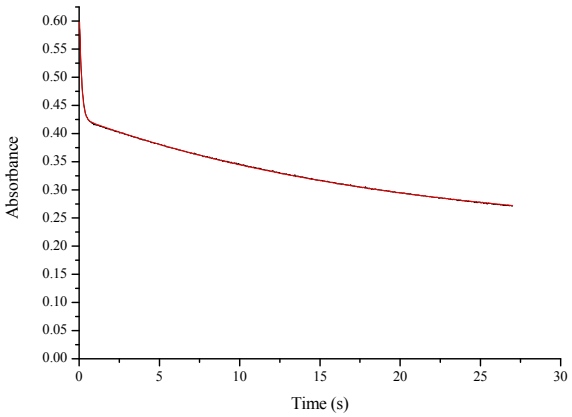

Figure 2: Kinetic trace of the protonation induced reactions at (Ar -BIAN)$PtPh_2$ **1e** with HBF_4.Et2O obtained by the absorbance decrease at 590 nm over 25 seconds at -40 °C.

Previous report of UV-vis monitoring of the protonation reaction of (Ar-BIAN)$PtPh_2$ **1e** complex in acetonitrile dichloromethane solvent mixtures at -80 °C resulted in a drastic absorbance decrease above 350 nm.[173] The protonation reaction produces a (Ar-BIAN)Pt(IV)$Ph_2H(NCMe)^+$ **2e** complex which UV-vis signature shows a zero absorbance above 540 nm. At near ambient temperature (Ar-BIAN)Pt(IV)$Ph_2H(NCMe)^+$ **2e** eliminates benzene and the formation of (Ar-BIAN)Pt(II)$PhNCMe^+$ **4e** results in an absorbance increase above 304 nm. The transition from the Pt(IV) intermediate to the Pt(II) complex gave rise to an isobestic point at 304 nm. The UV-vis spectrum of that complex shows a zero absorbance above 600 nm. From these observations we assume that the first step observed is a protonation step. According to the mechanism of the protonolysis of such diimine Pt complex already reported[185] the protonation proceeds via a (Ar-BIAN)Pt(IV)Ph_2H^+ intermediate, to the formation of (Ar-BIAN)Pt(II)Ph(η^2-C_6H_6)$^+$ **3e** complex after reductive coupling. This π-benzene complex is formed rapidly at -78 °C and is unstable at -50 °C, as reported by NMR observations. Consequently, we assign the identity of the second UV-vis signature to the π-benzene complex, and the third one to the (Ar-BIAN)Pt(II)Ph(solv)$^+$ **6e** complex, where solv is a weakly coordinated solvent molecule.

5.2.2 Protonation of (Ar-BIAN)$PtPh_2$ 1b complex with $HBF_4.Et_2O$ and consecutive benzene substitution reaction

The protonation reaction of (Ar-BIAN)$PtPh_2$ **1b** with $HBF_4.Et_2O$ in ether-dichloromethane solvent mixtures was previously reported and resulted in the formation of (Ar -BIAN)$PtPh(\eta^2$-$C_6H_6)^+$ **3b**. [157,173] The protonation was completed in a few minutes at ca -35 °C and the π-benzene complex was reported to decompose by slow liberation of benzene from ca -35 °C under NMR experimental conditions. The temperature difference in formation and stability of the two complexes was attributed to the steric shielding of the metal provided by the 2,6 substitution pattern of the *N*-Aryl group of the diimine ligand.[173]

Monitoring of the reaction by UV-vis spectroscopy between -10 and 20 °C resulted in the observation of three distinct isobestic points at 360, 452, and 535 nm, Figure 3.

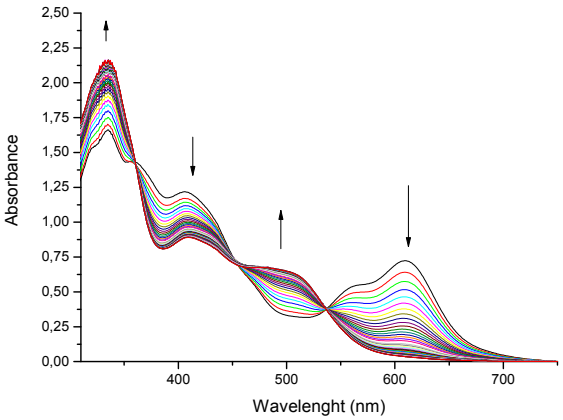

Figure 3: UV-vis spectra evolution observed during protonation and subsequent elimination of (Ar -BIAN)$PtPh_2$ **1b** Experimental conditions: [$HBF_4.Et_2O$] = 4 mM, [Pt] = 0.125 mM, 0.96 M Et_2O, 20 °C. Time scale of the experiment 10 seconds

This made us confident that a clean reaction without accumulation of intermediates could be monitored. With similarities to the (Ar-BIAN)$PtPh_2$ **1e** complex UV-vis behaviour upon protonation, two consecutive steps could however be discerned. As shown Figure 4 (right), a first step was characterized by a small decay of absorbance at 605 nm (ca 0.05 units in 30 ms at 20 °C), and is followed by a larger absorbance decay over 10 s. The reaction was complete within 10 s at 20 °C under UV-vis experimental conditions, Figure 3.

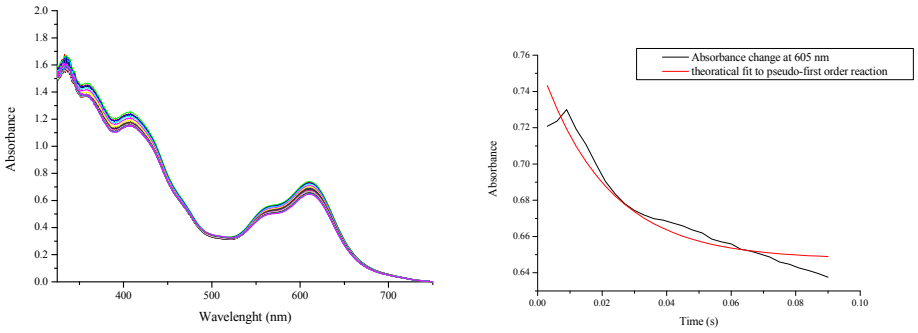

Figure 4: Time-resolved UV-vis spectral evolution upon reaction of the (Ar -BIAN)$PtPh_2$ **1b** with $HBF_4.Et_2O$ left, and kinetic fit and absorbance change extracted at 605 nm, right. Time scale 90 ms at 20 °C

Variation of the ether concentration (0.96 and 1.92 M) did not affect the pseudo-first-order rate constant of the process investigated. The [$HBF_4.Et_2O$] influence on the rate of the UV-vis absorbance decay was investigated over a concentration range of 2.3- 9.3 mM, Figure 5. From the good linear fit regression of the plot of k_{obs} as a function of [$HBF_4.Et_2O$], the second-order rate constant was determined as k = 46.8 ± 1.4 M^{-1} s^{-1} at 20 °C.

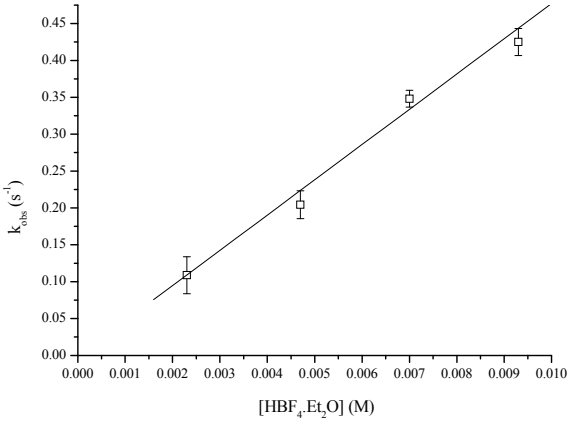

Figure 5: [$HBF_4.Et_2O$] influence on the reaction investigated. Experimental conditions, 0.125 mM [Pt], 0.96 M [Et_2O], T = 20 °C

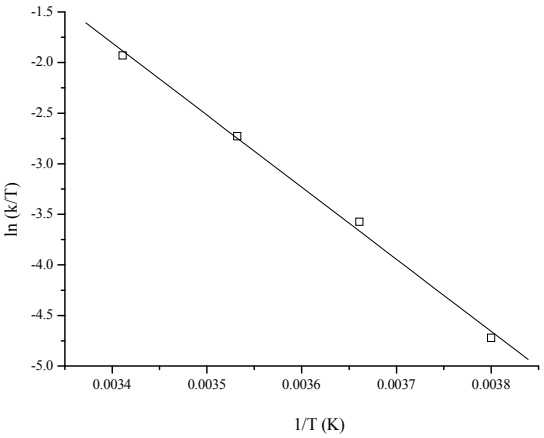

Figure 6: Eyring plot for the reaction of Pt complex with $HBF_4.Et_2O$ solution in ether - dichloromethane solvent mixture. Experimental conditions: 0.125 mM [Pt], 4.7 mM [HBF_4], 0.96 M [Et_2O] in dichloromethane

The temperature dependence was investigated between -10 and 20 °C and the resulting activation parameters extracted from the slope and intercept of the Eyring plot, Figure 6, were calculated as $\Delta H^{\#}$ = 59.2 ± 2.5 kJ mol^{-1} and $\Delta S^{\#}$ = -11.0 ± 8.9 J K^{-1} mol^{-1} . Pressure dependence experiments were conducted with a 9.3 mM $HBF_4.Et_2O$ solution at 25 °C, and the activation volume, was determined in the usual way from the slope of the $\ln(k_{obs})$ as a function of pressure,[173,185] as $\Delta V^{\#}$ = -32 ± 5 cm^3 mol^{-1}, Figure 7.

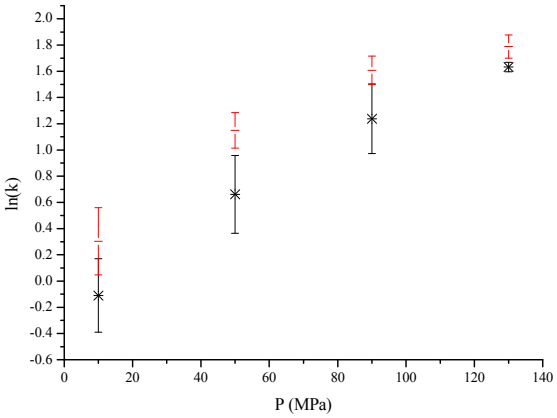

Figure 7: Evolution of the pseudo rate order constant as a function of pressure for evaluation of the activation volume $\Delta V^{\#}$. Experimental conditions: [Pt] = 0.06 mM, [$HBF_4.Et_2O$] = 9.3 mM, 298 K, 0.96 M [Et_2O].

Although $\Delta S^{\#}$ appears modest, the large negative value of $\Delta V^{\#}$ and the [$HBF_4.Et_2O$] dependence are supportive for the associative nature of the reaction investigated.

5.2.3 Protonation of (Ar-BIAN)$PtPh_2$ 1b with triflic acid and benzene substitution reaction

The acid of formula $HBF_4.Et_2O$ previously employed in ether containing solutions is more precisely described as ($HOEt_2.BF_4$), where the proton source is protonated ether instead of HBF_4.[106] In order to assure that no solvent effect where involved in the studies when triflic acid (TfOH) was used, a solution of triflic acid in ether was used. In such media the true identity of the acid is no more TfOH but protonated ether of formula $HOEt_2.TfO$. The identity of the acid was confirmed by ^1H NMR where the same spectra were obtained whether HBF_4 or TfOH were used to protonate ether.

The reaction was monitored, when protonation is performed with triflic acid, by UV-vis spectroscopy, in the same conditions as previously and resulted in the same UV-vis spectral evolution, although the reaction appeared faster, Figure 8.

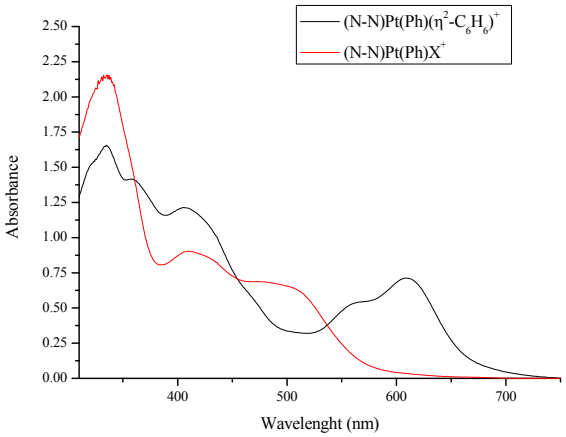

Figure 8: Starting material and final product after protonation of (Ar -BIAN)$PtPh_2$ **1b** with triflic acid. (X = dichloromethane or ether) at 20 °C.

Observation of the exact same three isobestic points also suggested a clean reaction with no discernable accumulation of intermediate, and that the same reaction was observed. The rate

constant did not appeared dependent neither in [TfOH] (2 - 8 mM), nor in [Et_2O] (0.96 and 1.92 M) and the pseudo-first-order rate constant was measured as $k_{obs(TfOH)} = 0.64 \pm 0.08\ s^{-1}$ at 20 °C. Temperature dependent kinetic measurements were conducted between -10 and 20 °C, Figure 9, and the resulting activation parameters were extracted as previously as $\Delta H^{\#} = 90 \pm 2$ kJ mol^{-1} and $\Delta S^{\#} = + 59 \pm 8$ J K^{-1} mol^{-1}. Pressure dependence measurements were conducted, and resulted in a too small variation of the rate constant upon pressure between 10 and 130 MPa to be objectively significant ($\Delta V^{\#}$ ca -3 cm^3 mol^{-1}).

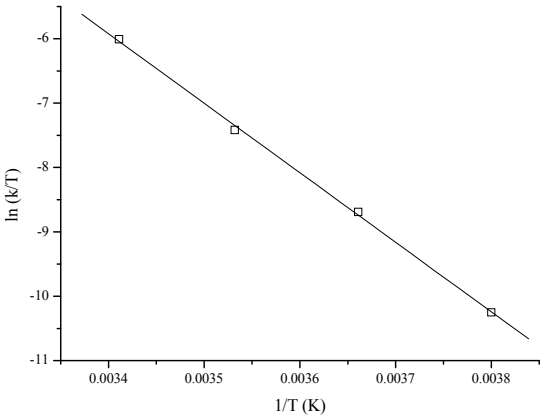

Figure 9: Eyring plot for the reaction of (Ar-BIAN)$PtPh_2$ **1b** with triflic acid. Experimental conditions: [Pt] = 0.125 mM, [TfOH] = 4 mM, 10 % (v/v) ether solution in dichloromethane.

These data, no acid concentration dependence, large $\Delta H^{\#}$ and large positive $\Delta S^{\#}$, strongly support the dissociative character of the reaction investigated.

5.2.4 Ion pair and salt inhibition effect

An additional set of experiments was conducted in which a solution of NBu_4BF_4 salt and triflic acid in ether co-solvent mixture was prepared before reaction with the complex solution at 20 °C. The solution was prepared by dissolution of the BF_4 salt in a dichloromethane containing ether solution of triflic acid (0.96 M in ether and 4 mM in acid). The evolution of k_{obs} as a function of [BF_4^-] added is presented Figure 10.

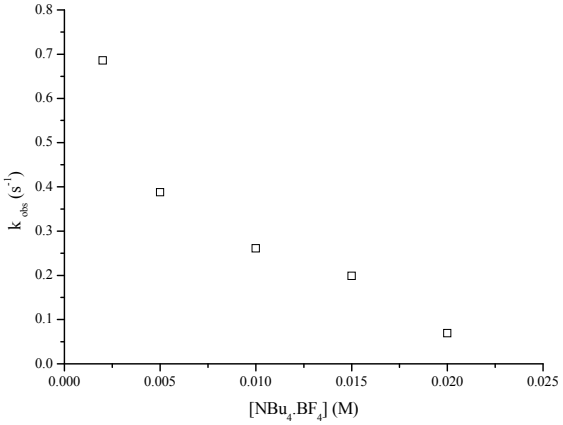

Figure 10: k_{obs} as a function of [NBu_4BF_4] added to a solution of triflic acid in ether- dichloromethane mixture prior to reaction with (Ar -BIAN)$PtPh_2$ **1b**. Experimental conditions: [TfOH] = 4 mM, [Pt] = 0.125 mM, 0.96 M ether solution in dichloromethane, 20 °C.

From the curve depicted Figure 10, we observed that the addition of BF_4^- salt has a decelerating influence on the rate of the reaction investigated.

BF_4^- is considered a more coordinating,[190] or strongly interacting counter anion than TfO^- and cationic (N-N)Pt(II) complexes are known to form ion pairs in low dielectric constant solvents, such as dichloromethane.[187,191] Reactions occurring at contact ion pairs, a sub-class of ion pairs as defined elsewhere,[187] can be inhibited by the addition of salts because of ion exchanges between two ion pairs and formation of the more stable ion pairs.[187] In our case, the addition of BF_4^- salt displaced equilibrium 1 to the right by forming the presumably more stable [Pt][BF_4] ion pair. At the same acid concentration (4 mM) we observe that $k_{obs(HBF4)}$ (ca 0.19 s^{-1} at 20 °C) is smaller than $k_{obs(TfOH)}$ (0.64 s^{-1} at 20 °C), which support the notion that ion pair formed with the complex and the BF_4^- counter anion is more stable than the complex;TfO ion pair.

Equilibrium 1

$$[Pt\text{-}C_6H_6]^+;\ TfO^- \underset{}{\overset{+\,NBu_4BF_4}{\rightleftharpoons}} [Pt\text{-}C_6H_6]^+;\ BF_4^-$$

Such ion pairing effect has been observed in arene C-H activation by cationic Ir(III) complexes where the less interacting ion pair induced faster kinetics.[192]

5.3. Discussion

The UV-vis spectral observations reported herein can be rationalized by the two plausible mechanisms depicted Scheme 2. At temperatures of ca. -78 °C and -35 °C respectively the (Ar-BIAN)$PtPh_2$ **A** complexes (**1b** and **1e**) undergo a rapid protonation, most probably at the metal,[27-30,188] which is followed by a reductive coupling step to yield (Ar-BIAN)$PtPh(\eta^2\text{-}C_6H_6)^+$ **C**. The kinetics of the protonation reaction of (Ar-BIAN)$PtPh_2$ **1b** were previsouly monitored by NMR between -60 and -45 °C, *i.e.* the reaction was completed within a few minutes at -45 °C, under NMR experimental conditions, see Chapter 3.[102,157,173,185] These π-benzene complexes have limited thermal stability and have been reported to start to decompose by liberation of benzene respectively at ca -50 °C, for the Ar-BIAN complex **1e** , and at -30 °C for complex **1b** based on NMR investigations.[185] The identity of the resulting complex has not been demonstrated but complex **E** represents a reasonable candidate. It is envisaged that complex **E** resulted from the slow dissociation of benzene from **C**, followed by rapid coordination of a solvent molecule.

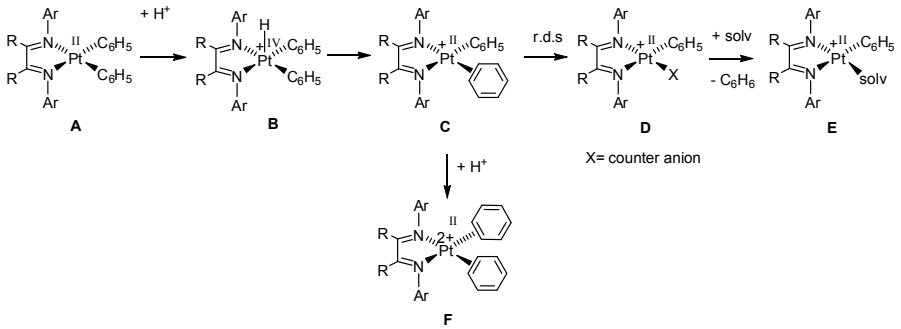

Scheme 2: Protonation and benzene liberation reactions at (diimine)Pt(II)Ph_2 complex in ether dichloromethane solvent mixtures.

Kinetic data obtained for the protonation of (Ar-BIAN)$PtPh_2$ **1b** with $HBF_4.Et_2O$ are in agreement with the associative nature of the process investigated. The rate law can be expressed as $k = k_{obs}[Pt][HBF_4.Et_2O]$. In this expression the term $[HBF_4.Et_2O]$ may refer to $[H^+]$ or to $[BF_4^-]$. It has been reported that double protonation at (diimine)Pt complexes could occur.[173] In this case the $[HBF_4.Et_2O]$ term should refer to $[H^+]$. Double protonation of (diimine)Pt complex has been reported when the reaction was conducted in acetonitrile-dichloromethane mixtures, and yielded to (diimine)$Pt(NCMe)_2^{2+}$ **7** after two successive

sequences of protonation and benzene elimination.[108,157,173] However the second protonation at (Ar-BIAN)PtPh(NCMe)$^+$ **4b** appeared much slower than the process investigated here,[157,173] and we haven't observed double protonation of (diimine)$PtPh_2$ complexes in ether-dichloromethane solvent mixtures by NMR previously.

The benzene substitution reaction at (Ar-BIAN)PtPh(η^2-C_6H_6)$^+$ **3b** in the presence of acetonitrile has been reported to be associative in nature, and was monitored by NMR between -70 to -60 °C. It is then reasonable to envisage that BF_4^-, a considerably less nucleophilic agent than acetonitrile, can promote a similar benzene substitution at higher temperatures. In this case the term [$HBF_4.Et_2O$] refers to [BF_4^-] and the substitution reaction rate increase when increasing acid concentration, as reported in the results section.

Kinetic data obtained when the protonation reaction is performed with TfOH suggested the dissociative character of the reaction. Noteworthy is the absence of [TfOH] dependence in the rate law, which conflicts with the double protonation scenario envisaged previously. At the same temperature (20 °C) and concentration (4 mM) conditions the reaction appears faster in the case of TfOH (k_{obs} 0.64 s^{-1}) than in the case of HBF_4 (k_{obs} 0.19 s^{-1}). The reaction appeared inhibited by addition of [NBu_4BF_4] salt to a solution of complex and triflic acid. These observations support the notion that the π-benzene complex forms a more stable ion pair with the BF_4 counter anion. However, it appears conflicting with the k_{obs} increase observed upon increase concentration of HBF_4.

5.4. Conclusion

UV-vis stop-flow techniques were used to study the protonation and subsequent benzene elimination reactions of two (Ar-BIAN)$PtPh_2$ **1e, 1e** complexes in ether dichloromethane solvent mixtures. Protonation, a fast process at the temperature investigated, is followed by reductive coupling to form (Ar-BIAN)PtPh(η^2-C_6H_6)$^+$ **3b, 3e**. The consecutive benzene releasing step was investigated by UV-vis spectroscopy after reaction of the neutral complex with HBF_4 or TfOH. The results suggest that either a second protonation is involved or that the benzene releasing step can occur by two different mechanisms, an associative or a dissociative one when HBF_4 and TfOH are used respectively. The data presented here do not allow conclusive distinction between both scenarios. The kinetic data suggest the involvement of ion pair interactions between (Ar-BIAN)PtPh(η^2-C_6H_6)$^+$ **3** and the counter anion. The ion pair formed with BF_4^- appears more stable than the one formedg with TfO^-.

6. Conclusion and perspectives

In conclusion, progress has been made in the understanding of the benzene C-H activation mechanism by studying its microscopic reverse, *i.e.* protonation of (diimine)$PtPh_2$ complexes. As a major contribution, a new diimine Ar-BICAT ligand structure has been successfully introduced and the use of the well known Ar-BIAN diimine ligand structure has been employed. Both diimine structures formed air and moisture stable Pt diphenyl complexes that were fully characterized. The use of ^{195}Pt NMR spectroscopy was determinant in the assessment of the electronic influence of the diimine structure and allowed the first rationalization and classification of the relative electronic properties brought by the arms and the backbone of the diimine. The backbone diimine structure appeared to modulate the electronic properties of the metal in a greater extent in comparison to the N-aryl arms. The protonolysis mechanism appeared more sensitive to steric parameters. The combined UV-vis and NMR experiments presented along the thesis both support the discussed mechanism. Some uncertainties remain but it can be summarized as a metal centre protonation followed by trapping of incoming acetonitrile ligand to form a Pt(IV) hydride. This unstable intermediate eliminates benzene upon warming, in a successive acetonitrile dissociation and reductive coupling reactions to form an otherwise observed Pt(II) π-benzene complex. The benzene is then associatively substituted by acetonitrile and a (diimine)$PtPh(NCMe)^+$ cation can be isolate. This cationic species is susceptible to undergo a second protonation and benzene elimination sequence, for which we haven't been able to collect major mechanistic information. The relative rate of acetonitrile dissociation and reductive coupling appeared greatly influenced by the diimine substitution pattern. In the case of an Ar-DAB diimine the former appeared rate determining, whereas both appeared to proceed at similar rate in the case of Ar-BIAN and Ar-BICAT diimines, independently of steric parameters. Importantly we have been able to review some previous mechanistic proposal regarding the proton exchange reaction that occurred between the phenyl and the benzene ligand at (diimine)$PtPh(C_6H_6)^+$ complex. In opposition to the previously envisaged oxidative cleavage – reductive coupling sequence, a direct σ-bond metathesis pathway, as first suggested by DFT calculation, appeared more likely.

These represented great input in the field, but since time is limited, a series of experiment haven't been performed. First of all, the fact that all diimine Pt complexes used here reacted in a similar manner upon protonation suggest but doesn't prove that they all will be able to

activated C-H bond. Therefore, it will be interesting to investigate such reaction. Additionally, the proton exchange reaction between phenyl and benzene ligand although undermine as occurring for each set of ligand hasn't been characterized with the Ar-BIAN and Ar-BICAT diimine complexes. Concerning these two set of ligand the protonolysis study presents evidence that the reductive coupling is involved in the rate limiting step of the benzene elimination. As such it will also be valuable to measure kinetic isotope effect in that case, as it involves the breaking of a Pt-H(D) bond.

Additionally, the current thesis has been focused exclusively on reaction relevant to benzene C-H activation mechanism. The use of the newly introduced diimine structures should also be employed in methane and other arenes mechanism investigations.

7. References

(1) Moss, G. P.; Smith, P. A. S.; Tavernier, D. *Pure and Applied Chemistry* **1995**, *67*, 1307-1375.

(2) Lashof, D. A.; Ahuja, D. R. *Nature* **1990**, *344*, 529-531.

(3) Periana, R. A.; Mironov, O.; Taube, D.; Bhalla, G.; Jones, C. J. *Science* **2003**, *301*, 814-818.

(4) Gradassi, M. J.; Green, N. M. *Fuel. Proc. Technol* **1995**, *42*.

(5) Periana, R. A.; Taube, D. J.; Gamble, S.; Taube, H.; Satoh, T.; Fujii, H. *Science* **1998**, *280*, 560-564.

(6) Yardley-Jones, A.; Anderson, D.; Parke, D. V. *British journal of industrial medicine* **1991**, *48*, 437-444.

(7) Huff J. *International journal of occupational and environmental health* **2007**, *13*, 213-221.

(8) Friedel, C.; Crafts, J.-M. *C. R. Acad. Sci.* **1877**, *84*, 1392-1395.

(9) Friedel, C.; Crafts, J.-M. *C. R. Acad. Sci.* **1877**, *84*, 1450-1454.

(10) Friedel, C.; Crafts, J.-M. *C. R. Acad. Sci.* **1877**, *85*, 74-77.

(11) Spryskov *J.Gen. Chem. USSR* **1960**, *30*.

(12) Lauer, W. M.; Noland, W. E. *J. Am. Chem. Soc.* **1953**, *75*, 3689-3692.

(13) de la Mare, P. B. D.; Dunn, T. M.; Harvey, J. T. *J. Chem. Soc.* **1957**, 923.

(14) Labinger, J. A. *J. Mol. Catal. A: Chem.* **2004**, *220*, 27-35.

(15) Davico, G. E.; Bierbaum, V. M.; DePuy, C. H.; Ellison, G. B.; Squires, R. R. *J. Am. Chem. Soc.* **1995**, *117*, 2590-2599.

(16) Labinger, J. A.; Bercaw, J. E. *Nature* **2002**, *417*, 507-514.

(17) Bergman, R. G. *Nature* **2007**, *446*, 391-393.

(18) Lersch, M.; Tilset, M. *Chem. Rev.* **2005**, *105*, 2471-2526.

(19) Periana, R. A.; Bhalla, G.; Tenn, W. J.; Young, K. J. H.; Liu, X. Y.; Mironov, O.; Jones, C. J.; Ziatdinov, V. R. *J. Mol. Catal. A: Chem.* **2004**, *220*, 7-25.

(20) Janowicz, A. H.; Bergman, R. G. *J. Am. Chem. Soc.* **1982**, *104*, 352-354.

(21) Hoyano, J. K.; Graham, W. A. G. *J. Am. Chem. Soc.* **1982**, *104*, 3723-3725.

(22) Jones, C. J.; Taube, D.; Ziatdinov, V. R.; Periana, R. A.; Nielsen, R. J.; Oxgaard, J.; Goddard III, W. A. *Angew. Chem., Int. Ed.* **2004**, *43*, 4626-4629.

(23) Sen, A.; Benvenuto, M. A.; Lin, M.; Hutson, A. C.; Basickes, N. *J. Am. Chem. Soc.* **1994**, *116*, 998-1003.

(24) Kao, L. C.; Hutson, A. C.; Sen, A. *J. Am. Chem. Soc.* **1991**, *116*, 700-701.

(25) Lin, M.; Hogan, T. E.; Sen, A. *J. Am. Chem. Soc.* **1996**, *118*, 4574-4580.

(26) Lin, M.; Sen, A. *Nature* **1994**, *368*, 613-615.

(27) Arndtsen, B. A.; Bergman, R. G. *Science* **1995**, *270*, 1970-1973.

(28) Burger, P.; Bergman, R. G. *J. Am. Chem. Soc.* **1993**, *115*, 10462-10463.

(29) Luecke, H. F.; Bergman, R. G. *J. Am. Chem. Soc.* **1997**, *119*, 11538-11539.

(30) Golden, J. T.; Andersen, R. A.; Bergman, R. G. *J. Am. Chem. Soc.* **2001**, *123*, 5837-5838.

(31) Hodges, R. J.; Garnett, J. L. *J. Phys. Chem.* **1968**, *72*, 1673-1682.

(32) Garnett, J. L.; Hodges, R. J. *J. Am. Chem. Soc.* **1967**, *89*, 4546-4547.

(33) Gol'dshleger, N. F.; Shteinman, A. A.; Shilov, A. E.; Eskova, V. V. *Zh. Fiz. Khim.* **1972**, *46*, 1353-1354.

(34) Gol'dshleger, N. F.; Tyabin, M. B.; Shilov, A. E.; Shteinman, A. A. *Zh. Fiz. Khim.* **1969**, *43*, 2174-2175.

(35) Crabtree, R. H. *J. Organomet. Chem.* **2004**, *689*, 4083-4091.
(36) Shilov, A. E.; Shul'pin, G. B. *Chem. Rev.* **1997**, *97*, 2879-2932.
(37) Stahl, S. S.; Labinger, J. A.; Bercaw, J. E. *Angew. Chem., Int. Ed.* **1998**, *37*, 2180-2192.
(38) Fekl, U.; Goldberg, K. I. *Adv. Inorg. Chem.* **2003**, *54*, 259-320.
(39) Paul, A.; Musgrave, C. B. *Organometallics* **2007**, *26*, 793-809.
(40) Arndtsen, B. A.; Bergman, R. G.; Mobley, T. A.; Peterson, T. H. *Acc. Chem. Res.* **1995**, *28*, 154.
(41) Crabtree, R. H. *J. Chem. Soc., Dalton Trans.* **2001**, 2437-2450.
(42) Tyabin, M. B.; Shilov, A. E.; Shteinman, A. A. *Dokl. Akad. Nauk.* **1971**, *198*, 380.
(43) Mylvaganam, K.; Bacskay, G. B.; Hush, N. S. *J. Am. Chem. Soc.* **2000**, *122*, 2041-2052.
(44) Kua, J.; Xu, X.; Periana, R. A.; Goddard, W. A. *Organometallics* **2002**, *21*, 511-525.
(45) Xu, X.; Kua, J.; Periana, R. A.; Goddard, W. A. *Organometallics* **2003**, *22*, 2057-2068.
(46) Halpern, J. *Inorg. Chim. Acta.* **1985**, *100*, 41-48.
(47) Jones, W. D.; Feher, F. J. *J. Am. Chem. Soc.* **1984**, *106*, 1650-1653.
(48) Vigalok, A.; Kraatz, H.-B.; Konstantinovsky, L.; Milstein, D. *Chem. Eur. J.* **1997**, *3*, 253-260.
(49) Peterson, T. H.; Golden, J. T.; Bergman, R. G. *J. Am. Chem. Soc.* **2001**, *123*, 455-462.
(50) Chin, R. M.; Dong, L.; Duckett, S. B.; Jones, W. D. *Organometallics* **1992**, *11*, 871-876.
(51) Chin, R. M.; Dong, L.; Duckett, S. B.; Partridge, M. G.; Jones, W. D.; Perutz, R. N. *J. Am. Chem. Soc.* **1993**, *115*, 7685-7695.
(52) Churchill, D. G.; Janak, K. E.; Wittenberg, J. S.; Parkin, G. *J. Am. Chem. Soc.* **2003**, *125*, 1403-1420.
(53) Cordone, R.; Taube, H. *J. Am. Chem. Soc.* **1987**, *109*, 8101-8102.
(54) Cronin, L.; Higgitt, C. L.; Perutz, R. N. *Organometallics* **2000**, *19*, 672-683.
(55) Iverson, C. N.; Lachicotte, R. J.; Müller, C.; Jones, W. D. *Organometallics* **2002**, *21*, 5320-5333.
(56) Jones, W. D.; Dong, L. *J. Am. Chem. Soc.* **1989**, *111*, 8722-8723.
(57) Jones, W. D.; Feher, F. J. *J. Am. Chem. Soc.* **1986**, *108*, 4814-4819.
(58) Sweet, J. R.; Graham, W. A. G. *J. Am. Chem. Soc.* **1983**, *105*, 305-306.
(59) Berenguer, J. R.; Forniés, J.; Martín, L. F.; Martín, A.; Menjón, B. *Inorg. Chem.* **2005**, *44*, 7265-7267.
(60) Johansson, L.; Tilset, M.; Labinger, J. A.; Bercaw, J. E. *J. Am. Chem. Soc.* **2000**, *122*, 10846-10855.
(61) Vigalok, A.; Uzan, O.; Shimon, L. J. W.; Ben-David, Y.; Martin, J. M. L.; Milstein, D. *J. Am. Chem. Soc.* **1998**, *120*, 12539-12544.
(62) Krumper, J. R.; Gerisch, M.; Magistrato, A.; Rothlisberger, U.; Bergman, R. G.; Tilley, T. D. *J. Am. Chem. Soc.* **2004**, *126*, 12492-12502.
(63) Perutz, R. N.; Sabo-Etienne, S. *Angew. Chem., Int. Ed.* **2007**, *46*, 2578-2592.
(64) Jones, W. D. *Acc. Chem. Res.* **2003**, *36*, 140-146.
(65) Churchill, D. G.; Janak, K. E.; Wittenberg, J. S.; Parkin, G. *J. Am. Chem. Soc.* **2003**, *125*, 1403-1420.
(66) Stahl, S. S.; Labinger, J. A.; Bercaw, J. E. *J. Am. Chem. Soc.* **1995**, *117*, 9371-9372.

(67) Stahl, S. S.; Labinger, J. A.; Bercaw, J. E. *J. Am. Chem. Soc.* **1996**, *118*, 5961-5976.
(68) Jenkins, H. A.; Yap, G. P. A.; Puddephatt, R. J. *Organometallics* **1997**, *16*, 1946-1955.
(69) Fekl, U.; Zahl, A.; van Eldik, R. *Organometallics* **1999**, *18*, 4156-4164.
(70) Hill, G. S.; Rendina, L. M.; Puddephatt, R. J. *Organometallics* **1995**, *14*, 4966-4968.
(71) Holtcamp, M. W.; Labinger, J. A.; Bercaw, J. E. *Inorg. Chim. Acta.* **1997**, *265*, 117-125.
(72) Hinman, J. G.; Baar, C. R.; Jennings, M. C.; Puddephatt, R. J. *Organometallics* **2000**, *19*, 563-570.
(73) Holtcamp, M. W.; Henling, L. M.; Day, M. W.; Labinger, J. A.; Bercaw, J. E. *Inorg. Chim. Acta.* **1998**, *270*, 467-478.
(74) Procelewska, J.; Zahl, A.; van Eldik, R.; Zhong, H. A.; Labinger, J. A.; Bercaw, J. E. *Inorg. Chem.* **2002**, *41*, 2808-2810.
(75) Zhong, H. A.; Labinger, J. A.; Bercaw, J. E. *J. Am. Chem. Soc.* **2002**, *124*, 1378-1399.
(76) Wik, B. J.; Lersch, M.; Tilset, M. *J. Am. Chem. Soc.* **2002**, *124*, 12116-12117.
(77) Heiberg, H.; Johansson, L.; Gropen, O.; Ryan, O. B.; Swang, O.; Tilset, M. *J. Am. Chem. Soc.* **2000**, *122*, 10831-10845.
(78) Johansson, L.; Tilset, M. *J. Am. Chem. Soc.* **2001**, *123*, 739-740.
(79) Tilset, M.; Johansson, L.; Lersch, M.; Wik, B. J. In *Activation and Functionalization of C-H Bonds*; Goldberg, K. I., Goldman, A. S., Eds.; American Chemical Society: Washington, D.C., 2004, p 264-282.
(80) Wik, B. J.; Ivanovic-Burmazovic, I.; Tilset, M.; van Eldik, R. *Inorg. Chem.* **2006**, *45*, 3613-3621.
(81) Wik, B. J.; Lersch, M.; Krivokapic, A.; Tilset, M. *J. Am. Chem. Soc.* **2006**, *128*, 2682-2696.
(82) Johansson, L.; Ryan, O. B.; Rømming, C.; Tilset, M. *J. Am. Chem. Soc.* **2001**, *123*, 6579-6590.
(83) Zhong, H. A.; Labinger, J. A.; Bercaw, J. E. *J. Am. Chem. Soc.* **2002**, *124*, 1378-1399.
(84) Heyduk, A. F.; Driver, T. G.; Labinger, J. A.; Bercaw, J. E. *J. Am. Chem. Soc.* **2004**, *126*, 15034-15035.
(85) Gerdes, G.; Chen, P. *Organometallics* **2003**, *22*, 2217-2225.
(86) Holtcamp, M. W.; Labinger, J. A.; Bercaw, J. E. *J. Am. Chem. Soc.* **1997**, *119*, 848-849.
(87) Thomas, J. C.; Peters, J. C. *J. Am. Chem. Soc.* **2001**, *123*, 5100-5101.
(88) Driver, T. G.; Day, M. W.; Labinger, J. A.; Bercaw, J. E. *Organometallics* **2005**, *24*, 3644-3654.
(89) Vedernikov, A. N.; Pink, M.; Caulton, K. G. *Inorg. Chem.* **2004**, *43*, 3642-3646.
(90) Song, D.; Jia, W. L.; Wang, S. *Organometallics* **2004**, *23*, 1194-1196.
(91) Song, D.; Wang, S. *Organometallics* **2003**, *22*, 2187-2189.
(92) Thomas, J. C.; Peters, J. C. *J. Am. Chem. Soc.* **2003**, *125*, 8870-8888.
(93) Iverson, C. N.; Carter, C. A. G.; Baker, R. T.; Scollard, J. D.; Labinger, J. A.; Bercaw, J. E. *J. Am. Chem. Soc.* **2003**, *125*, 12674-12675.
(94) Harkins, S. B.; Peters, J. C. *Organometallics* **2002**, *21*, 1753-1755.
(95) Labinger, J. A.; Bercaw, J. E.; Tilset, M. *Organometallics* **2006**, *25*, 805-808.
(96) Gerdes, G.; Chen, P. *Organometallics* **2006**, *25*, 809-811.

(97) Moret, M.-E.; Chen, P. *Organometallics* **2007**, *26*, 1523-1530.
(98) Reinartz, S.; White, P. S.; Brookhart, M.; Templeton, J. L. *J. Am. Chem. Soc.* **2001**, *123*, 12724-12725.
(99) Norris, C. M.; Templeton, J. L. *Organometallics* **2004**, *23*, 3101-3104.
(100) Fekl, U.; Goldberg, K. I. *J. Am. Chem. Soc.* **2002**, *124*, 6804-6805.
(101) Fekl, U.; Kaminsky, W.; Goldberg, K. I. *J. Am. Chem. Soc.* **2001**, *123*, 6423-6424.
(102) Li, J.-L.; Geng, C.-Y.; Huang, X.-R.; Zhang, X.; Sun, C.-C. *Organometallics* **2007**, *26*, 2203-2210.
(103) Harris, R. K.; Becker, E. D.; Cabral De Menezes, S. M.; Goodfellow, R.; Granger, P. *Pure Appl. Chem.* **2001**, *73*, 1795-1818.
(104) van Eldik, R.; Gaede, W.; Wieland, S.; Kraft, J.; Spitzer, M.; Palmer, D. A. *Rev. Sci. Instrum.* **1993**, *64*, 1355-1357.
(105) van Eldik, R.; Palmer, D. A.; Schmidt, R.; Kelm, H. *Inorg. Chim. Acta* **1981**, *50*, 131-135.
(106) van Eldik, R.; Hubbard, C. D.; Riad Manaa, M. *Chemistry at Extreme Conditions* **2005**, *Chapter 4*, 109-164.
(107) Koppel, I. A.; Burk, P.; Koppel, I.; Leito, I.; Sonoda, T.; Mishima, M. *Journal of the American Chemical Society* **2000**, *122*, 5114-5124.
(108) Driver, T. G.; Williams, T. J.; Labinger, J. A.; Bercaw, J. E. *Organometallics* **2007**, *26*, 294-301.
(109) Koppel, I. A.; Burk, P.; Koppel, I.; Leito, I.; Sonoda, T.; Mishima, M. *J. Am. Chem. Soc.* **2000**, *122*, 5114-5124.
(110) We thank a reviewer for suggesting this experiment and for useful comments.
(111) Wik, B. J.; Lersch, M.; Tilset, M. *J. Am. Chem. Soc.* **2002**, *124*, 12116-12117.
(112) Seeman, J. I. *Chem. Rev.* **1983**, *83*, 83-134.
(113) Bercaw, J. E. *J. Am. Chem. Soc.* **2008**, *130*, 17654-17655.
(114) Romeo, R.; D'Amico, G. *Organometallics* **2006**, *25*, 3435-3446.
(115) Arthur, K. L.; Wang, Q. L.; Bregel, D. M.; Smythe, N. A.; O'Neil, B. A.; Goldberg, K. I.; Moloy, K. G. *Organometallics* **2005**, *24*, 4624-4628.
(116) Crumpton-Bregel, D. M.; Goldberg, K. I. *J. Am. Chem. Soc.* **2003**, *125*, 9442-9456.
(117) Karshtedt, D.; McBee, J. L.; Bell, A. T.; Tilley, T. D. *Organometallics* **2006**, *25*, 1801-1811.
(118) Kloek, S. M.; Goldberg, K. I. *J. Am. Chem. Soc.* **2007**, *129*, 3460-3461.
(119) Khaskin, E.; Zavalij, P. Y.; Vedernikov, A. N. *Angew. Chem., Int. Ed.* **2007**, *46*, 6309-6312.
(120) Hill, G. S.; Irwin, M. J.; Levy, C. J.; Rendina, L. M.; Puddephatt, R. J. *Inorg. Synth.* **1998**, *32*, 149-153.
(121) tom Dieck, H.; Svoboda, M.; Greiser, T. *Z. Naturforsch., B: Chem. Sci.* **1981**, *36B*, 823-832.
(122) Song, D.; Wang, S. *J. Organomet. Chem.* **2002**, *648*, 302-305.
(123) Luinstra, G. A.; Wang, L.; Stahl, S. S.; Labinger, J. A.; Bercaw, J. E. *J. Organomet. Chem.* **1995**, *504*, 75-91.
(124) Stahl, S. S.; Labinger, J. A.; Bercaw, J. E. *J. Am. Chem. Soc.* **1995**, *117*, 9371-9372.
(125) Hill, G. S.; Vittal, J. J.; Puddephatt, R. J. *Organometallics* **1997**, *16*, 1209-1217.
(126) Hill, G. S.; Puddephatt, R. J. *Organometallics* **1998**, *17*, 1478-1486.
(127) Hill, G. S.; Puddephatt, R. J. *J. Am. Chem. Soc.* **1996**, *118*, 8745-8746.

(128) Puddephatt, R. J. *Coord. Chem. Rev.* **2001**, *219-221*, 157-185.
(129) Periana, R. A.; Taube, D. J.; Gamble, S.; Taube, H.; Satoh, T.; Fujii, H. *Science* **1998**, *280*, 560-564.
(130) Kua, J.; Xu, X.; Periana, R. A.; Goddard, W. A., III *Organometallics* **2002**, *21*, 511-525.
(131) Periana, R. A.; Mironov, O.; Taube, D.; Bhalla, G.; Jones, C. J. *Science* **2003**, *301*, 814-818.
(132) Periana, R. A.; Bhalla, G.; Tenn, W. J., III; Young, K. J. H.; Liu, X. Y.; Mironov, O.; Jones, C. J.; Ziatdinov, V. R. *J. Mol. Catal. A: Chem.* **2004**, *220*, 7-25.
(133) Young, K. J. H.; Meier, S. K.; Gonzales, J. M.; Oxgaard, J.; Goddard, W. A., III; Periana, R. A. *Organometallics* **2006**, *25*, 4734-4737.
(134) Ziatdinov, V. R.; Oxgaard, J.; Mironov, O. A.; Young, K. J. H.; Goddard, W. A., III; Periana, R. A. *J. Am. Chem. Soc.* **2006**, *128*, 7404-7405.
(135) van Asselt, R.; Elsevier, C. J. *J. Mol. Catal.* **1991**, *65*, L13-L19.
(136) van Asselt, R.; Elsevier, C. J. *Tetrahedron* **1994**, *50*, 323-334.
(137) van Asselt, R.; Elsevier, C. J.; Smeets, W. J. J.; Spek, A. L. *Inorganic Chemistry* **1994**, *33*, 1521-1531.
(138) van Asselt, R.; Elsevier, C. J.; Smeets, W. J. J.; Spek, A. L.; Benedix, R. *Recl. Trav. Chim. Pays-Bas* **1994**, *113*, 88-98.
(139) van Asselt, R.; Gielens, E. E. C. G.; Rülke, R. E.; Vrieze, K.; Elsevier, C. J. *J. Am. Chem. Soc.* **1994**, *116*, 977-985.
(140) van Asselt, R.; Rijnberg, E.; Elsevier, C. J. *Organometallics* **1994**, *13*, 706-720.
(141) van Asselt, R.; Elsevier, C. J. *Organometallics* **1992**, *11*, 1999-2001.
(142) van Asselt, R.; Gielens, E. E. C. G.; Rulke, R. E.; Elsevier, C. J. *J. Chem. Soc., Chem. Commun.* **1993**, 1203-1205.
(143) Tempel, D. J.; Johnson, L. K.; Huff, R. L.; White, P. S.; Brookhart, M. *J. Am. Chem. Soc.* **2000**, *122*, 6686-6700.
(144) Ittel, S. D.; Johnson, L. K.; Brookhart, M. *Chem. Rev.* **2000**, *100*, 1169-1203.
(145) Svejda, S. A.; Brookhart, M. *Organometallics* **1999**, *18*, 65-74.
(146) Gates, D. P.; Svejda, S. A.; Oñate, E.; Killian, C. M.; Johnson, L. K.; White, P. S.; Brookhart, M. *Macromolecules* **2000**, *33*, 2320-2334.
(147) Shiotsuki, M.; White, P. S.; Brookhart, M.; Templeton, J. L. *J. Am. Chem. Soc.* **2007**, *129*, 4058-4067.
(148) Groen, J. H.; Delis, J. G. P.; van Leeuwen, P. W. N. M.; Vrieze, K. *Organometallics* **1997**, *16*, 68-77.
(149) van Asselt, R.; Elsevier, C. J.; Amatore, C.; Jutand, A. *Organometallics* **1997**, *16*, 317-328.
(150) Klein, R. A.; Witte, P.; van Belzen, R.; Fraanje, J.; Goubitz, K.; Numan, M.; Schenk, H.; Ernsting, J. M.; Elsevier, C. J. *Eur. J. Inorg. Chem.* **1998**, 319-330.
(151) Sprengers, J. W.; de Greef, M.; Duin, M. A.; Elsevier, C. J. *Eur. J. Inorg. Chem.* **2003**, 3811-3819.
(152) Adams, C. J.; Fey, N.; Weinstein, J. A. *Inorg. Chem.* **2006**, *45*, 6105-6107.
(153) Adams, C. J.; Fey, N.; Parfitt, M.; Pope, S. J. A.; Weinstein, J. A. *Dalton Trans.* **2007**, 4446-4456.
(154) Adams, C. J.; Fey, N.; Harrison, Z. A.; Sazanovich, I. V.; Towrie, M.; Weinstein, J. A. *Inorg. Chem.* **2008**, *47*, 8242-8257.
(155) Hansch, C.; Leo, A.; Taft, R. W. *Chem. Rev.* **1991**, *91*, 165-195.
(156) Paulovicova, A.; El-Ayaan, U.; Shibayama, K.; Morita, T.; Fukuda, Y. *Eur. J. Inorg. Chem.* **2001**, 2641-2646.

(157) Parmene, J.; Ivanovic-Burmazovic, I.; Tilset, M.; van Eldik, R. *Inorg. Chem.* **2009**, *48*, 9092-9103.
(158) Pregosin, P. S. *Coord. Chem. Rev.* **1982**, *44*, 247-291.
(159) Skvortsov, A. N. *Russ. J. Gen. Chem.* **2000**, *70*, 1023-1027.
(160) Still, B. M.; Kumar, P. G. A.; Aldrich-Wright, J. R.; Price, W. S. *Chem. Soc. Rev.* **2007**, *36*, 665-686.
(161) Coventry, D. N.; Batsanov, A. S.; Goeta, A. E.; Howard, J. A. K.; Marder, T. B. *Polyhedron* **2004**, *23*, 2789-2795.
(162) Johansson, L.; Ryan, O. B.; Rømming, C.; Tilset, M. *Organometallics* **1998**, *17*, 3957-3966.
(163) Yang, K.; Lachicotte, R. J.; Eisenberg, R. *Organometallics* **1997**, *16*, 5234-5243.
(164) Yang, K.; Lachicotte, R. J.; Eisenberg, R. *Organometallics* **1998**, *17*, 5102-5113.
(165) Norris, C. M.; Templeton, J. L. *Organometallics* **2004**, *23*, 3101-3104.
(166) Siemens Analytical X-ray Instruments Inc.: Madison, WI, 1995.
(167) Sheldrick, G. M.; University of Göttingen: Göttingen, Germany, 1997.
(168) Altomare, A.; Cascarano, G.; Giacovazzo, C.; Guagliardi, A.; Burla, M. C.; Polidori, G.; Camalli, M. *J. Appl. Crystallogr.* **1994**, *27*, 435.
(169) Altomare, A.; Burla, M. C.; Camalli, M.; Cascarano, G. L.; Giacovazzo, C.; Guagliardi, A.; Moliterni, A. G. G.; Polidori, G.; Spagna, R. *J. Appl. Crystallogr.* **1999**, *32*, 115-119.
(170) Betteridge, P. W.; Carruthers, J. R.; Cooper, R. I.; Prout, K.; Watkin, D. J. *J. Appl. Crystallogr.* **2003**, *36*, 1487.
(171) Gasperini, M.; Ragaini, F.; Cenini, S. *Organometallics* **2002**, *21*, 2950-2957.
(172) Lindauer, D.; Beckert, R.; Doering, M.; Fehling, P.; Goerls, H. *Journal für Praktische Chemie/Chemiker-Zeitung* **1995**, *337*, 143-152.
(173) Parmene, J.; Krivokapic, A.; Tilset, M. *Submitted.* **2009**.
(174) Norris, C. M.; Reinartz, S.; White, P. S.; Templeton, J. L. *Organometallics* **2002**, *21*, 5649-5656.
(175) Crabtree, R. H. *The Organometallic Chemistry of the Transition Metals, Fourth Edition, John Wiley and Sons, Inc* **2005**.
(176) Procelewska, J.; Zahl, A.; Liehr, G.; van Eldik, R.; Smythe, N. A.; Williams, B. S.; Goldberg, K. I. *Inorg. Chem.* **2005**, *44*, 7732-7742.
(177) Plutino, M. R.; Monsu Scolaro, L.; Romeo, R.; Grassi, A. *Inorg. Chem.* **2000**, *39*, 2712-2720.
(178) Frey, U.; Helm, L.; Merbach, A. E.; Romeo, R. *J. Am. Chem. Soc.* **1989**, *111*, 8161-8165.
(179) Alibrandi, G.; Minniti, D.; Scolaro, L. M.; Romeo, R. *Inorg. Chem.* **1989**, *28*, 1939-1943.
(180) Alibrandi, G.; Bruno, G.; Lanza, S.; Minniti, D.; Romeo, R.; Tobe, M. L. *Inorg. Chem.* **1987**, *26*, 185-190.
(181) Minniti, D.; Alibrandi, G.; Tobe, M. L.; Romeo, R. *Inorg. Chem.* **1987**, *26*, 3956-3958.
(182) Lanza, S.; Minniti, D.; Moore, P.; Sachinidis, J.; Romeo, R.; Tobe, M. L. *Inorg. Chem.* **1984**, *23*, 4428-4433.
(183) Raffaello Romeo, Maria R. P. A. R. *Helvetica Chimica Acta* **2005**, *88*, 507-522.
(184) Marrone, A.; Re, N.; Romeo, R. *Organometallics* **2008**, *27*, 2215-2222.

(185) Parmene, J.; Ivanovic-Burmazovic, I.; Tilset, M.; van Eldik, R. *Manuscript in preparation*.
(186) Pearson, R. G.; Gray, H. B.; Basolo, F. *J. Am. Chem. Soc.* **1960**, *82*, 787-792.
(187) Macchioni, A. *Chem. Rev.* **2005**, *105*, 2039-2074.
(188) Tellers, D. M.; Yung, C. M.; Arndtsen, B. A.; Adamson, D. R.; Bergman, R. G. *J. Am. Chem. Soc.* **2002**, *124*, 1400-1410.
(189) Romeo, R.; Grassi, A.; Monsu Scolaro, L. *Inorg. Chem.* **1992**, *31*, 4383-4390.
(190) Brookhart, M.; Grant, B.; Volpe, A. F. *Organometallics* **1992**, *11*, 3920-3922.
(191) Macchioni, A.; Zuccaccia, C.; Clot, E.; Gruet, K.; Crabtree, R. H. *Organometallics* **2001**, *20*, 2367-2373.
(192) Loupy, A.; Tchoubar, B.; Astruc, D. *Chem. Rev.* **1992**, *92*, 1141-1165.

Paper I

Combined low temperature rapid scan and ^{1}H NMR mechanistic study of the protonation and subsequent benzene elimination from a (diimine)platinum(II) diphenyl complex relevant to arene C-H activation

Jerome Parmene, Ivana Ivanović-Burmazović, Mats Tilset, and Rudi van Eldik

Inorganic Chemistry, **2009**, *48*, 9092-9103

This article is removed.

Paper II

Synthesis, Characterization, and Protonation Reactions of new Ar-BIAN and Ar-BICAT Diimine Platinum Diphenyl Complexes

Jerome Parmene, Alexander Krivokapic, and Mats Tilset

Eur. J. Inorg. Chem., **2010**, published on the web

This article is removed.

Paper III

Steric and electronic effect investigation on the protonolysis reaction mechanism at a serie of (N-N)$PtPh_2$ ((N-N) = diimine = Ar-BIAN with Ar = 2,6-$Me_2C_6H_3$ (a), 2,4,6-$Me_3C_6H_2$ (b), 4-Br-2,6-$Me_2C_6H_2$ (c), 3,5-$Me_2C_6H_3$ (d), 4-MeC_6H_4 (e), and Ar'BICAT with Ar'= 4-MeC_6H_4 (f)) complexesby complementary ^1H NMR and UV-Vis spectroscopy

Jerome Parmene, Ivana Ivanović-Burmazović, Mats Tilset, and Rudi van Eldik

Manuscript in preparation

This article is removed.